วิทยาแร่และศิลาวรรณนาของหินสการ์นที่เขาเหล็ก อำเภอหนองบัว จังหวัดนครสวรรค์

นายมามินีรีนา แอนเดรียนารีมานานา

วิทยานิพนธ์นี้เป็นส่วนหนึ่งของการศึกษาตามหลักสูตรปริญญาวิทยาศาสตรมหาบัณฑิต
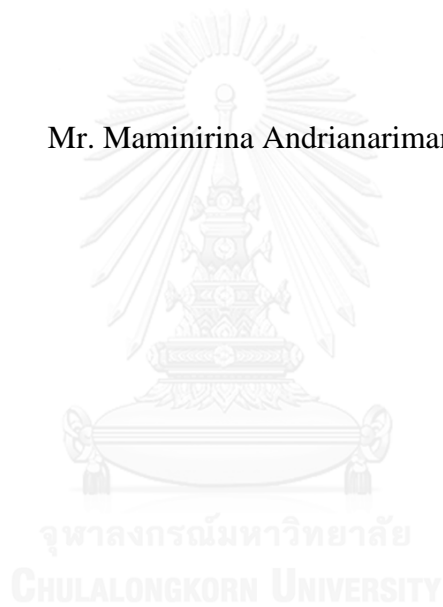สาขาวิชาธรณีวิทยา ภาควิชาธรณีวิทยา
คณะวิทยาศาสตร์ จุฬาลงกรณ์มหาวิทยาลัย
ปีการศึกษา 2559
ลิขสิทธิ์ของจุฬาลงกรณ์มหาวิทยาลัย

MINERALOGY AND PETROGRAPHY OF SKARN AT KHAO LEK,

AMPHOE NONG BUA, CHANGWAT NAKHON SAWAN

Mr. Maminirina Andrianarimanana

A Thesis Submitted in Partial Fulfillment of the Requirements
for the Degree of Master of Science Program in Geology
Department of Geology
Faculty of Science
Chulalongkorn University
Academic Year 2016

| | |
|---|---|
| Thesis Title | MINERALOGY AND PETROGRAPHY OF SKARN AT KHAO LEK, AMPHOE NONG BUA, CHANGWAT NAKHON SAWAN |
| By | Mr. Maminirina Andrianarimanana |
| Field of Study | Geology |
| Thesis Advisor | Abhisit Salam, Ph.D. |
| Thesis Co-Advisor | Associate Professor Chakkaphan Sutthirat, Ph.D. |

Accepted by the Faculty of Science, Chulalongkorn University in Partial Fulfillment of the Requirements for the Master's Degree

........................................................... Dean of the Faculty of Science
(Associate Professor Polkit Sangvanich, Ph.D.)

THESIS COMMITTEE

........................................................... Chairman
(Professor Montri Choowong, Ph.D.)

........................................................... Thesis Advisor
(Abhisit Salam, Ph.D.)

........................................................... Thesis Co-Advisor
(Associate Professor Chakkaphan Sutthirat, Ph.D.)

........................................................... Examiner
(Associate Professor Pitsanupong Kanjanapayont, Dr.rer.nat.)

........................................................... External Examiner
(Ladda Tangwattananukul, Ph.D.)

มามินีรีนา แอนเดรียนารีมานานา : วิทยาแร่และศิลาวรรณนาของหินสการ์นที่เขาเหล็ก อำเภอหนอง
บัว จังหวัดนครสวรรค์ (MINERALOGY AND PETROGRAPHY OF SKARN AT KHAO
LEK, AMPHOE NONG BUA, CHANGWAT NAKHON SAWAN) อ.ที่ปรึกษาวิทยานิพนธ์
หลัก: ดร. อภิสิทธิ์ ซาลำ, อ.ที่ปรึกษาวิทยานิพนธ์ร่วม: รศ. ดร. จักรพันธ์ สุทธิรัตน์, 86 หน้า.

แหล่งแร่เขาเหล็กตั้งอยู่อำเภอหนองบัว จังหวัดนครสวรรค์ ซึ่งหินสการ์นเกิดได้ดีในหินต้นกำเนิดที่
เป็นหินปูนมากกว่าหินภูเขาไฟ แสดงโซนการเกิดแร่ที่ชัดเจน อย่างเช่น สการ์นการ์เนต สการ์นไพรอกซีน สการ์น
ไพรอกซีนการ์เนต และสการ์นโวลาสโทไนส์ไพรอกซีน แต่อย่างไรก็ตามสการ์นไพรอกซีนเท่านั้นที่พบในหิน
ภูเขาไฟ โดยไพรอกซีนจะเกิดเป็นสายแร่เล็ก ๆ ตัดเข้ามาในหินภูเขาไฟ สการ์นมีความหลากหลายภายในแต่โซน
ตัวอย่างเช่น สการ์นการ์เนตพบทางด้านทิศตะวันตกของบ่อเหมือง มีการ์เนตสีน้ำตาลเข้ม ขนาดกลางถึงหยาบ ที่
อยู่ร่วมกับแร่แคลไซต์ แต่ทางด้านทิศตะวันออก มีการ์เนตสีน้ำตาลแดงถึงสีเขียวเหลือง ซึ่งอยู่ร่วมกับแร่ไพรอก
ซีน ความแตกต่างของแร่ในสการ์นแต่ละโซนบ่งบอกถึงระยะใกล้หรือไกลจากหินอัคนีแทรกซอน จากการ
วิเคราะห์โดยอีพีเอ็มเอ โซนการ์เนตที่อยู่ใกล้หินอัคนีแทรกซอนพบเป็น สเปสซาไทท์- กรอสซูลาร์-แอนดราไดต์
ส่วนที่อยู่ไกลจะเป็นแอนดราไดต์ การที่การ์เนตมีองค์ประกอบที่แตกต่างดังที่กล่าวข้างต้น สะท้อนถึงที่มาของ
น้ำแร่และชนิดของหินต้นกำเนิดและระยะใกล้ไกลจากหินอัคนีแทรกซอน คล้ายกับในกรณีของสการ์นไพรอกซี
นซึ่งพบแร่ไดออพไซด์ในหินต้นกำเนิดภูเขาไฟ ส่วนแร่ไพรอกซีนที่อยู่ใกล้กับหินปูนจะเป็นเฟอโรออไจต์ โซน
แร่แมกเนไทท์ (เหล็ก) เป็นการเข้าไปแทนที่ในเอนโดสการ์น ซึ่งเกิดตามรอยเลื่อนในแนวตะวันออกเฉียงเหนือ-
ตะวันตกเฉียงใต้ การเกิดแร่แมกเนไทท์จะเกิดในช่วงของการเกิดรีโทรเกรดสการ์น ส่วน        รีโทรเกรดสการ์น
จะเกิดตามรอยเลื่อนที่กล่าวข้างต้น โดยเฉพาะในส่วนของหินพื้น (ด้านตะวันตกเฉียงใต้ของบ่อ) ซึ่งสัมพันธ์กับ
สายแร่เอปิโดท-คลอไรต์-แคลไซต์ แหล่งสการ์นที่เขาเหล็กถูกจัดเป็นแคลซิคสการ์น โดยพิจารณาจากชนิดแร่
เมื่อพิจารณาชนิดของแหล่งแร่ที่เกิดในสการ์น สามารถจัดเป็นแหล่งแร่แบบสการ์น ไอรอน±คอปเปอร์ ซึ่งมีโลหะ
เด่น ได้แก่ ทองแดง ทอง ตะกั่ว-สังกะสี เหล็ก โมลิบดีนัม ทังสเตน และดีบุก

| | | |
|---|---|---|
| ภาควิชา    ธรณีวิทยา | ลายมือชื่อนิสิต | _____ |
| สาขาวิชา    ธรณีวิทยา | ลายมือชื่อ อ.ที่ปรึกษาหลัก | _____ |
| ปีการศึกษา   2559 | ลายมือชื่อ อ.ที่ปรึกษาร่วม | _____ |

v

# # 5872126423 : MAJOR GEOLOGY

KEYWORDS: MINERALOGY / PETROGRAPHY / SKARN / KHAO LEK / IRON / EPMA / ALTERATION

MAMINIRINA ANDRIANARIMANANA: MINERALOGY AND PETROGRAPHY OF SKARN AT KHAO LEK, AMPHOE NONG BUA, CHANGWAT NAKHON SAWAN. ADVISOR: ABHISIT SALAM, Ph.D., CO-ADVISOR: ASSOC. PROF. CHAKKAPHAN SUTTHIRAT, Ph.D., 86 pp.

Khao Lek deposit is located at Amphoe Nong Bua, Changwat Nakhon Sawan. Skarn is better developed in limestone than volcanics protoliths. It shows mineralogical zonations represented by garnet skarn, pyroxene skarn, garnet-pyroxene, pyroxene-wollastonite. However, in volcanics protolith, pyroxene skarn is the only skarn type identified and it is characterized by pyroxene veinlets or pyroxene infilled vugs in volcanic unit mainly in the footwall. Mineralogically, skarn may vary within each skarn zone for example in garnet skarn in the western part of the zone is represented by dark brown, medium- to coarse-grained associated with calcite whereas, at the eastern part garnet is reddish brown to yellowish green closely associated with pyroxene. Skarn variation may reflect distance from intrusion or proximal to more distal. This is consistence with composition obtained from EPMA analyzes in which garnet at proximal has composition of spessartite-grossular-andradite series whereas, at the distal become andradite. These reflect source of fluid and type of protolith and proximal and distal from source intrusion. Similar to pyroxene where diopside represent pyroxene hosted in volcanic whereas, pyroxene hosted in or close to limestone protolith is represented by ferroaugite.Magnetite orebody is likely replacing the major endoskarn which was emplaced along NE-SW major fault as a dyke. This magnetite mineralization could well be formed during retrograde skarn formation. Retrograde skarn is better developed along major faults particularly the footwall (southwest of the pit). It characterized by epidote-chlorite $\pm$ calcite vein/veinlets. The skarn at Khao Lek can be classified as calcic skarn based on its mineralogy. When consider in terms of ore deposits that are hosted by skarns, this deposit can be classified as skarn deposit. It is classified as iron $\pm$ copper skarn deposit which is based on the dominant metal i.e., Cu, Au, Pb-Zn, Fe, Mo, W and Sn

| | | | |
|---|---|---|---|
| Department: | Geology | Student's Signature | |
| Field of Study: | Geology | Advisor's Signature | |
| Academic Year: | 2016 | Co-Advisor's Signature | |

# ACKNOWLEDGEMENTS

# CONTENTS

# List of figures

# Chapter I
# Introduction

1.1 Introduction

The Khao Lek deposit is located at Amphoe Nong Bua, Changwat Nakhon Sawan, central Thailand (latitude 16º 18´ and longitude 100º 40´) and lies within the Loei Fold Belt (LFB; Fig 1.1). This is iron skarn deposit which is about 245 km north of Bangkok. The deposit is among few iron skarn deposits in the LFB which was successfully discovered from basic exploration techniques by local investor. Subsequently, it has developed into a mine (open pit mine) in which iron ore has been produced till very recent years. It is considered as small deposit operated by local company for the past 10 years. The current operation is shifted to industrial material or construction materials from both volcanic host rocks and marble of the previous iron mine area particularly. The mineral resource (iron ore) at Khao Lek has not been reported. However, its geology and the nature of the deposit itself could delimit it as small reserve or resources.

Skarn is a product of metamorphic and metasomatic process between intrusive granitic rocks of intermediate to felsic composition with carbonate rocks, at least limestones. However, skarn could be formed in almost any rock type, including shale, sandstone, granite, iron formation. It is characterized by its calc-silicate minerals which are composed mainly of garnet and pyroxene with associated minerals, and is segregated in zones according of the evolution of temperature (T), stress (P), and the prevailing chemical elements during their formation process.

Independent of any geologic epoch, skarn deposits form and offer different commodities to the humanity. They have been mined for variety of metals such as Fe, W, Cu, Pb, Zn, Mo, Ag, Au, U, rare earth elements (REE), F, B, and Sn. (Meinert et al., 2005). Major source of the world's copper, gold, silver, and zinc come from intrusive related hydrothermal ore deposits which embrace a variety of porphyry, skarn, and vein types. Numerous researches have suggested that there have been genetic,

temporal, spatial relationships between porphyry-skarn deposits and their magmatic history.
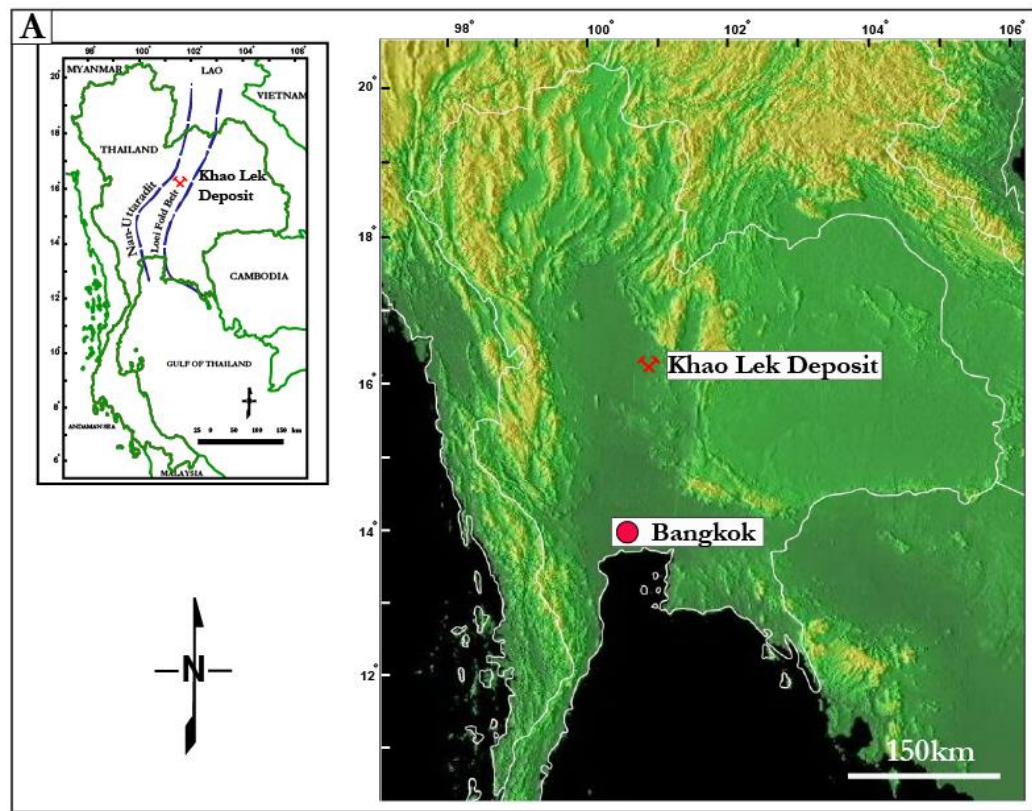


*Figure 1. 1* Map showing LFB and study area. (after Salam, 2013)

1.2 Objectives of Study

1. To characterize mineralogy and petrography of iron skarn in Khao Lek area, Changwat Nakhon Sawan.

2. To compare Khao Lek deposit with others Skarn deposits in the Loei Fold Belt.

The broad aim of this study is to describe the geology and the mineralization characteristics of the Khao Lek deposit using pit mapping combined with studies in laboratory. The main laboratory-based work includes petrographic (skarn, ore) and microanalysis study for Khao Lek ore samples and skarn alteration samples to provide

information for further detailed geochemical background through Electron Microprobe Analysis (EPMA).

## 1.3 Study Area

The study area, the Khao Lek open pit located at the east of Ban Sap Sawan, Amphoe Nong Bua, is marked on the coordinates 0690529 mE and 1758083 mN, in the Changwat Nakhon Sawan, central Thailand (Figs. 1.1 and 1.2). It is estimated about 245 km north of Bangkok. FromBangkok, the area could be reach by the highway number 32 to the In Buri then take the highway No. 11 (Tak Fa-Phisanulok highway) to Nong Bua. From Nong Bua uses road No. 225 to the study area which is located at Ban Sap Sawan.

## 1.4 Physiography

The study area is located on the southern edge of the mountain range that appears as a half circular (Fig. 1.2.) surrounded by low land area. Further to the west and east, laying with several isolated granitic mountains and hills. The highest mountains peak in the area is about 450 meters above mean sea level which is situated in the northwest of the area. while the lowest elevation is the main Khao Lek peak, which is about 303 meters located on the southeast of the area. These mountains, trending NW-SE, are surrounded by low terrains around 160 m. above the sea level.

## 1.5 Climate - Vegetation

Khao Lek is located in the upper central plain of Thailand where the climate is governed by the tropical savanna under the influence of monsoons which lead a heavy rainfall in during rainy season. Average annual rainfall is between 930 to 1,170mm. Temperature ranges from 20°C to 40°C. Wet season commences in August to the end of September with temperature about 25°C - 33°C. Cold season occurs during December to January with temperature about 21°C - 32°C. The weather become warmer on February to May with temperature about 25°C - 36°C. April is generally the hottest month of the year. The mountainous area at and around the Khao Lek are mainly covered by shrub (natural and/or cultivated). Only small trees are still preserved on the hilly area. However, the low land area surrounding the mine is mainly used for growing corn, sugar cane etc.

***Figure 1. 2*** Topographic map showing the study area of Khao Lek. (map series L 7017, sheet 51401)

1.6 Methodology

**1.6.1. Field investigation methods**

Field seasons for this study have been undertaken during end August 2016. The field geological checking was done using pre-existing district-scale geologic maps (e.g., DMR, 1976) to confirm geology particularly rock units during the field work. Approximate 60 host rocks and mineralized samples were described and collected for further laboratory-based analyses.

**1.6.2. Laboratory research methods**

*1.6.2.1 Petrographic study*

Petrographic investigations using transmitted and reflected lights were conducted for both host rocks (e.g., volcanics and limestone protoliths), and skarn alteration. The study was performed at the Department of Geology, Faculty of Sciences, University of Chulalongkorn. Skarn alteration minerals such as garnet, pyroxene is analysed for their composition.

*1.6.2.2 Method for EPMA analyzes*

Polished rock samples' surfaces are bombarded by accelerated and focused beam of electrons which excite atoms of the selected mineral grain to produce characteristic X-ray. Associated software collects, compiles and manages the specific energies corresponding to theses X-ray inputs for the determination of the intensity related to the concentrations of the oxides belonging to the analyzed mineral.

**Advantage**

Nondestructive, analysis performed with EPMA is rapid and in *situ*; micrometer size of mineral can be used for analysis. All elements with atomic number ranging from 4 (Be) to 92 (U) can be detected by this technique. Among standard techniques in mineralogy and petrology, EPMA has high spatial resolution, good resolution, good accuracy and reasonably low detection limits. Moreover, it requires fairly simple specimen preparation.

**Sample preparation**

Samples for EPMA analysis should be prepared as polished section or polished-thin section before their polished surface is coated with a vacuum-evaporated carbon of about 20 nm thick for the best flow of the incident electrons from beam source.

**Ferric/ Ferrous calculation**

As reported above, the EPMA analyses are presented in weight% oxides. However, this technique cannot distinguish $Fe^{2+}/Fe^{3+}$; iron oxides are then given as total iron oxide ($FeO_{total}$). Droop, G.T.R., (1987) suggested equations which are requested for the determination of ferric/ ferrous ratio in crucial ferromagnesian minerals. His equations were therefore applied for appropriate minerals, i.e., pyroxene and garnet.

## 1.7 Thesis structure and conventions

For overview of the thesis structures, the thesis is divided into the following Chapters:

- Chapter 2 includes (a) reviewing tectonic setting of mainland SE Asia(b) reviewing regional geology of area surrounding the deposit (c) reviews distribution of major mineral deposits in the LFB including skarn deposits and occurrences.

- Chapter 3 documenting deposit-scale geology of volcanics and limestone, intrusive rocks that might related to skarn alteration

- Chapter 4 describes detailed skarn alterations including zoning, and details petrography for each zone with emphasizing on garnet and pyroxene. Petrographic description of iron mineralization and retrograde skarn alteration were also undertaken in this chapter.

- Chapter 5 describes the detailed minerals chemistry with emphasizing on garnet, pyroxene.

- Chapter 6 firstly comparison several skarn deposit/occurrences in the LFB and secondly interpretation, discussion and conclusions of all collected data during this study, and introduces genesis Khao Lek iron skarn system.

# Chapter 2
# Tectonic Setting and Regional Geology

## 2.1. Introduction

This Chapter reviews regional tectonic setting, geological framework of mainland SE Asia including Thailand, major mineral deposits, especially the skarn deposits/occurrences in the Loei Fold Belt (LFB). In addition, regional geology surrounding the study area is herein described.

## 2.2. Tectonic setting

The tectonic evolution of the mainland southeast Asia has been a subject of interest and debate in several aspects such as geometry of subduction, position of Paleo-Tethys, and timing of collision of Shan-Thai and Indochina Terranes (or blocks). However, one of the common points of views is the existence of Paleotethys ocean between Shan-Thai and Indochina Terranes prior to their collision to form the Nan-Uttaradit Suture.

Thailand and its adjacent areas of mainland SE Asia are located on the southern part of the Red River Fault zone, south China, and comprise two major tectonic terranes: Indochina in the east and Shan-Thai on the west (Fig. 2.1). These two terranes are delimited by Sukhothai Fold Belt (SFB) in the west and Loei Fold Belt (LFB) in the east. The Shan-Thai terrane is an elongate continental block comprising of the west Myanmar, east Myanmar, western Thailand, western Malaysia Peninsular and Sumatra. It is widely believed to have been rifted from the northwestern Australian part of Gondwanaland (or Gondwana in current literatures) in the early Permian (Bunopas and Vella, 1983; Gatinsky et al., 1984; Hutchison, 1989). This is also supported by the presence of glaciomarine siliciclastic rocks of Early Permian Phuket Group in the southern Thailand (part of the Shan-Thai Terrane), which can be strongly correlated with the Gondwana glacial stratigraphy.(Metcalfe, 1988; Shi and Waterhouse, 1991).

The Indochina block, enclosed the central and east Thailand, Cambodia, Lao PDR, and Vietnam. South China Terrane was part of northeastern Gondwana in the

Early Paleozoic (Audley-Charles et al., 1988; Metcalfe, 1988). Prior the collision with Shan-Thai, Indochina Terrane is believed to have already been amalgamated to the South China along the Song Ma Suture during Silurian (Carter and Clift, 2008; Carter et al., 2001). However, Gatinsky et al. (1984); Intasopa (1993) believed Devonian or Early Carboniferous is more likely timing of the amalgamation. The Truong Son Fold Belt (TSFB) located in northern Lao PDR and northern-central Vietnam (Fig. 2.1) included in the Indochina Terrane is linked to the closure of Laos-North Vietnam Strait of Paleotethys (Intasopa, 1993).

The Shan-Thai and Indochina Terranes moved north from Australia into Paleo-Tethys Ocean during Phanerozoic and this process caused opening and closing of the Paleo-Tethys and Meso-Tethys between them and they were subsequently amalgamated into Asia (Metcalfe, 2002). Most workers agreed the paired subduction occurred on the both side of this Paleo-Tethys Ocean underneath Shan-Thai and Indochina Terranes (Bunopas, 1981; Charusiri, 1989; Hutchison, 1989; Intasopa, 1993). However, Ueno and Hisada (2001) introduced single eastward subduction underneath Indochina Terrane form the SFB (now known as Sukhothai Arc).

Permo-Triassic volcanic rocks in SFB are believed to be related to eastward subduction underneath the Indochina Terrane. Subsequently, the subduction was followed by the I-type granitoid emplacement in the area during Late Triassic to Jurassic. However, recently many authors regard Nan-Uttaradit-Sra Kaeo Suture as remnant of back arc basin situating behind Sukhothai Arc and Indochina Terrane. LFB is no longer mentioned in recent literatures (Sone, 2008a). Khin Zaw et al. (2007, 2010) suggested that the Permo-Triassic subduction related magmatic rocks are widely distributed in both along SFB and LFB and are predominantly of I-type affinity. This is conflicting with the idea proposed by (Sone, 2008a). Recently published works also suggested similar finding, for example Salam (2013) reported that the emplacement of volcanic rocks (ranging in composition from basalt to rhyolite) and plutonic rocks (granite to gabbro of I-type affinity) occurred in the LFB is the results of the Late Permian subduction of the oceanic crust underneath Indochina.

***Figure 2. 1*** Map showing tectonic setting of the mainland SE Asia (Sone, 2008a).

The collision and accretion of Shan-Thai and Indochina Terranes in Late Triassic are generally accepted (Bunopas, 1981; Intasopa, 1993; Metcalfe, 2002; Phajuy et al., 2005; Salam, 2013). This collision was subsequently followed by post-collision magmatism represented by the occurrence of granitoid rocks in SFB and LFB (Salam, 2013). Later India-Eurasia collision during Cenozoic also affected this region resulting

in reactivation of the several strike-slip faults such as Red River Fault (Tapponier, 1982). In Thailand, Three Pagoda and Mae Ping (or Wang Chao) Faults are among of them.

## 2.3. Major Skarn Deposits/Occurrences in LFB

In LFB, there are a number of skarn occurrences and the skarns are divided into two types namely, oxidized skarn and reduced skarn (Kamvong and Zaw, 2009). Some skarns in this region are clearly related to porphyry intrusions or porphyry-related skarn type which is mainly characterized by Cu-Au and Au deposit (Fig. 2.2.). Major intrusive rocks associated with skarn formation are mainly of intermediate to felsic composition (granodiorite and diorite) that hosted in both volcaniclastic and limestone protolith. Major skarn deposits in the LFB are summarized below:

### 2.3.1. Phu Kham deposit

The Phu Kham copper-gold deposit (192 Mt at 0.62 % Cu, 0.24 g/t Au) is hosted in Late Carboniferous to Early Permian volcaniclastic rocks and associated intrusions (Tate, 2005). The porphyry-related alteration assemblages include: (1) biotite + magnetite ± K-feldspar alteration; (2) sericite-quartz- pyrite ± epidote alteration; (3) epidote-calcite-quartz + chlorite alteration; and (4) muscovite-pyrophyllite- quartz alteration. Skarn-related alteration includes: (1) garnet skarn (proximal zone) and (2) garnet-epidote skarn (distal zone). The Cu-Au mineralization at Phu Kham is mostly confined to the skarn zones, and economic Cu-Au veins occur predominantly as stockwork veins in retrograde stage.

### 2.3.2. Puthep deposit

The Puthep (PUT1 and PUT2) porphyry-related Cu-Au skarn deposits occur in fractures and as veins typically centered on at least two dioritic to granodiorite intrusions (Fig. 2.2). These intrusions were emplaced into Carboniferous sedimentary rocks (Wang Saphung Formation) including siltstone, limestone and sandstone. The Puthep 1 (PUT1) deposit is previously known as Phu Hin Lek Fia and the deposit has a resource of 183 Mt at 0.5% Cu and 0.13 g/t Au. U-Pb zircon dating of the PUT1 intrusions yielded Early to Middle Triassic ages of 242.4 ± 1.3 Ma and laser ablation Ar- Ar dating of biotite from the same intrusion indicates an age of 248 ± 2 Ma and 247

± 6 Ma.

The Re-Os dating of molybdenite is between the zircon and biotite ages at 245.9 ± 0.9 Ma indicating mineralization and intrusion appear to have occurred between 248-242 Ma. The intrusions display younger feldspar Ar-Ar ages (164 ± 0.6 Ma). The hypogene alteration at PUT1 is characterized by porphyry-style alteration and mineralization and skarn-style alteration and mineralization outboard from the PUT1 stock. Mineralization includes both oxide (magnetite) and sulfide (pyrite-chalcopyrite ± chalcocite) minerals, and the best copper grades are significantly associated with skarn-style mineralization that occurs in the retrograde skarn assemblages.

The PUT2 deposit is also known as Phu Thong Daeng and has an inferred resource of 36.4 Mt grading 0.43 % Cu and U-Pb zircon age of the associated intrusions yielded Early to Middle Triassic age ranging between 234-244 Ma. Porphyry and skarn alteration and mineralization at PUT2 are characterized by the earlier phyllic alteration consisting of sericite replacing feldspar and chlorite after mafic minerals (e.g., biotite) in the host igneous rock and followed by argillic alteration and retrograde quartz-carbonate +epidote assemblages. In contrast to PUT1, early prograde skarn minerals such as garnet and pyroxene are not recorded in the PUT2 deposit.

### 2.3.3. Phu Lon skarn deposit

The Phu Lon skarn deposit (resource of 5.4 Mt at 2.4 % Cu and 0.64 g/t Au) is hosted in volcanosedimentary units and limestone of the Devonian age (Fig. 2.2). The LA ICP-MS U-Pb zircon dating from the volcaniclastic unit yielded 359 + 6 Ma (Late Devonian) age. These rocks are intruded by plutons of oxidized, calc- alkaline quartz monzonite and diorite-monzodiorite (granodiorite) porphyry.
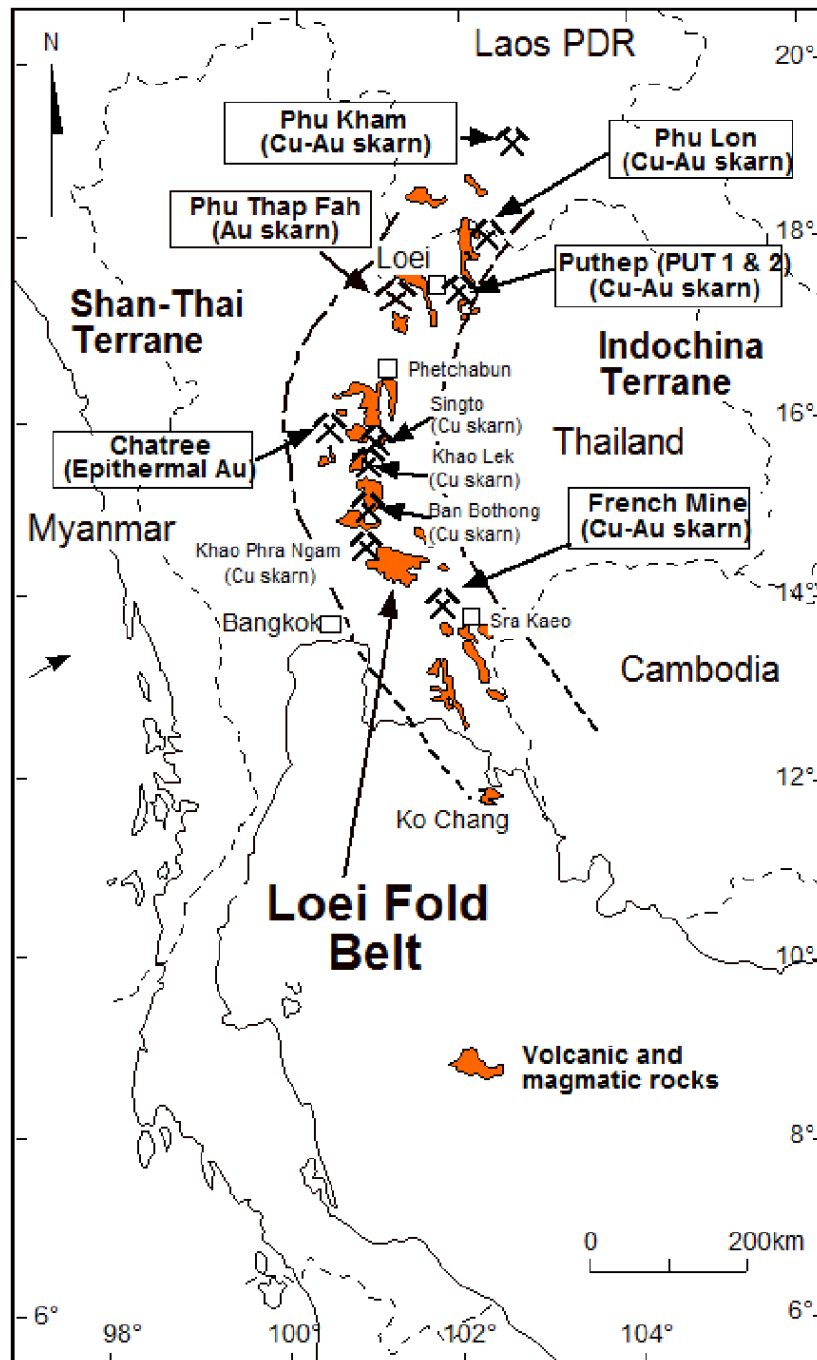
***Figure 2. 2***.Map showing major skarn deposits and occurrences in LFB (Khin Zaw et al., 2009).

The presence of primary magnetite and titanite, combined with the absence of ilmenite, indicates that the plutons associated with mineralization are derived from oxidized magmas (Kamvong and Zaw, 2009; Kamvong et al., 2006).

Three paragenetic sequences of the mineralized skarn formation are differentiated by the separate calc- silicate mineral assemblages: (I) Pre-ore Stage − garnet + tremolite + calcite + quartz ± vesuvianite ± magnetite ± sulfides; (II) Ore-skarn Stage − (IIA) garnet + clinopyroxene + magnetite, and (IIB) epidote + actinolite + chalcopyrite + pyrite ± calcite ± quartz ± tremolite; and (III) Post-ore Stage − calcite + quartz + chlorite + sericite ± epidote ± actinolite (Kamvong et al., 2006).

### 2.3.4. Phu Thap Fah

The Phu Thap Fah is a reduced gold skarn deposit in LFB (Zaw et al., 2014) (Fig. 2.2). It is hosted in the Permian sedimentary sequence consisting of shale, crystalline limestone, muddy sandstone, carbonaceous siltstone and shale intruded by Early Triassic granodiorite (U-Pb zircon age of 245 ± 3 Ma) and Late Triassic andesitic dikes (U- Pb zircon age of 221 ± 5 Ma). The Late Triassic andesitic dyke cross-cuts the mineralized skarn zone suggesting skarn alteration and gold mineralization probably occurred during the Middle to Early Triassic .

The deposit contains gold reserves of and 747,000 tones at 7.97 g/t Au. The skarn mineralogy is characterized by early development garnet- clinopyroxene skarn followed by retrograde alteration and mineralization. The retrograde skarn assemblages consist of amphiboles, epidote, chlorite, carbonate and quartz. Gold occurs as electrum, gold-bismuth and gold-bismuth- telluride association and majority of gold is confined to the massive pyrrhotite and pyrite with chalcopyrite in the retrograde zone (Khin Zaw et al., 2006, 2008).

### 2.3.5. Khao Phanom Pha

The Khao Phanom Pha deposit in the LFB is hosted by N-S trending volcaniclastic rocks ranging in composition from basaltic andesite to rhyolite and microdiorite intrusions (Salam personal communication). This deposit is located at Amphoe Wang Sai Poon, Changwat Phichit (Fig. 2.2). Gold mineralization occurs as quartz-sulfide-gold veins and veinlets in zones of almost north-south trending. Recently, the mineralization is identified as skarn which occurs both as endoskarn (in diorite) and exoskarn developed in Late Permian-Early Triassic volcanics protolith.

This volcanics is the same sequence as the host of the Chatree low-sulfidation Au-Ag epithermal deposit (Salam et al., 2014). The volcaniclastic rock unit shows fault contact with the fossiliferous limestone roof-pendants, which are locally found in the volcanic rocks adjacent to the ore bodies and have been recrystallized to marble and calc-silicate. It is noticeable that the presence of wollastonite was reported in the calc-silicate roof pendant unit.

Finally, the volcanic and carbonate host rocks at the Khao Phanom Pha deposit and it vicinities have been occasionally intruded by sparsely K-feldspar megacrystic, medium-grained, porphyritic hornblende-biotite Triassic granite. It is also noticeable that the Khao Pong – Khao Mo gold deposit (Chatree Gold Mine) is located approximately 20 Km east of the Khao Phanom Pha deposit (Salam, 2013).

2.3.6. French Mine Cu-Au skarn deposit

The French Mine Cu-Au skarn deposit is hosted in Early Triassic volcanosedimentary units (U-Pb zircon $247 \pm 6$ Ma), in the Amphoe Kabin Buri, eastern Thailand (Fig. 2.2) and the sequence was intruded Late Triassic diorite (U-Pb zircon age $203 \pm 8$ Ma). Drilling has shown that this is a low-grade deposit, although 16.8 g/t Au has been determined in some drilling chips (Müller, 1999). Prograde skarn is characterized by garnet-pyroxene zone, pyroxene-garnet- wollastonite-vesuvianite. Gold mineralization is associated tremolite-actinolite± clinozoisite- quartz ± prehnite-chlorite ± calcite veins/veinlets. Gold associates with magnetite, pyrite, chalcopyrite and sphalerite). The late stage veining is represented by illite-montmorillonite ± hematite.

2.4. Regional Geology

Regional-scale geology surrounding the study area is given in Figure 2.3. Here, the oldest rock unit which forms as high mountainous area on the eastern part of the study area is the Permian Tak Fa Formation of Saraburi Group. In the area, the Tak Fa Formation is composed mainly of thick-bedded limestone partly interbedded with shale, slaty shale and sandstone (Fig. 2.3). This limestone contains fossils such as corals, brachiopods bryozoa and fusulinids, *Verbekina sp., Parafusulina sp. and*

*Neoschwagerina sp*. which indicate the Artinskians-Kungurian age (Nakornsri, 1981). The Tak Fah Formation was overlain by Permo-Triassic volcaniclastic rocks (Fig. 2.3) composing basalt, andesite, rhyolite porphyry, and pyroclastic rocks (tuff and agglomerate).

The basaltic rock occurs in flat area on the eastern central part of the study area. Andesite porphyry forms as small hills in the central part while the pyroclastic rocks occur in flat area and mountains in western part of the area. The rhyolite porphyry forms as small hills in the south-eastern part. Four varieties of intrusive rocks are associated with the volcanic rocks of the area, they are mapped as gabbro, diorite, quartz diorite and hornblende-biotite granodiorite. Diorite occurs as a large north-south elongated sill (1.5 x 6 km$^2$) intruded parallel to the bedding plane of Permian limestone on the eastern part of the area. Diorite intrusion was cross cut by a small quartz diorite sill/dyke on the southeastern corner. Hornblende-biotite granodiorite forms as circular bodies exposed in the middle and west-central parts, while gabbro occurs as small stock on the western part. Both hornblende-biotite granodiorite and gabbro intruded the older Permo-Triassic volcanic rocks.

Basaltic rock covers about 25 km$^2$ of the central part of the study area. It is very fine-grained, black. It overlies the Permian limestone and has also been found as xenoliths in quartz diorite and basaltic andesite. In the field, it was cut by a 2-3 m. thick diorite dike. Flow structure has not been found in the basalt which might have been eroded away. This basaltic rock was proposed as the oldest volcanic rock in this area by Jungyusuk et al. (1985). Pyroclastic rocks including mafic agglomerate and tuff covered the western part of the map. This rock unit overlies the Permian limestone.

The andesite porphyry covers the central part of the study area. It is fine-grained, grayish green, porphyritic and contains phenocrysts of hornblende. The rock contains xenoliths of basalt therefore it is younger than basalt. The southeastern part of the area is covered rhyolite porphyry which occurs as small hills. The rock is yellowish brown, porphyritic and contains plagioclase phenocrysts. Cross-cutting relationship of this rock with other rock units has not been found in the field.

Fold, fault, bedding and flow structure of volcanic rocks are the main geological structures found in the area. Synclinal with fold axis oriented in the N-W direction was reported outside the study area. Faults occur in two directions, NW-SE and NE-SW. Bedding in the Permian limestone has the strike in the N-S direction 24 with 10 – 30° east dipping. Finally, flow structure was found to have two directions, NE-SW and NW-SE (Jungyusuk et al.,1985).
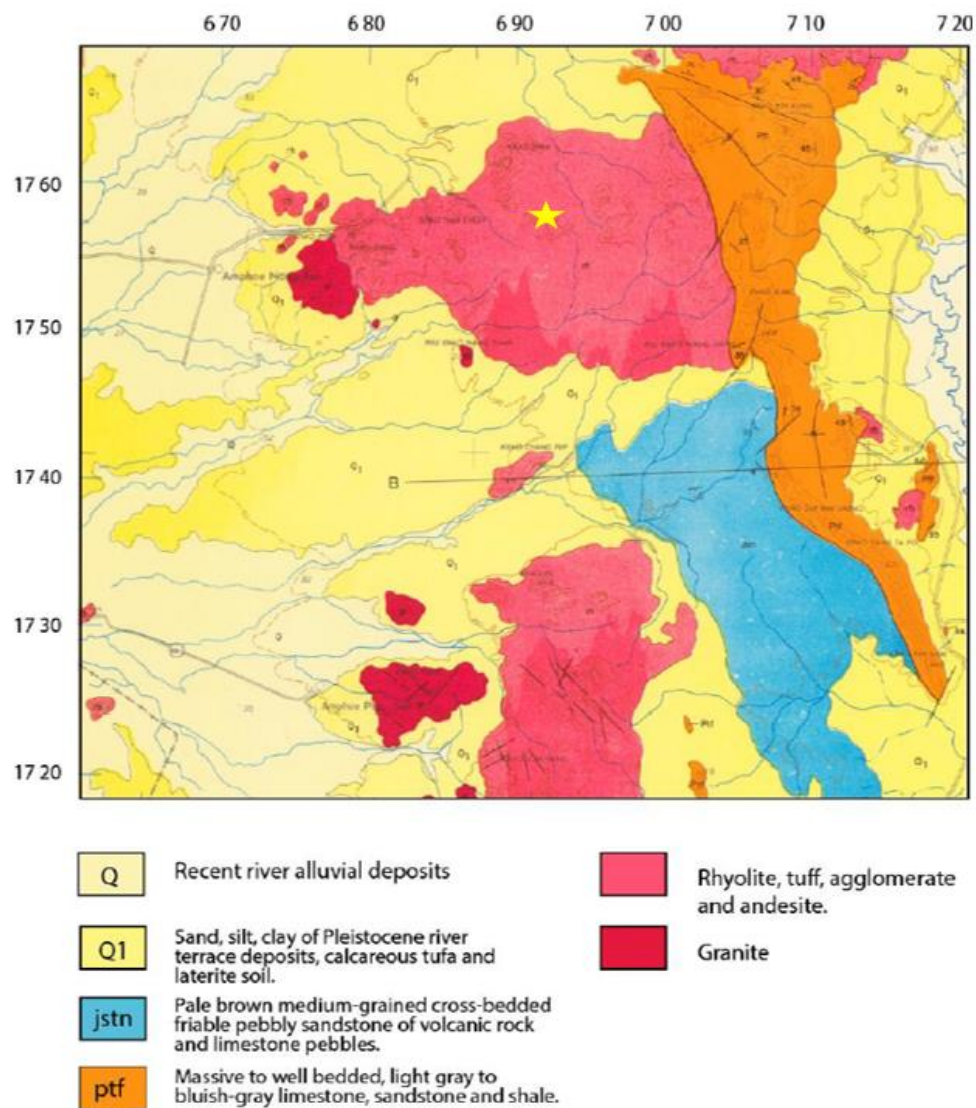


***Figure 2. 3*** Geological map showing major rock units of Khao Lek (yellow star) and adjacent area (after DMR 1979, Amphoe BAN MI, ND 47-4).

## Chapter 3
## Geology of Khao Lek skarn deposit

3.1 Introduction

This chapter documents rock units in and around the study area. The geologic map covering the deposit area and its adjacent is given in Figure 3.1. Detailed petrographic description of rock units will be outlined below:

3.2. Geology of Deposit

The oldest rock in the study area is Permian limestone of Tak Fa Formation, Ratchaburi Group which is characterized by massive to well bedded, light gray to bluish-gray limestone, sandstone and shale (Department of Mineral Resources, 1977). The nearest limestone exposures (including marble and calc-silicate) to the mine area is on the small hill, northwest of the mine area. It is overlain by Permo-Triassic volcanic rocks consisting of rhyolite, tuff, agglomerate and andesite. Triassic granite to diorite are mainly cropped out in low land area in the east and northeast of study area (Figs. 3.1 and 3.2).

3.2.1. Marble and calc-silicate unit

At Khao Lek, there are few small exposures of Permian limestone. It crops out about 1 kilometer northwest and southeast of the mine area respectively (Fig. 3.1). This limestone is mainly covered by widely distributed Permo-Triassic volcanic rocks. This formation is partly thermally metamorphosed to marble and calc-silicate particularly near the contact with diorite intrusion. The best example of calc-silicate and marble outside the pit area is a long road cut that cross cuts the Khao Lek mountain range, northwest of the mine area (Fig. 3.1). Here, marble is light gray to white forming well crystalline rock. However, it commonly contains chert nodules. The calc-silicate has been observed at some locations in this area where the original limestone is impure and formed as thin beds.
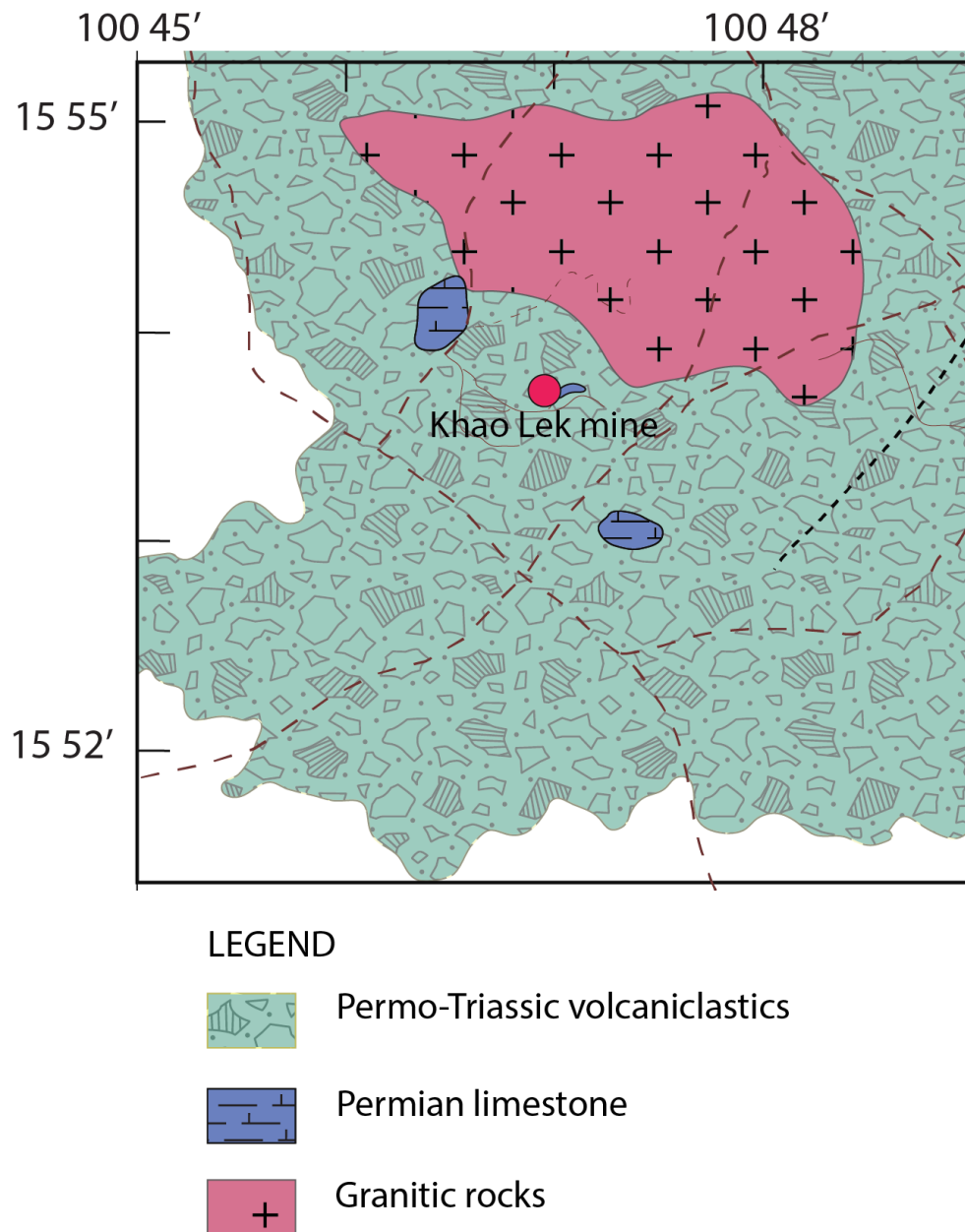
*Figure 3. 1* Geological map of Khao Lek and Khao Mae Kae areas showing distribution of rock units. Modified from (Khositanont, 2008)

At mine area, the limestone is a major protolith type for skarn alteration. Here, limestone was metamorphosed to medium- to coarse-grained marble (Figs. 3.2, 3.3, 3.4A and 3.4B). Marble unit exposes at the eastern pit wall and on the surface, may have been brought up to the surface by reversed fault (Figs. 3.2 and 3.3). However, the accessibility to the exposures is limited.
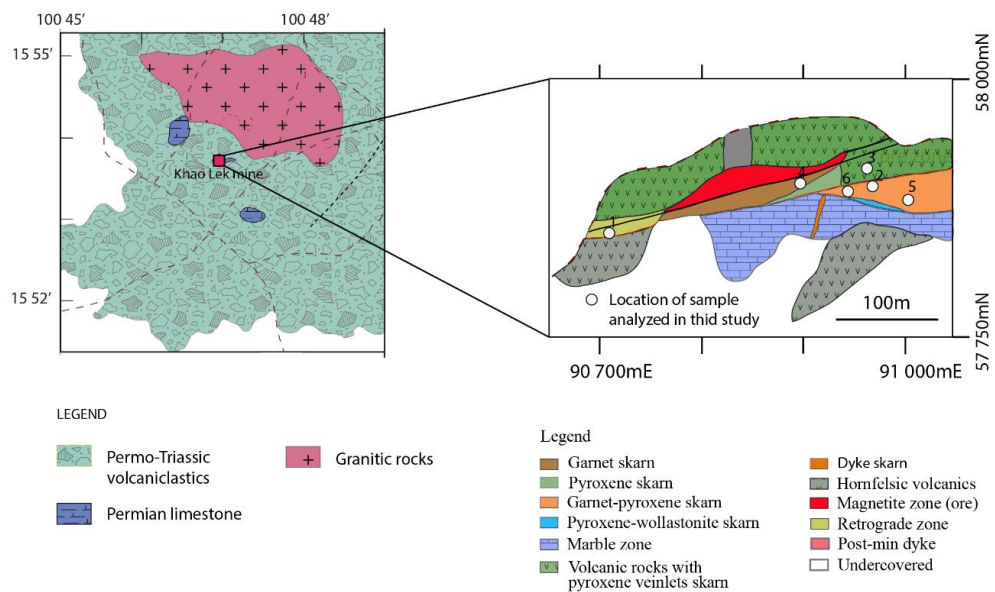
*Figure 3. 2* Simplified geological map of Khao Lek deposit showing rock types and skarn alteration zones, and locations of samples used for EPMA analyzes are given in number (e.g., 1, 2, 3 ...6).



*Figure 3. 3* Panorama view of Khao Lek open pit for eastern pit wall showing the end of main orebody (left of photograph), volcanics with pyroxene skarn veinlets, garnet-pyroxene skarn (brown), narrow pyroxene-wollastonite skarn and marble (white, right). Photograph looking northeast.

Under microscope, the marble consists of calcite about 70 to 75 % by volume and 25 to 30% of dolomite. Small amount of quartz and opaque minerals may also present. The rock shows a allotrioblastic-heterogranoblastic texture. Calcite and dolomite range in size from 0.2 to 1.5 mm, euhedral to subhedral crystals. It should be

noted that marble samples from the eastern part of the pit are finer grained in comparison to those at the center of pit close to the main garnet skarn zone.
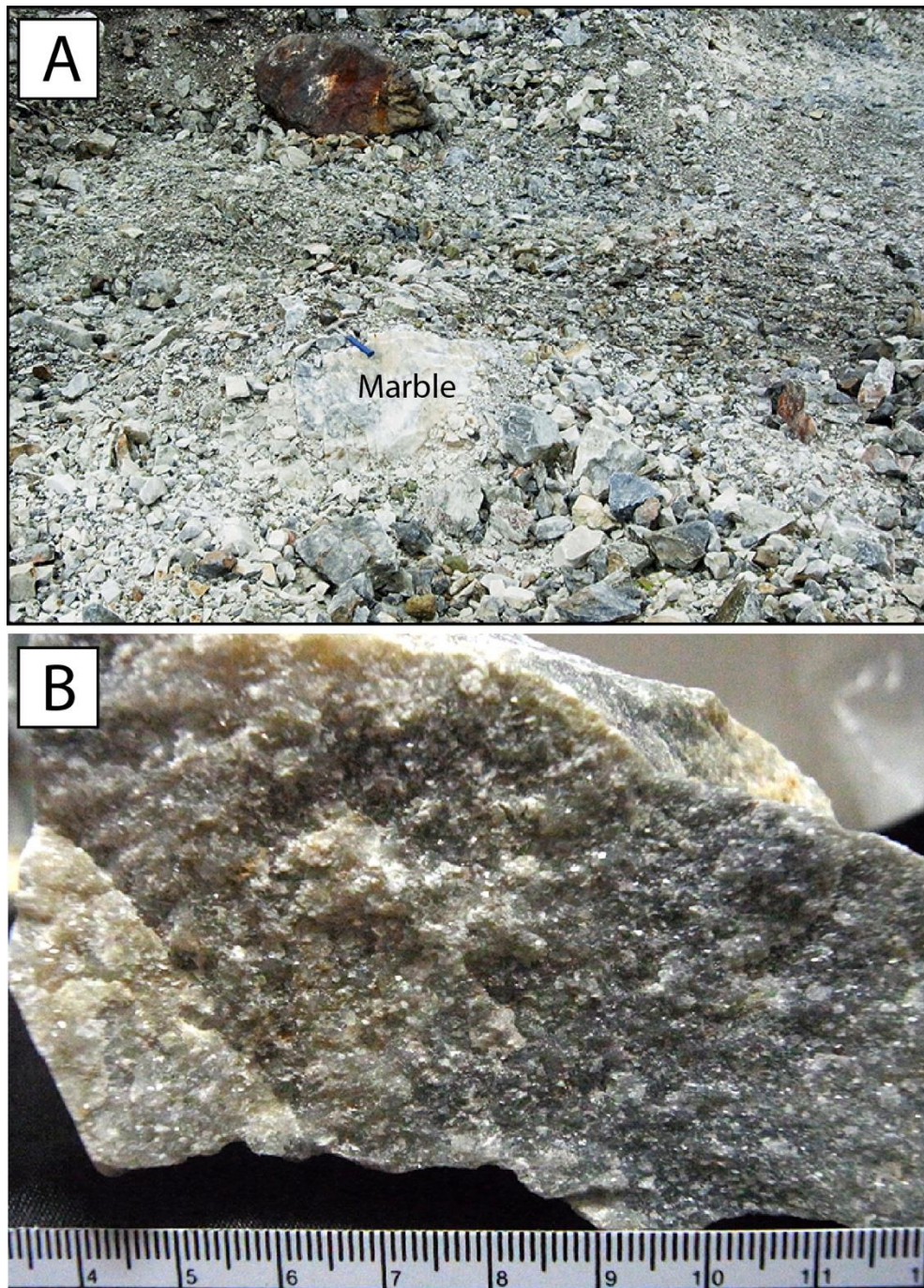


***Figure 3. 4*** Photograph of marble **A**. Marble exposure close to the main garnet skarn zone on pit floor. **B**. Hand specimen showing coarse-grained calcite.

3.2.2. Volcaniclastics Unit

Khao Lek volcanic rocks unit is a part of Thung Faeg-Sap Samran volcanics forming as a ring shape enclosing the diorite intrusion at Ban Khao Mae Kae (Fig. 3.1). These volcanic rocks were mapped as Permo-Triassic volcanics in geological map scaling 1: 250,000 (Department of Mineral Resources, 1979). Salam et al. (2014) suggested that these volcaniclastic rocks are similar in ages and composition to the volcaniclastics in Chatree area or "Chatree volcanics" in Amphoe Thap Khlo (Changwat Phichit) and Amphoe Chon Daeng (Changwat Phetchabun) about 50 km north of the study area in which the ages of host range from 258 to 250 Ma (Salam, 2013; Salam et al., 2014). The post-Chatree mineralization andesitic dykes which cut through Chatree epithermal mineralization have ages between 238 to 250 Ma (Salam et al., 2014).

At Khao Lek and its adjacent area, the volcanic rocks are characterized by dark greenish gray sandstone (tuff and lapilli tuff), breccia and lava ranging in composition from basalt to andesite. During this study, field observation reveals that the Late Permian-Early Triassic volcanic rocks are dominated by andesitic breccia, andesitic sandstone (or andesitic tuff) (Fig. 3.1) and minor coherent (or lava) basaltic andesite and basalt. However, at the mine area particularly in open pit, the coherent rocks (basaltic andesite and basalt) are quite dominant (Figs. 3.1 and 3.2). The volcanic sequence has strike northwest-southeast with moderate dipping about 20 to 30° to the east.

At Khao Lek, at least four types of volcanic rocks are classified namely: 1) Andesitic sandstone or andesitic tuff, 2) Andesitic breccia, 3) Andesitic basalt/basalt and 4) Basaltic dyke are found in and surrounding the mine area (Figs. 3.2 and 3.5).

***Andesitic tuff/andesitic lapilli tuff (andesitic sandstone)***

Megascopically, the rock is dark green to grayish green (Fig. 3.6). The composition varies from andesite to basalt and they are commonly polymictic in which majority of clasts size are least than 2mm in diameter consisting of andesite, basaltic andesite and basalt with trace of mudstone clasts. Clasts are angular to subangular with moderately sorted.

Under microscope, the rock consists mainly of andesite, basaltic andesite and porphyritic andesite clasts. Clasts are less than 2 mm in diameters, angular to subangular and moderately sorted (Fig. 3.7A and 3.7B).



***Figure 3. 5***.Panorama view of Khao Lek open pit showing volcanics protolith on footwall and the main orebody that is enclosed by garnet skarn zone (white) on pit floor. Photo looking northeast.



***Figure 3. 6*** Photograph of andesitic tuff (andesitic sandstone) contains chlorite-epidote veinlets.
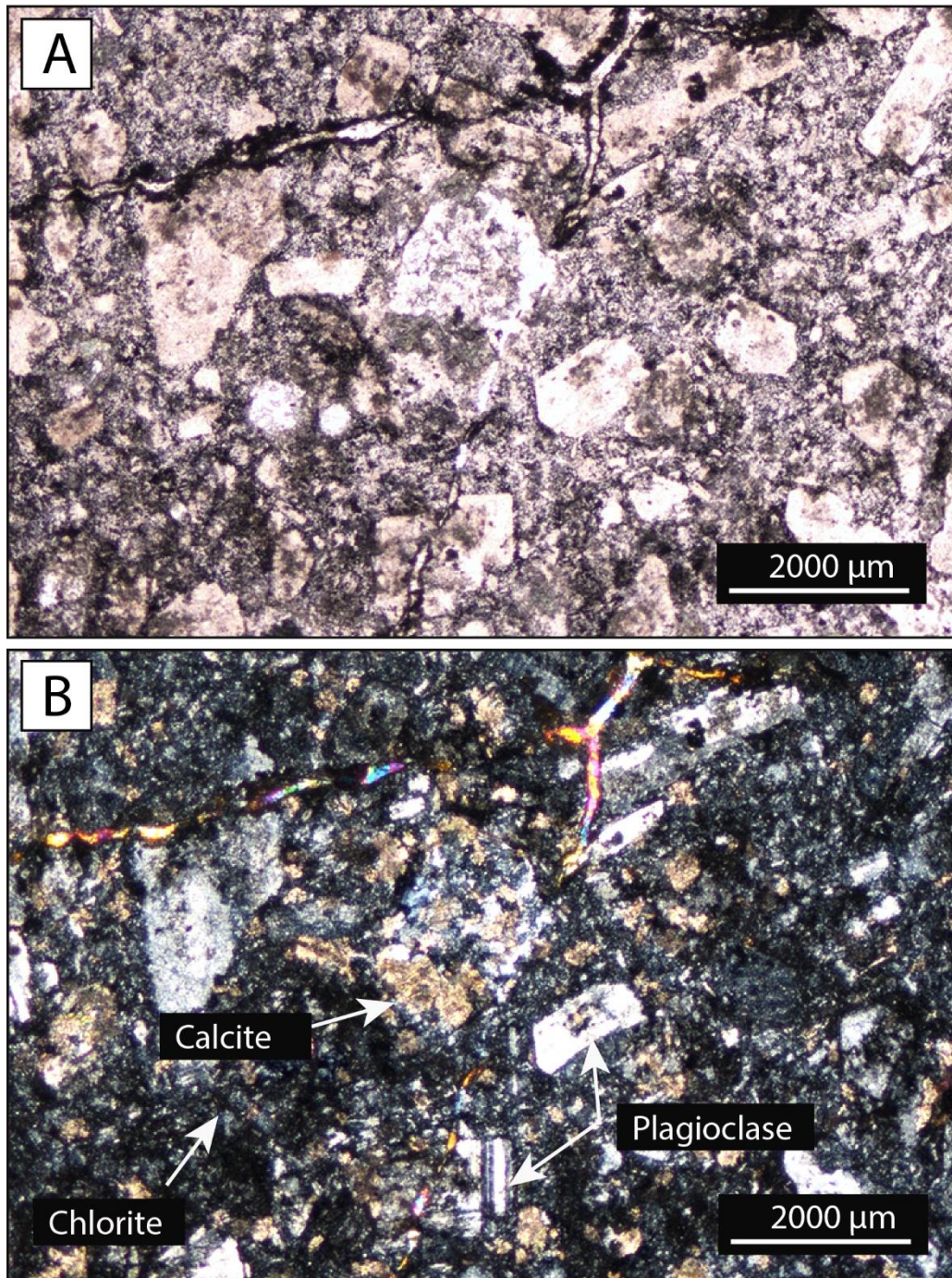
*Figure 3. 7* Photomicrograph of andesitic tuff, **A**. (ppl) and **B** (xpl) showing feldspar (mainly plagioclase), chlorite after mafic minerals (dark green) and some altered rock fragments (top left), Note epidote veinlets (top).

*Andesitic breccia*

Andesitic breccia has been observed mainly at the northwest part along the road cut within the mining concession area or about 100 meters from the open pit. However, the relationships with andesitic lapilli tuff, andesitic crystal tuff and coherent volcanic rocks (basaltic andesite and basalt) are not clear.

In hand specimen, the rock is dark green to grayish green (Fig. 3.8). The composition varies from andesite to basalt and they are commonly polymictic in which majority of clasts size ranges 2 mm to 2cm in diameter, subangular to angular. Majority of clasts are phyric basaltic andesite, porphyritic basaltic andesite and basaltic and matrix of similar composition. The rock is generally poorly sorted.
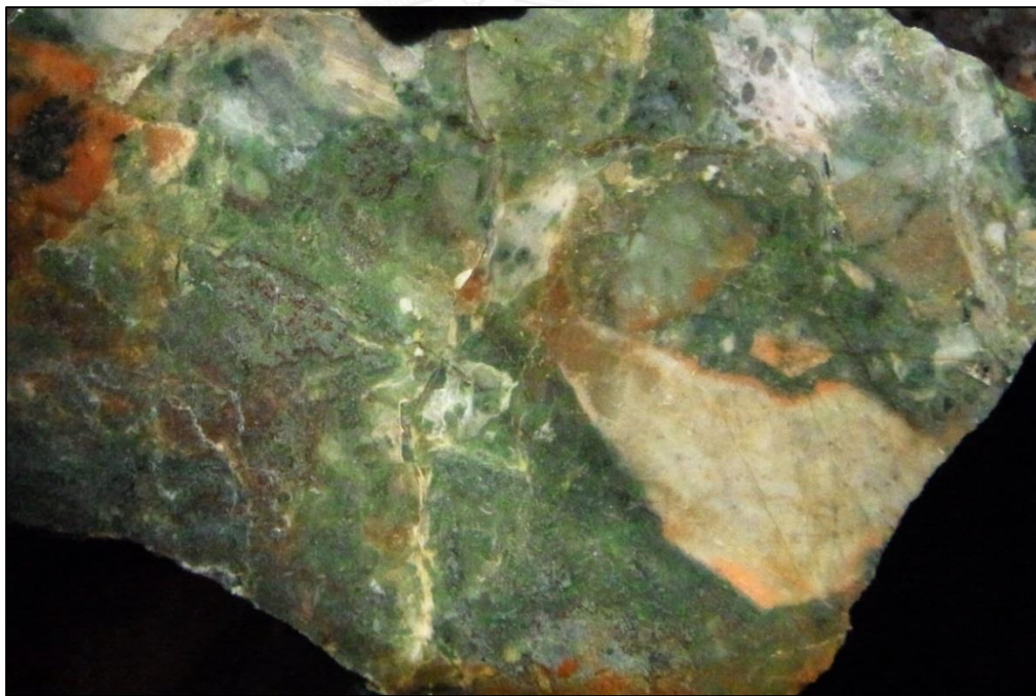


*Figure 3. 8* Photograph of hand specimen of andesitic breccia showing multiple clast types, strongly altered particularly in matrix which is characterized by chlorite-rich alteration.

*Basalt andesite and basalt*

Dykes of similar composition are observed on the footwall of Khao Lek open pit. Further away from the mine area or in the eastern side of the map (Fig. 3.1), shallow intrusive rocks of similar composition are commonly associated with basaltic andesite and basaltic.

The coherent (lava) volcanic rocks range in composition from andesite to basalt with basaltic andesite and basalt are dominated particularly in the mine area (Figs. 3.3 and 3.5). They have been observed both on hanging wall and footwall (Figs. 3.3 and 3.9A). However, the relationships with the andesitic breccia and andesitic tuff/lapilli tuff are less obvious due to limitation of outcrop and the area surrounding the open pit is mostly under covered. It is most likely that they are interbedded with andesitic breccia and andesitic sandstone. However, observation at some locations along the mining road at Khao Lek reveals that the coherent basaltic andesite is about 3-5 meters thick and interbedded/intercalated with andesitic sandstone and/or andesitic breccia. Its contact with andesitic sandstone and/or andesitic breccia is a gradational.

Megascopically, basaltic andesite is dark green in color, relatively fine-grained and weakly porphyritic in texture characterized by lath-shaped plagioclase (Fig. 3.9B). In contrast, the basalt is relatively fine-grained but equigranular with distinctive feldspar component. In hand specimens, the coherent basalt is also characterized by a uniform distribution of feldspar and mafic minerals (mostly pyroxene). The andesite displays a trachytic texture in which a groundmass of fine plagioclase feldspar laths encloses those plagioclase phenocrysts. The rock generally consists of plagioclase, K-feldspar and mafic minerals which are dominated by hornblende (Fig. 3.10A and 3.10B).
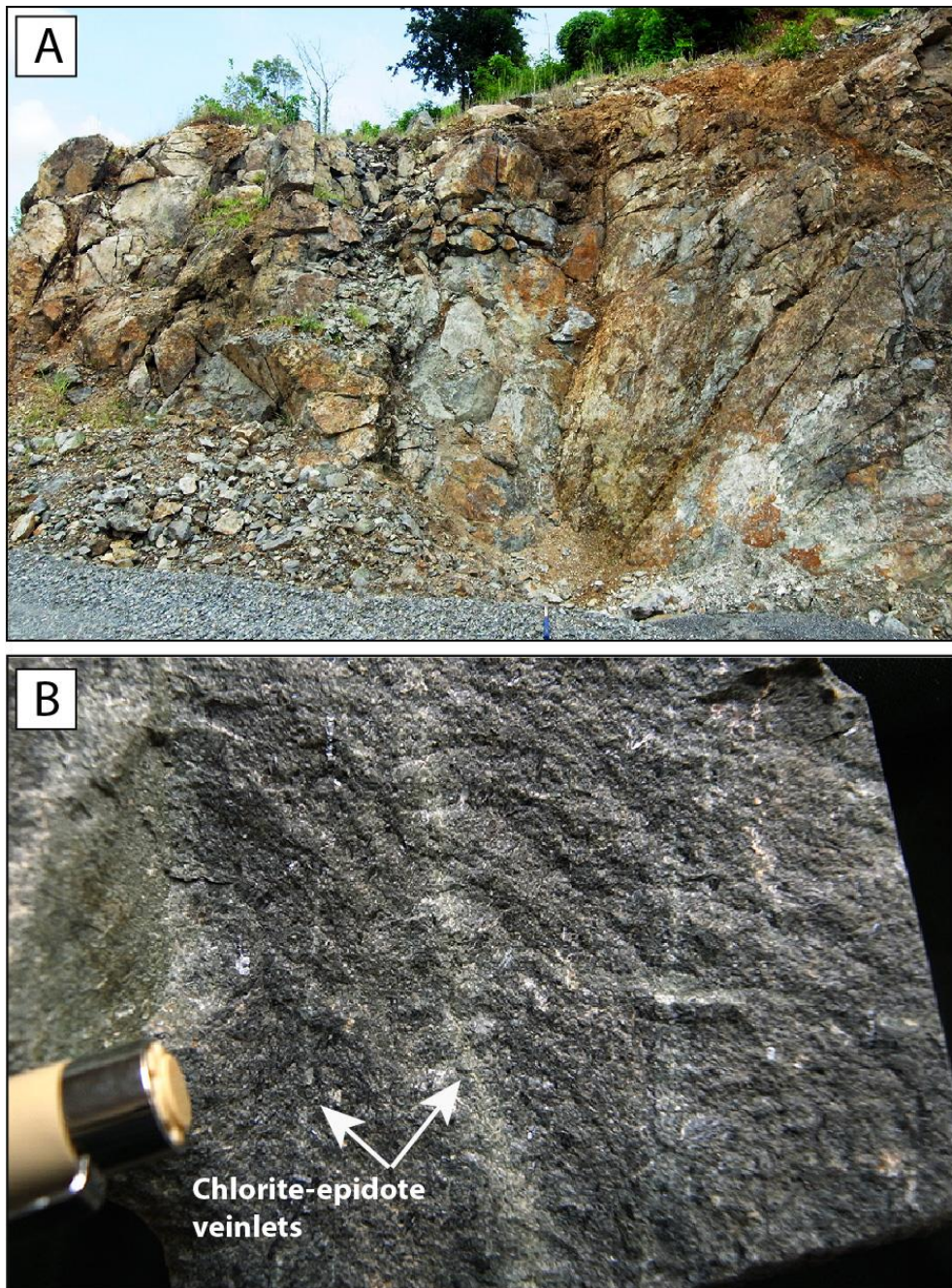
*Figure 3. 9* Basaltic andesite, **A**. Photograph of outcrop showing some faults, **B**. Hand specimen showing aphanitic texture with chlorite-epidote veinlets.
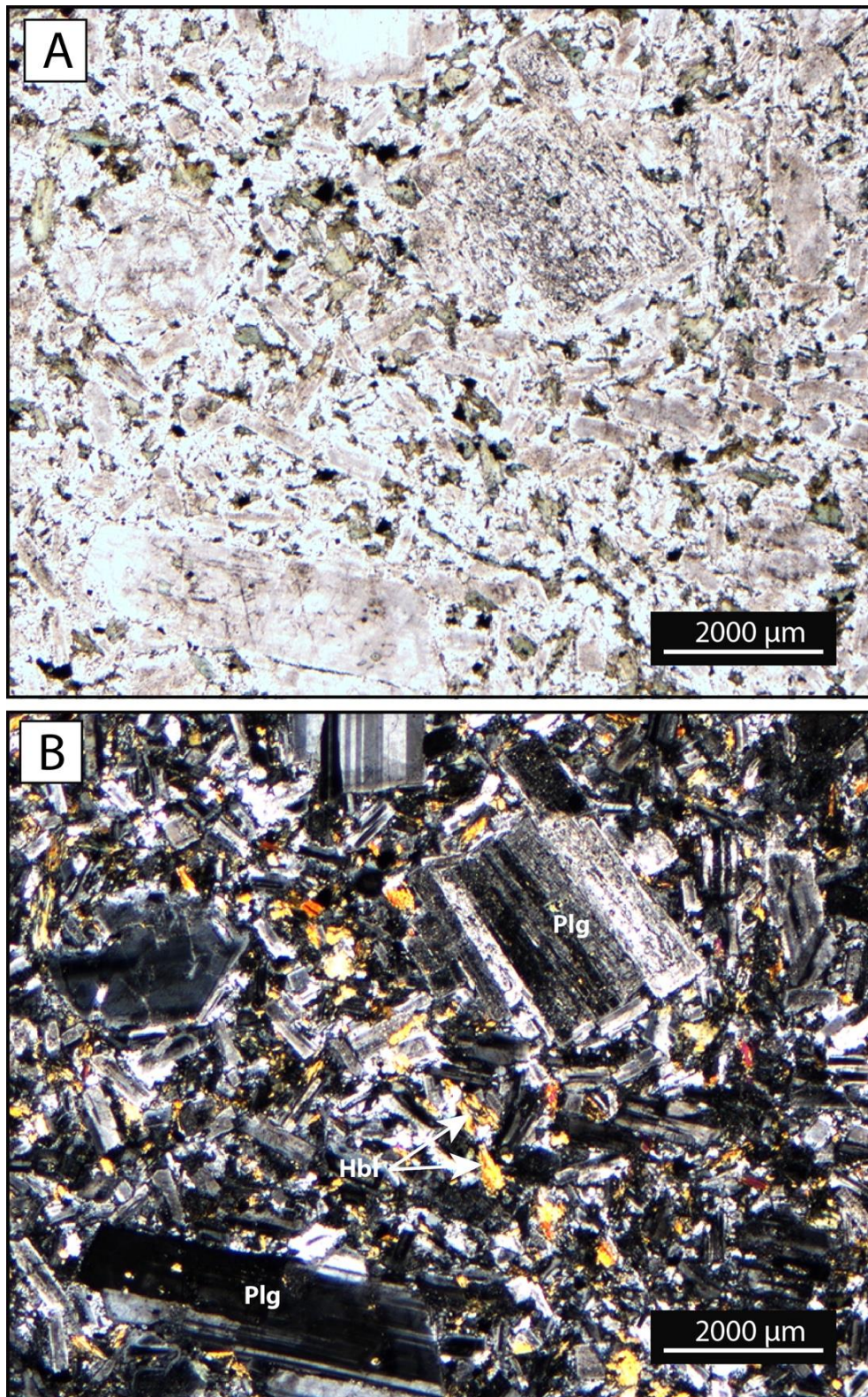
***Figure 3. 10*** Basaltic andesite, **A**. (ppl) and **B** (xpl) Photomicrograph showing feldspar (e.g., K-feldspar and plagioclase) and mafic mineral (mostly hornblende). Abbreviations; plg = Plagioclase, Hbl = Hornblende.

*Basaltic dyke*

In the mine area, basaltic dyke occurs at north wall (Figs. 3.2 and 3.11A) and is dark gray to black on fresh surface (Fig. 3.11B) with aphanitic texture. It is partly brecciated particularly at the foot of the pit wall (Fig. 3.11) and infilled with zeolite, a late stage and low temperature mineral. This basaltic dyke is about 7 to 10 meters wide, trending northwest to north-south with steep dipping to the northeast. This dyke has been cut by the main magnetite orebody as it is identified on the pit floor. However, the continuation of this dyke has not been identified on the hangingwall side. The major faults found at the southwest and northeast of the pit suggest that this fault is left lateral oblique movement. It is consistent with the presence of small block of basaltic rock at the northeast of the pit corner. It is likely that basaltic dyke has been displaced for 50 to 60 meters to the northeast. This dyke is also cross cut by quartz-amphibole-chlorite-sulfides veins or Stage 2 mineralization.

In the field, basaltic dyke is characterized by dark gray to black, aphanitic texture. It is locally brecciated particularly at the lower part of the body (near pit floor, Fig. 3.11B). The rock has been filled up by pale pinkish orange, low temperature late stage infilled fractures mineral known as laumontite or zeolite (see Chapter 4). It should be noted that there is no any skarn alteration developed within basaltic dyke and on volcanic wall rocks.
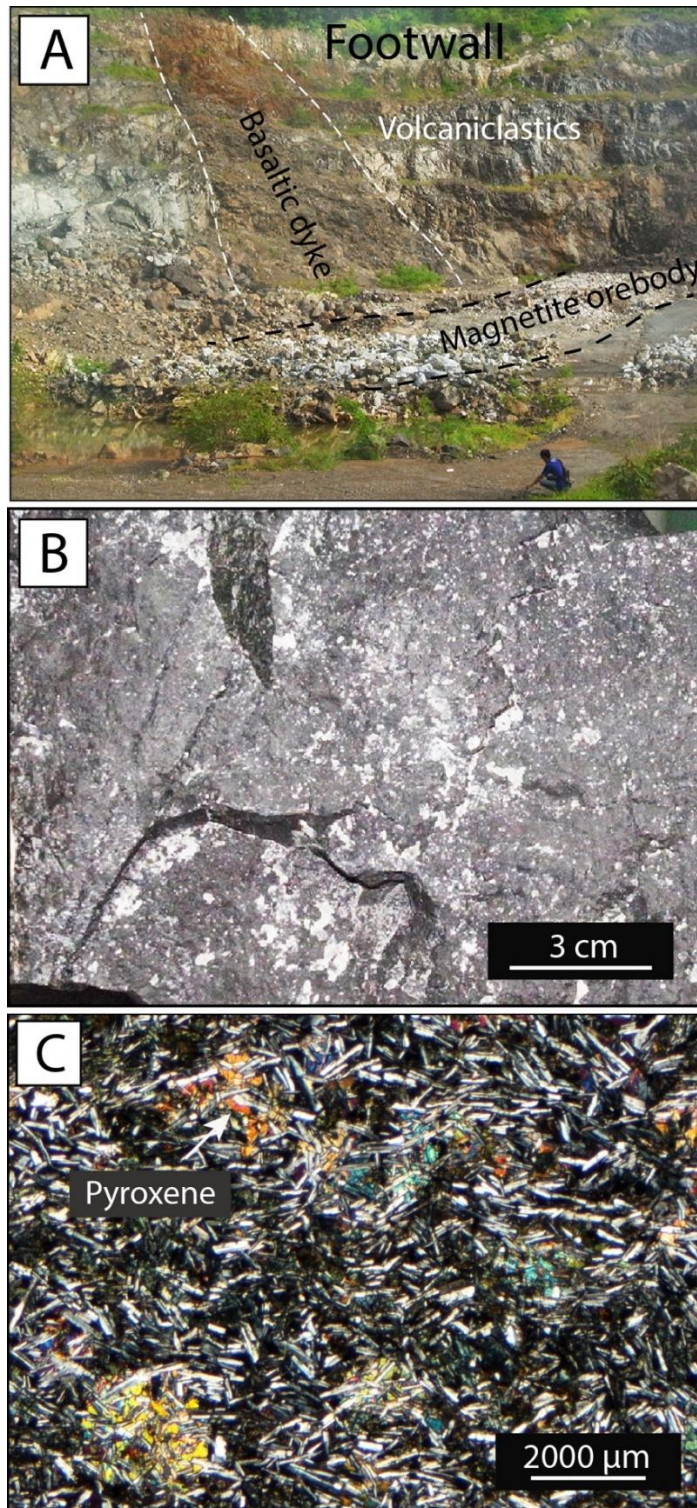
*Figure 3. 11* Basaltic dyke, **A**. Photograph of north wall showing basaltic dyke (center), **B**. Basaltic dyke showing aphanitic texture and **C**. Photomicrograph showing typical trachytic texture and patches of pyroxene (xpl).

### 3.2.3. Diorite and granodiorite Unit

Diorite and granodiorite unit exposes as a small discontinue exposures on low land area in northeast of Khao Lek hill throughout the area between Khao Lek and Khao Mae Kae (Fig 3.1) (Khositanont, 2008). This diorite has been dated by U-Pb zircon age technique and yielded age of $254 \pm 10$ Ma (Khositanont, 2008). It varies in composition from diorite to granodiorite, and locally gabbro. The rocks are dark gray to light gray in color and typically have a porphyritic texture.

Hand specimen of diorite is fine- to medium-grained and light gray in color. Its texture is slightly porphyritic with grains size ranging from 0.5 to 2 mm. Under microscope, the rock is characterized by short tabular crystals of plagioclase phenocrysts, floating in finer-grained groundmass components.

Mineralogically, diorite is composed mainly of plagioclase, hornblende and K-feldspar with some pyroxene (Fig. 3.12B and 3.12C). Quartz is present but in small amount. Accessory minerals include apatite and opaque minerals. While granodiorite contains more quartz and K-feldspar. Mineralogically, it consists of sparse plagioclase phenocrysts in fine- to medium-grained groundmass (Fig.3.1). Further detailed of diorite and granodiorite including its geochemistry are given by Wittayanonttawet (2017).

The contact between diorite and granodiorite with volcaniclastic rocks is not known. This is because the outcrop of diorite and granodiorite particularly in the area closes to the Khao Lek (mountainous area). Based on several outcrops of diorite and granodiorite exposed at east of Khao Lek, there are no pieces of evidence that o suggests the presence of skarn alteration (endo skarn) in Khao Lek diorite and granodiorite. It is evidenced that these intrusive rocks are responsible for contact metamorphism particularly marble and calc-silicate. It should be noted that this diorite is quite fresh and there are no pieces of evidence to suggest any skarn alteration.
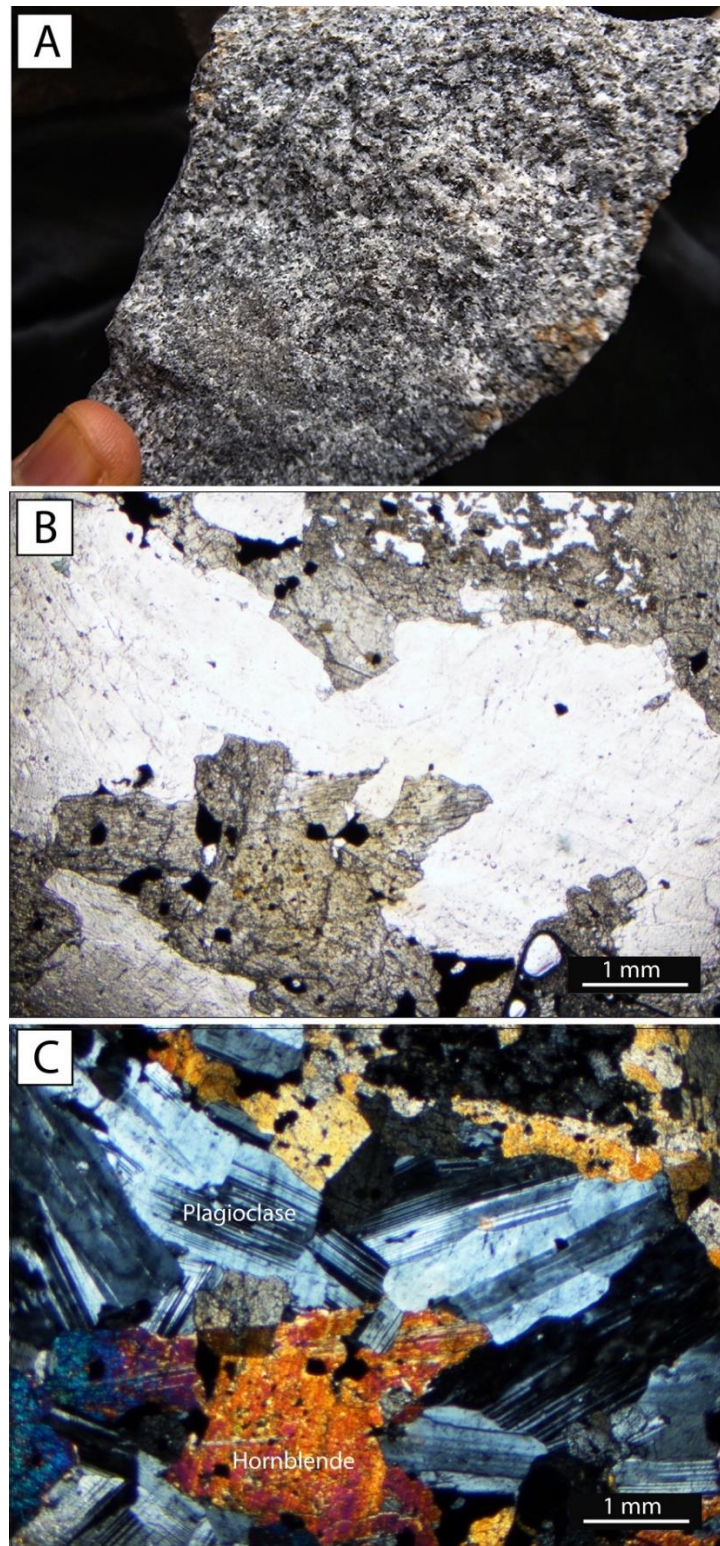
***Figure 3. 12* A** Diorite, **B**. (ppl) and **C**. (xpl) Photomicrograph showing medium-grained equigranular texture with major mineral assemblage including plagioclase and hornblende. Note that this rock has no affected from metamorphism or metasomatism.

### 3.2.4 Hornfelsic volcanic rock

Hornfelsic volcanic rock is mainly identified at southeast and southwest of the pit (Fig. 3.2) which can be observed on pit wall. The rock is grayish green in hand specimen and resemble to silicified volcanic rocks. They are locally cross cut by green epidote-chlorite ± calcite veinlets (see retrograde skarn).

Microscopically, these volcanic rocks are strongly altered in which feldspars are partly to completely altered. Characteristic minerals of this rock include quartz, and chlorite. Chlorite originally derived from volcanic rocks mainly basaltic andesite and basalt. It occurs at the southwest and southwest of the pit. It is locally cross cut by retrograde chlorite-epidote and calcite veins/veinlets. At southeast pit wall, it appears to have graded to prograde skarn alteration (Chapter 4). Based on field observation, occurrence of the hornfelsic volcanic rocks is confined to the southern part of the area.

### 3.3. Major structural features

The major faults in the mine area are represented by the ESE-WSW trending faulting with steep dipping about 70° to 80° (Figs. 3.2). Field evidences suggesting that this fault is reverse fault as indicated by lifting of the Permian limestone hangingwall (marble at present) to the current surface observed at eastern pit wall. This fault is reflected of major regional-scale faults in the region. Several smaller scale faults of similar orientation were also observed in the mine area particularly on both side of this major fault.

# Chapter 4
## Skarn Alteration and Iron Mineralization

### 4.1. Introduction

This chapter documents skarn alteration units of Khao Lek in which data were collected from an abundance open pit. Samples were limited to uncover pit floor and pit walls. Field geological observations and samples collection have been thoroughly undertaken to obtain best information and samples representing skarn alteration units. Petrographic description of these skarn units will be outlined below. Detailed skarn petrographic and iron mineralization will also be provided.

### 4.2. Skarn Alterations

Prior to mining, majority of the study area was probably covered by volcaniclastic (metavolcanics) unit. Small marble outcrops were observed on surface at the eastern part of the open pit. At present, the pit floor is estimated about 30 to 40 meters below the natural surface (Figs. 3.2, 3.3 and 3.5). Mapping of skarn alteration therefore mainly focus on the pit floor and lower level of pit wall as the rest of the area is inaccessible during this study. In addition, there is no diamond drill core available for deeper level study.

The prograde skarn has been observed both in limestone and volcanics protoliths. The lack of clarity of the intrusive body limits the study to exoskarn. However, narrow zones of skarn formation, containing narrow garnet, and garnet-pyroxene were found at the east and southeast of the pit (Figs. 3.2 and Section 4.2.3), where skarn has probably been developed in the intermediate intrusive bodies most likely diorite dyke. It should be noted that the intrusive rock is not clearly observed in the pit area. The obvious intrusive rocks (diorite and granodiorite) outcrops are about 1 kilometer to the north and east of the pit (see Chapter 3, Section 3.2.3). However, some samples collected from the main orebody is apparently magnetite replacing in coarse-grained intrusive rock. Some magnetite ore samples from the main orebody contain bands of garnet.

At Khao Lek, skarn occurs both in limestone and volcanic rocks and the main mineralization situated at the contact between limestone (hangingwall) and volcanic (footwall) protoliths. Small magnetite lenses also found in dyke skarn (see Section 4.2.3). Skarn is better developed in limestone in comparison to volcanic rocks and produced distinct types of skarn alteration for each type of protoliths. Details of their characters are described bellows.

### 4.2.1. Skarn in limestone protolith

Skarn in limestone has distinct alteration zones which could be mapped into at least four zones namely, 1) Garnet skarn zone, 2) Garnet-pyroxene zone, 3) Pyroxene-wollastonite zone and 4) Pyroxene zone (Fig. 3.2). Details of each skarn zone are described bellows.

### 4.2.1.1 Garnet skarn

The garnet skarn is best developed in limestone protolith which is parallel to the main orebody (Figs. 3.2 and 3.5). This zone occurs as lenticular shape about 4 to 10 meters wide. This zone contains predominantly of medium-grained to coarse-grained garnets in association with medium- to coarse-grained calcite with unevenly distributed of garnets particularly at the western side of the zone where medium- to coarse-grained garnet associated with calcite (Figs. 4.1A). However, fine-grained garnet about 1 mm in diameter is locally observed in garnet skarn zone. In general, garnet of this zone is euhedral and varying in color from dark brown (Fig. 4.1A) in the west to reddish brown or yellowish green in the eastern zone (Fig. 4.1B). However, the color of garnet as moving distal from magnetite orebody (possible intrusion) the color variation is less prominent.

Garnet skarn zone can be divided into three different varieties, namely 1) dark brown garnet with coarse-grained calcite (dominated in the western part of the zone), 2) reddish brown massive garnet ± pyroxene (dominated in the eastern part of the zone). Microscopically, the dark brown garnet that associated with medium- to coarse-grained calcite is often zoning. Zoning in this garnet is characterized by isotopic core and anisotropic rim (Figs. 4.2A and 4.2B). In general, garnet in this zone is identified as

spessartite-grossularite-andradite solid solution form (see Chapter 5). Coarse grained garnet is often fractured and commonly filled with carbonate mineral and/or partially altered to chlorite. Pyroxene constitutes in minor amount particularly toward the east of the zone.
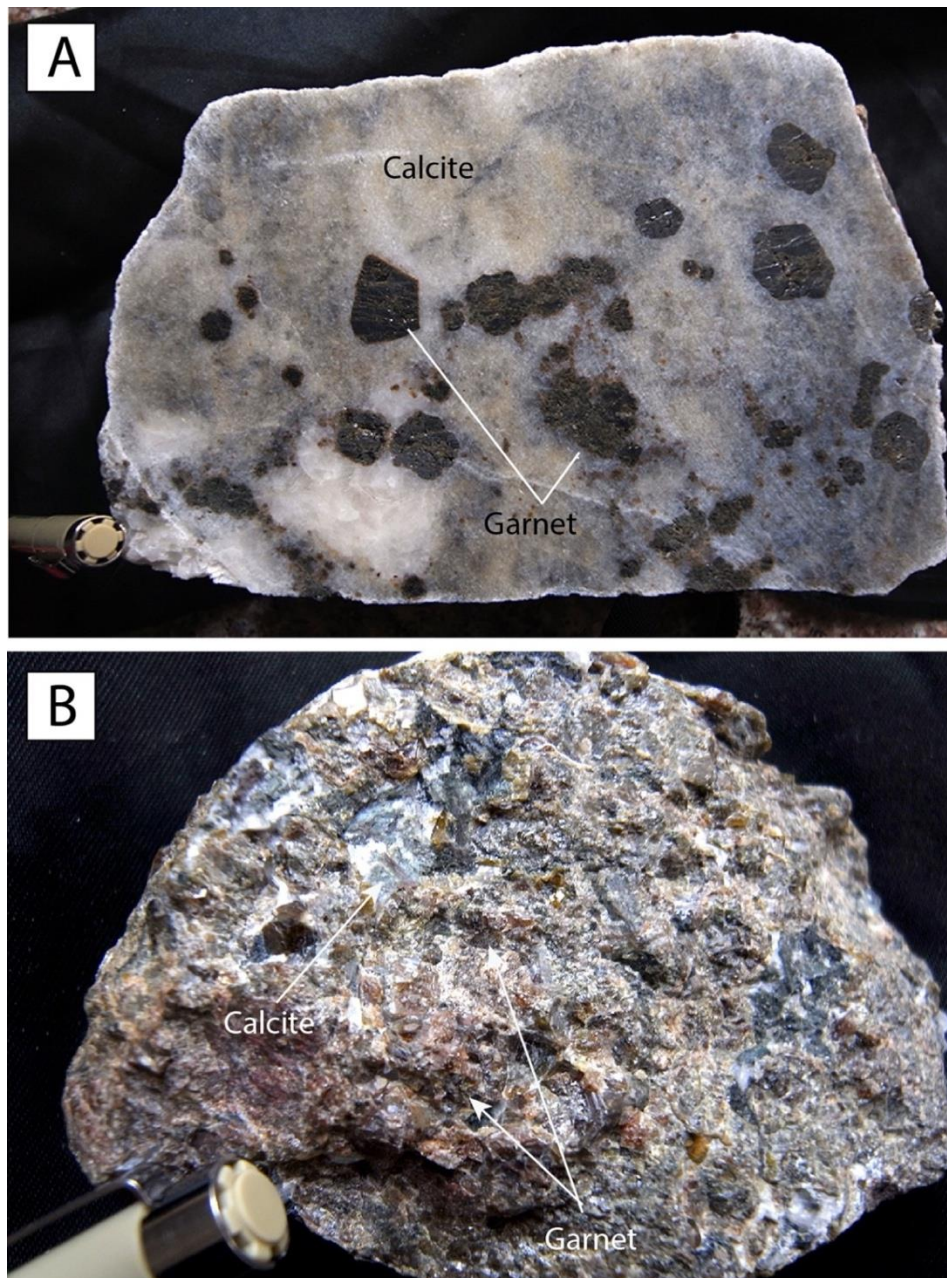


*Figure 4. 1* Photograph of hand specimen of garnet from the main garnet zone, **A**. Coarse-grained garnet associated with calcite from the western part, **B**. Medium- to coarse-grained reddish-brown garnet associated with calcite from the eastern part.
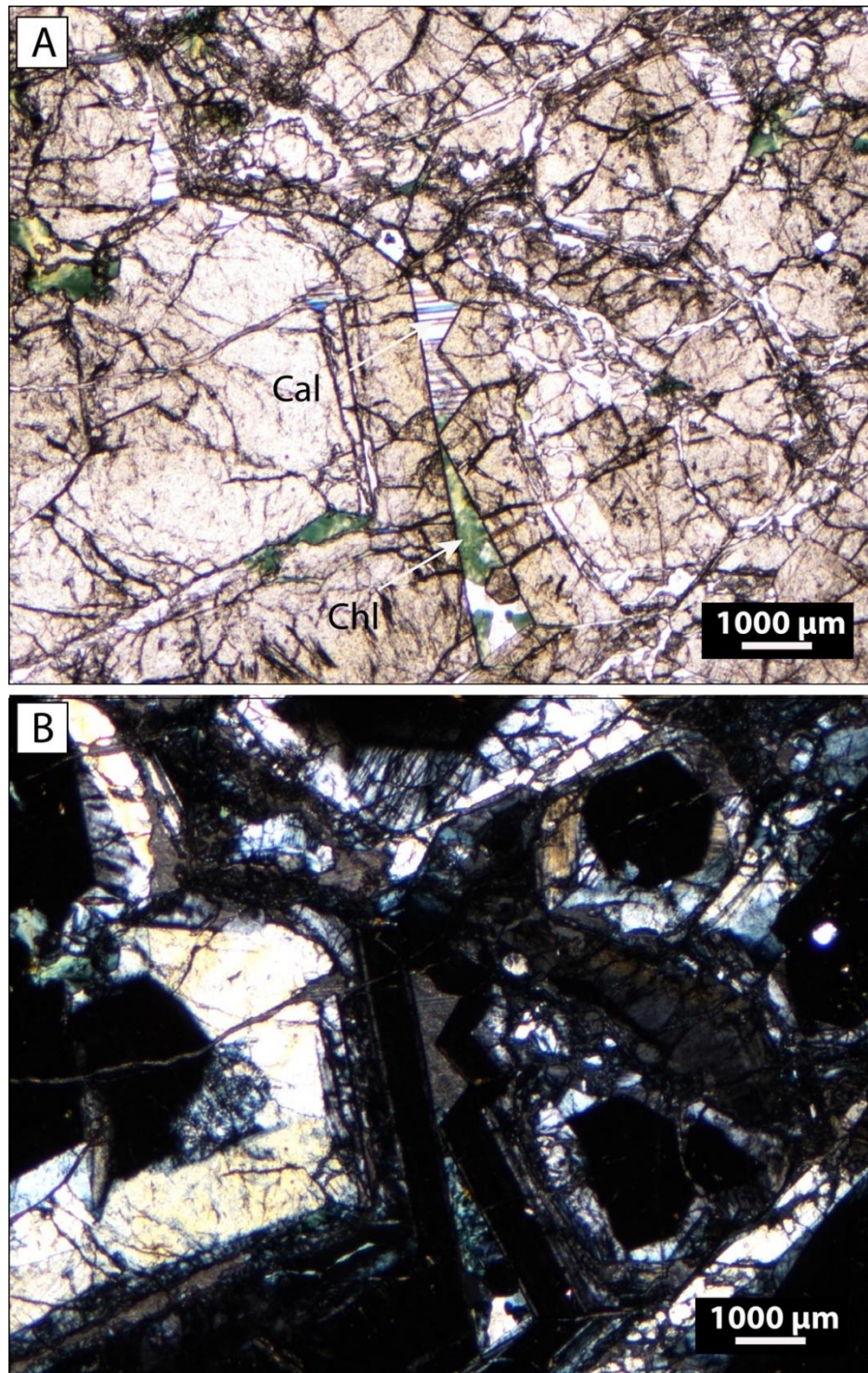
***Figure 4. 2*** Photomicrograph of garnet from main garnet skarn zone, **A**. (ppl) and **B.** (xpl) showing zonal in garnet illustrate isotropic (core) and anisotropic (rim), calcite and chlorite interstitially filled between garnet crystals and along fractures. Abbreviation: Cal = calcite, Chl = chlorite.

### 4.2.1.2. Garnet-pyroxene skarn

This zone occurs in the eastern part of the area (Fig. 3.2). It is exposed on pit floor and on the pit wall (Fig. 3.2, 3.3 and 4.3). This zone is about 10 to 20 meters wide and the length could further extend to the east into pit wall. It is bounded by fault with the volcanics containing pyroxene veinlet and patches. This skarn contains abundance of garnet which is varying in color from reddish brown to purple red in association with pyroxene (Fig. 4.4). Garnet in this zone is identified as andradite and spessartite-grossularite-andradite solid solution (see Chapter 5). Here, pyroxene is mainly clinopyroxene and minor orthopyroxene (Fig. 4.5). In some sample, small amount of wollastonite may also present particularly close to pyroxene-wollastonite zone. Some quartz present in these samples may have been replaced wollastonite. Small amount of calcite is interstitially associated with garnet. Pyroxene often altered to chlorite.



***Figure 4. 3*** Close from area in Fig. 3.3 showing garnet-pyroxene zone (brown), and a narrow zone of pyroxene-wollastonite close to marble (white). Photograph looking northeast.
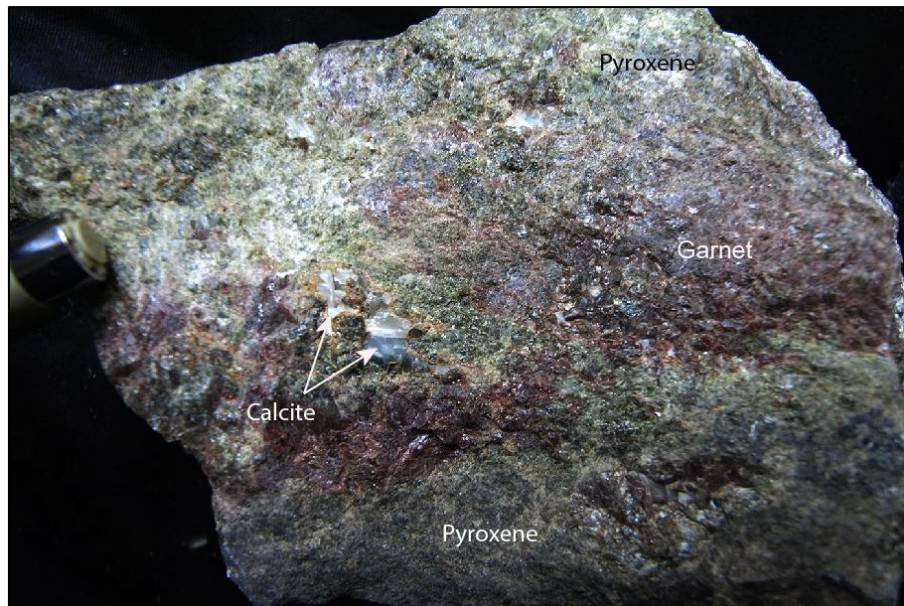
***Figure 4. 4*** Photograph of hand specimen of garnet-pyroxene zone showing purple red garnet, pyroxene (green) and calcite.
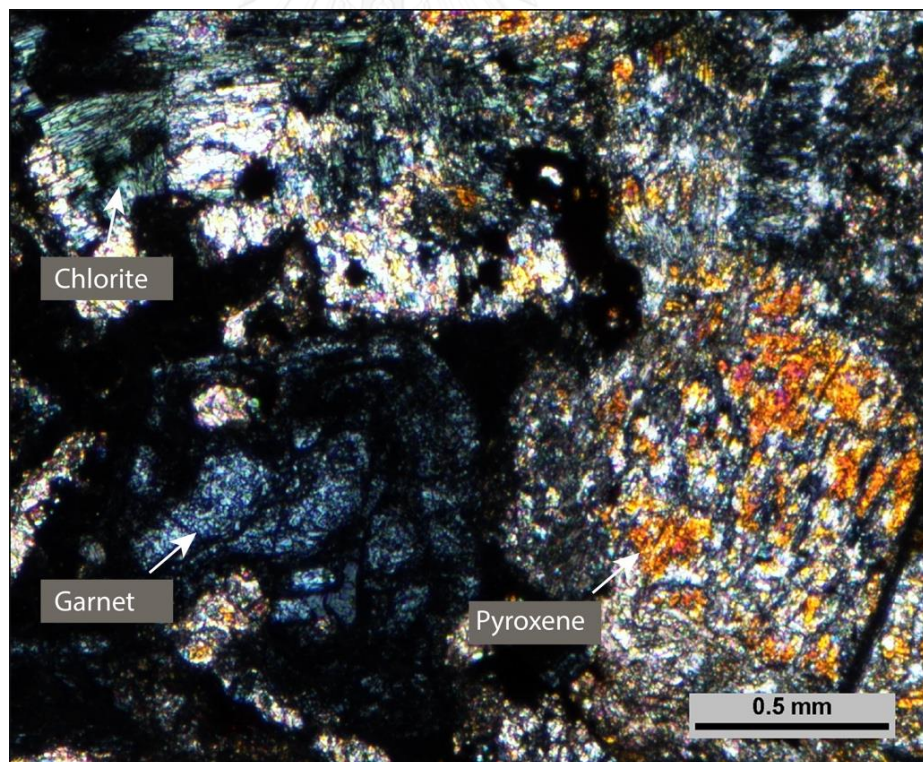


***Figure 4. 5*** Photomicrograph of garnet-pyroxene zone showing garnet and pyroxene that partly altered to chlorite (xpl).

### 4.2.1.3. Pyroxene-wollastonite skarn

Narrow zone of pyroxene-wollastonite has been mapped between the garnet-pyroxene zone and marble (Fig. 3.3). This zone is estimated about 2 to 3 meters wide (Fig. 3.2). In hand specimen, the rock is difficult to identify the present of wollastonite due to its fine-grained rather than forming as massive like others deposit.

Under microscope, wollastonite occurs as fine-grained ranging in size from 0.2 to 0.5 mm and closely associated with pyroxene (Fig. 4.6A and 4.6B). It is difficult to recognized particularly when quartz also present in the samples as some them may have been replaced by quartz.
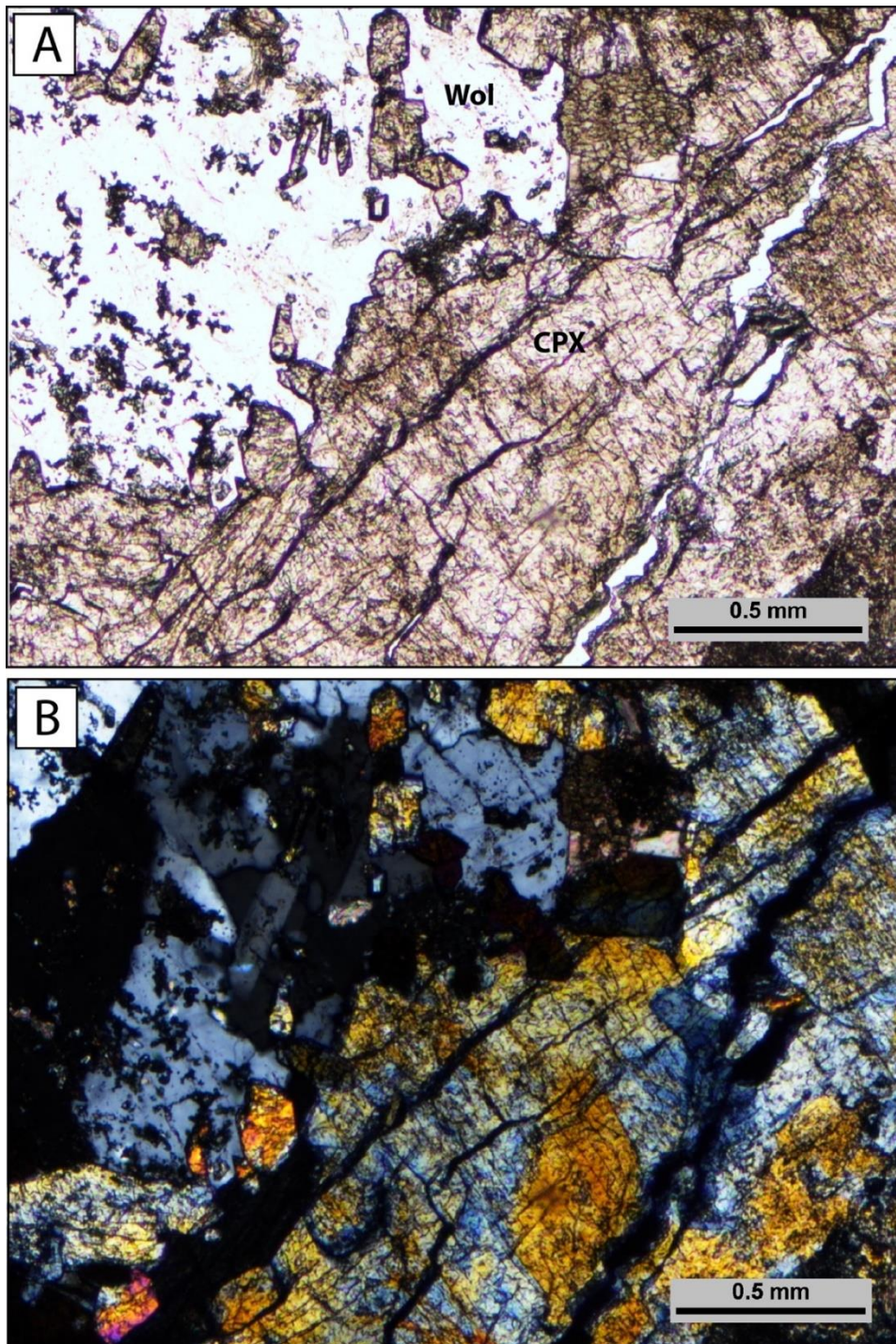
***Figure 4. 6*** Photomicrograph of pyroxene-wollastonite skarn, **A.** (ppl) and **B.** (xpl) Shows pyroxene (clinopyroxene) associated with wollastonite.

### 4.2.1.4. Pyroxene skarn

At Khao Lek, pyroxene skarn is less developed in limestone protolith in comparison to garnet skarn. Pyroxene tends to be formed better in volcanic rocks as pyroxene veinlets and infilled in vugs (see Section 4.2.2). However, narrow zone of pyroxene skarn has been mapped out between the garnet skarn and marble at center of the pit (Fig. 3.2). This zone is about few meters wide where it forms as small lenses hosted by marble. However, during field visit, part of the area that might be represent pyroxene zone was under covered by mining waste rocks. Therefore, the extension of skarn zone is not well understood.

### 4.2.2. Skarn in volcanics protolith

Garnet skarn has not been identified in basaltic andesite-basalt host sequence during this study. In volcanics host, pyroxene skarn is less pervasive but may quite extensive. It is confined to volcanics unit especially on the hangingwall of Khao Lek open pit. However, the extension of skarn alteration beyond the pit wall is not known due no thick vegetation. Here, pyroxene skarn occurs in two styles, 1) very narrow stripe at the contact with magnetite orebody on the footwall side, 2) pyroxene skarn veinlets and/or vugs. The first one occurs at the contact with magnetite orebody which is possible to have replace diorite intrusion.

### 4.2.2.1. Pyroxene skarn

As mentioned earlier that the pyroxene skarn is less obvious at the Khao Lek mine in comparison to garnet skarn. Pyroxene skarn in volcanic rocks is better observed from those samples collected from the footwall where volcanic rocks are close to the magnetite orebody (Fig. 3.5). The identification of pyroxene skarn should focus mainly on petrographic investigation due to skarn veinlets are too small to identify by naked eyes.

Based on petrographic investigation, it shown that pyroxene tends to occur as fine-grained replaces in volcanic rocks (Figs. 4.8 and 4.8B) and veinlet and/or infilled vugs (Figs. 4.8C and 4.8D). Those volcanics (e.g., basaltic andesitic tuff, andesitic breccia and basalt) located close to the garnet zone (or orebody) may developed narrow

pyroxene zones (Figs 4.7A and 4.7B). In some samples, larger pyroxene crystals (primary pyroxene) may have been replaced by pyroxene skarn.
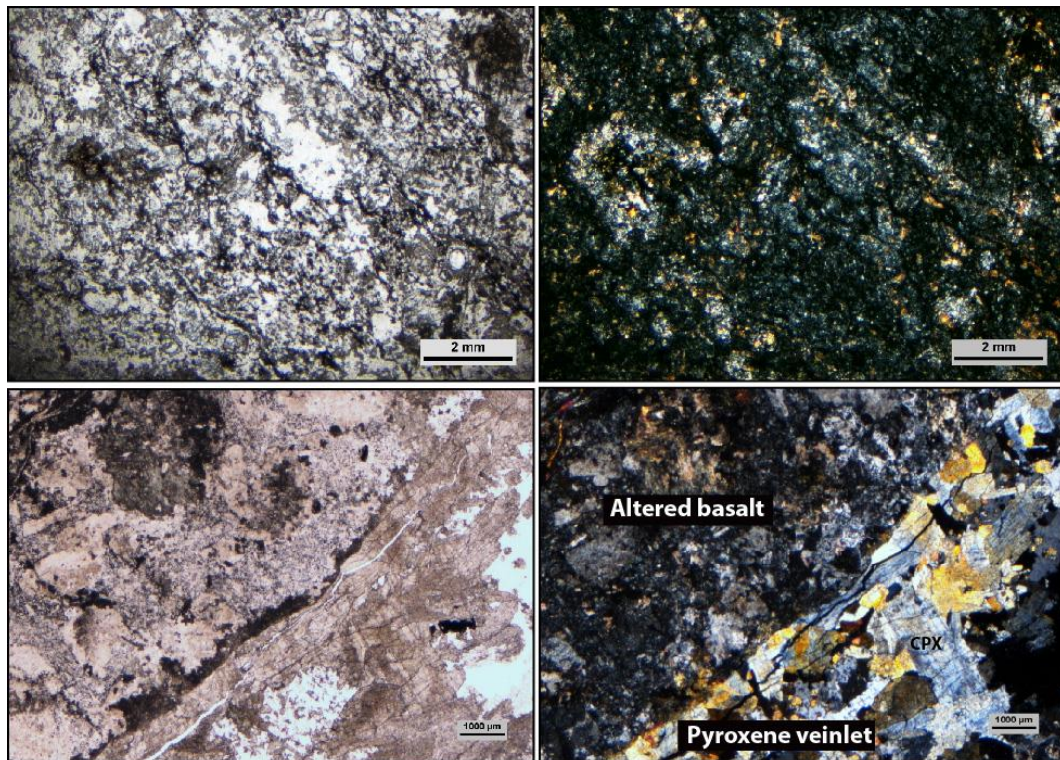


*Figure 4. 7* Photomicrograph of altered basaltic andesitic tuff and basalt, **A** and **B**. Pyroxene (yellow) disseminated in quartz-chlorite altered rock, **C** and **D**. Pyroxene (mainly clinopyroxene) veinlet cross cut basaltic andesite.

### 4.2.3. Dyke skarn

At Khao Lek, a distinctive endoskarn is identified as dyke skarn occurs at the center east of pit area (Figs. 3.2 and 4.8). This skarn is about 2 to 3 meter wide hosted in coarse-grained crystalline marble (or limestone protolith). Based on texture features of skarn and morphology, this skarn could have been confined to dyke and most likely is dioritic composition (Fig. 4.8). The contact between dyke skarn and marble is shape and there are no skarn minerals identified in coarse-grained marble wallrock. The extension of this dyke skarn is not known due it is under covered by mining waste rocks. This skarn is considered as endoskarn in which they are displayed distinctive zonation as indicated by garnet zone core (<1 meters wide), followed by garnet-pyroxene zone (<0.5 meter wide) and pyroxene-wollastonite zone (<0.5 meter wide, Fig. 4.8B). In

addition, magnetite lenses commonly associated with garnet zone (Fig. 4.9). It should be noted that this dyke skarn contains lenses of magnetite ore at the center and similar to that of major magnetite orebody. Wollastonite may forms as narrow zone next to pyroxene zone. Pyroxene skarn is well developed in this contaminated skarn (Fig. 4.10).
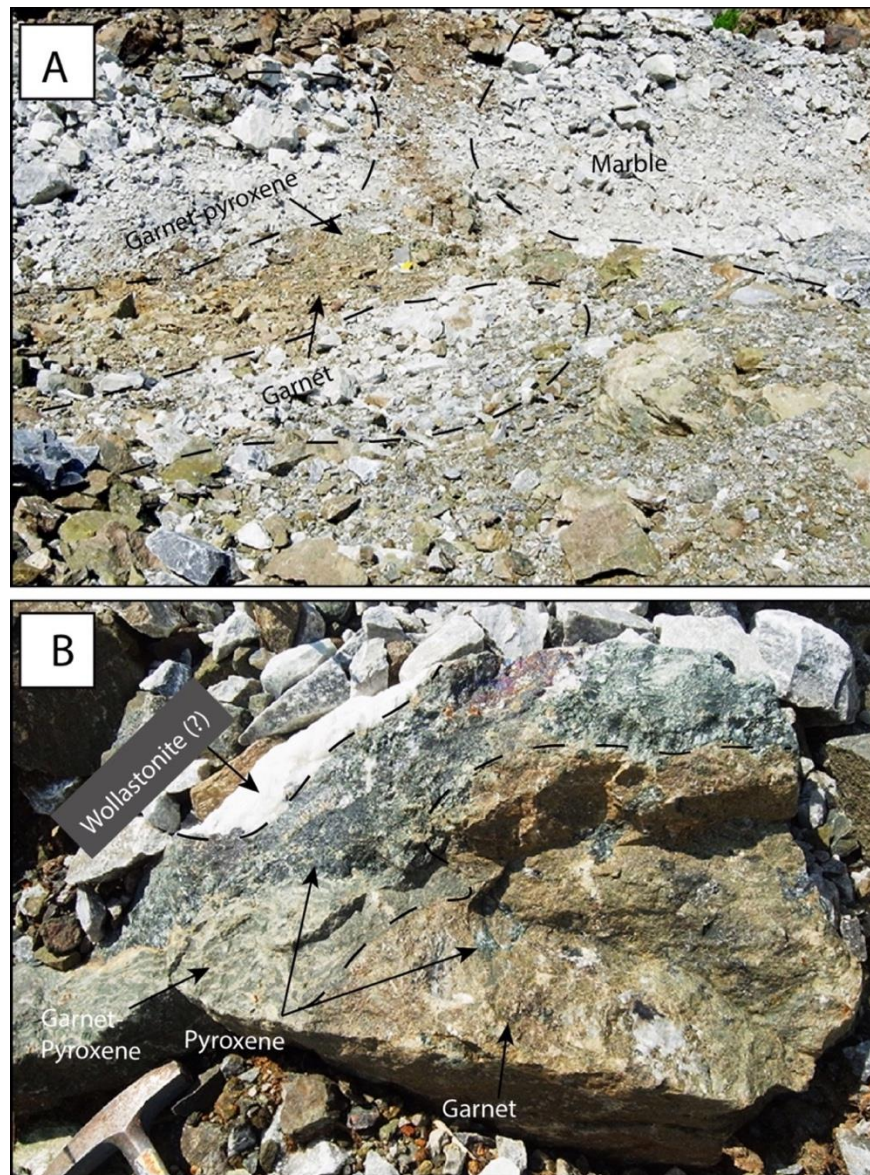


*Figure 4. 8* Photograph of dyke skarn, **A**. dyke skarn exposure on pit floor (brown) and marble (white), **B**. Large sample of dyke skarn showing garnet rich with some dark green pyroxene patches (brown, bottom right), pyroxene (dark green band, center), pyroxene-garnet (bottom left) and wollastonite (white). Location shown in Fig. 3.2.
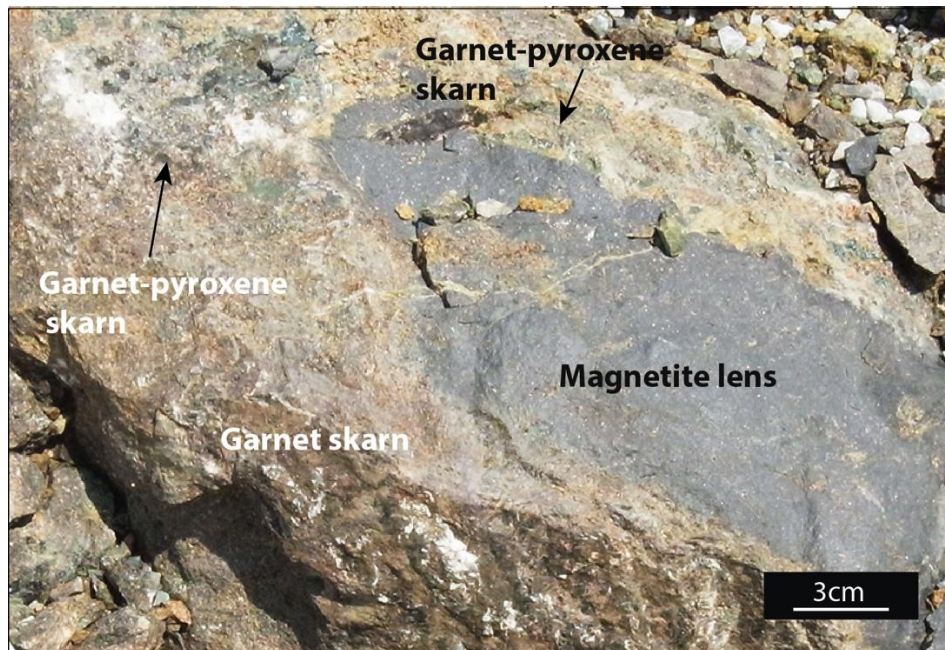
*Figure 4. 9* Photograph of dyke skarn showing magnetite (brownish gray), garnet, garnet-pyroxene (brown with green patches) and larger pyroxene patches (top left corner).



*Figure 4. 10* Photograph of dyke skarn showing green pyroxene skarn. Note that some magnetite patches present (top right).

## 4.3. Mineralization

Based on cross cutting relationships, mineral assemblages and textural features at least two mineralization has been identified namely, 1) Magnetite mineralization (or stage 1), and 2) Quartz-amphibole-chlorite-sulfides mineralization (or stage 2).

According to pit mapping, the iron mineralization is represented by massive magnetite orebody (stage 1 mineralization, Fig. 4.11A) occupying a major structure trending northeast-southwest to east-west (Figs. 3.2). At least, the orebody extends about 60 meters in length and 2 to 5 meters wide. The geometry of the orebody apparently widest at the center of the pit and narrow on both sides of body. However, due to there are no available drill hole at this mine, dipping and the vertical extension of the orebody could not have identified at this stage. Second ore zone is located the southeast of the pit where it is distinctive defined by brown to brownish green zone. Here, magnetite associated with brown garnet rich band (very narrow zone) followed by dark green to yellowish green zone and narrow zone of wollastonite (Fig. 4.9).

Massive magnetite orebody consists mainly magnetite (Fig. 4.11A) with small amounts of sulfides that form as patches or veinlets make up of pyrite and chalcopyrite. Under microscope, magnetite forms aggregate of fine-grained (Fig. 4.12A and 4.12B). In some samples, minor amount of pyrrhotite has been identified (Fig. 4.13). Based on textural relationships with magnetite and other sulfide minerals suggesting that pyrrhotite most likely forms same time as pyrite and chalcopyrite.

Quartz-amphibole-chlorite-sulfides stage occurs as small veinlets (<3 mm wide), is interpreted as second mineralization stage (or stage 2). Sulfide minerals of this stage are mainly pyrite and chalcopyrite (Fig. 4.14A) and major minerals are quartz and amphibole (mostly tremolite). It is accompanied by quartz-amphibole (tremolite)-chlorite alteration assemblage.
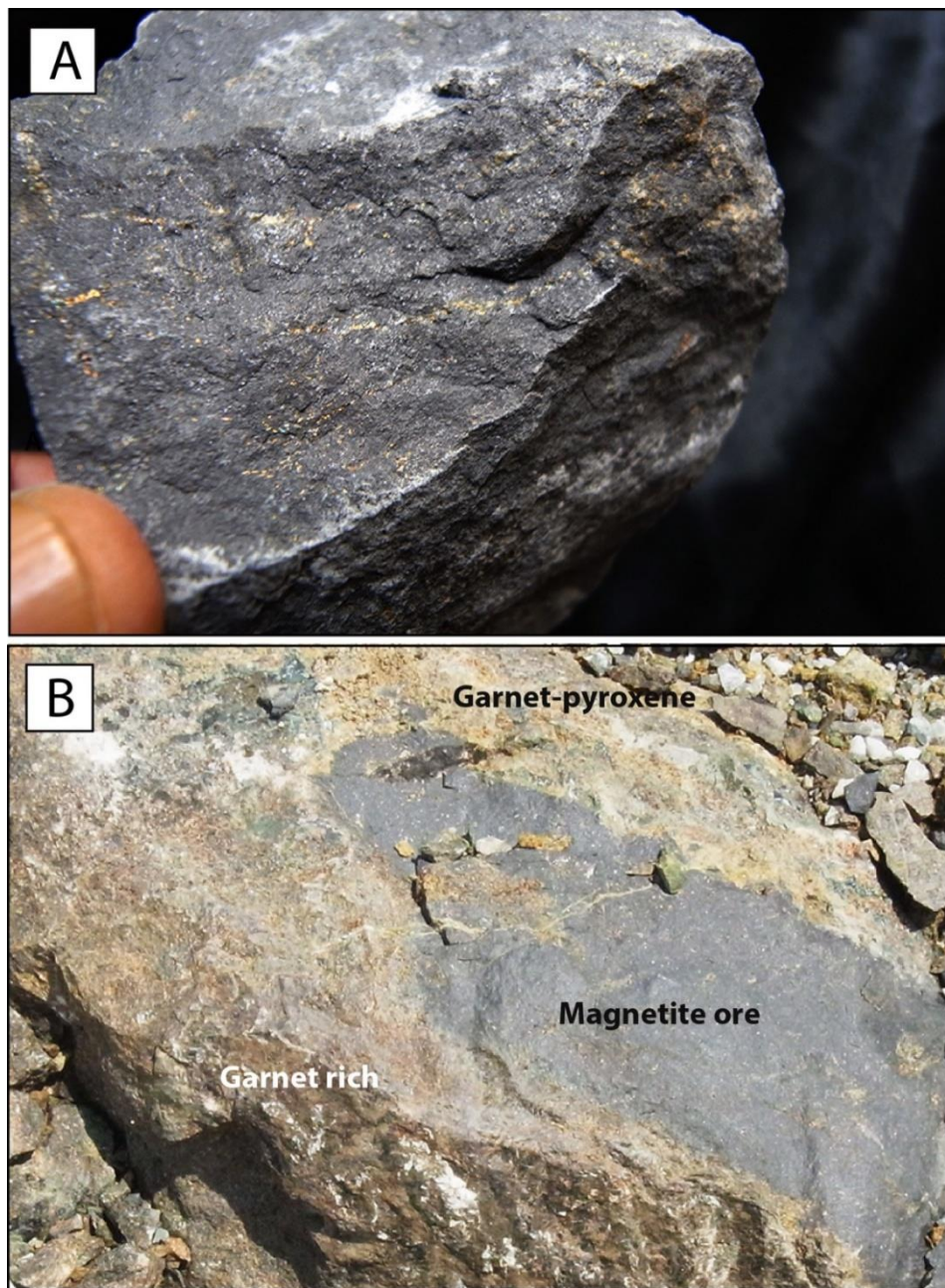
*Figure 4. 11* Photograph of massive magnetite, A. Magnetite from main orebody showing massive magnetite and small veinlets of quartz-amphibole-chlorite-sulfides, B. Magnetite (center) associated with skarns showing mostly magnetite.
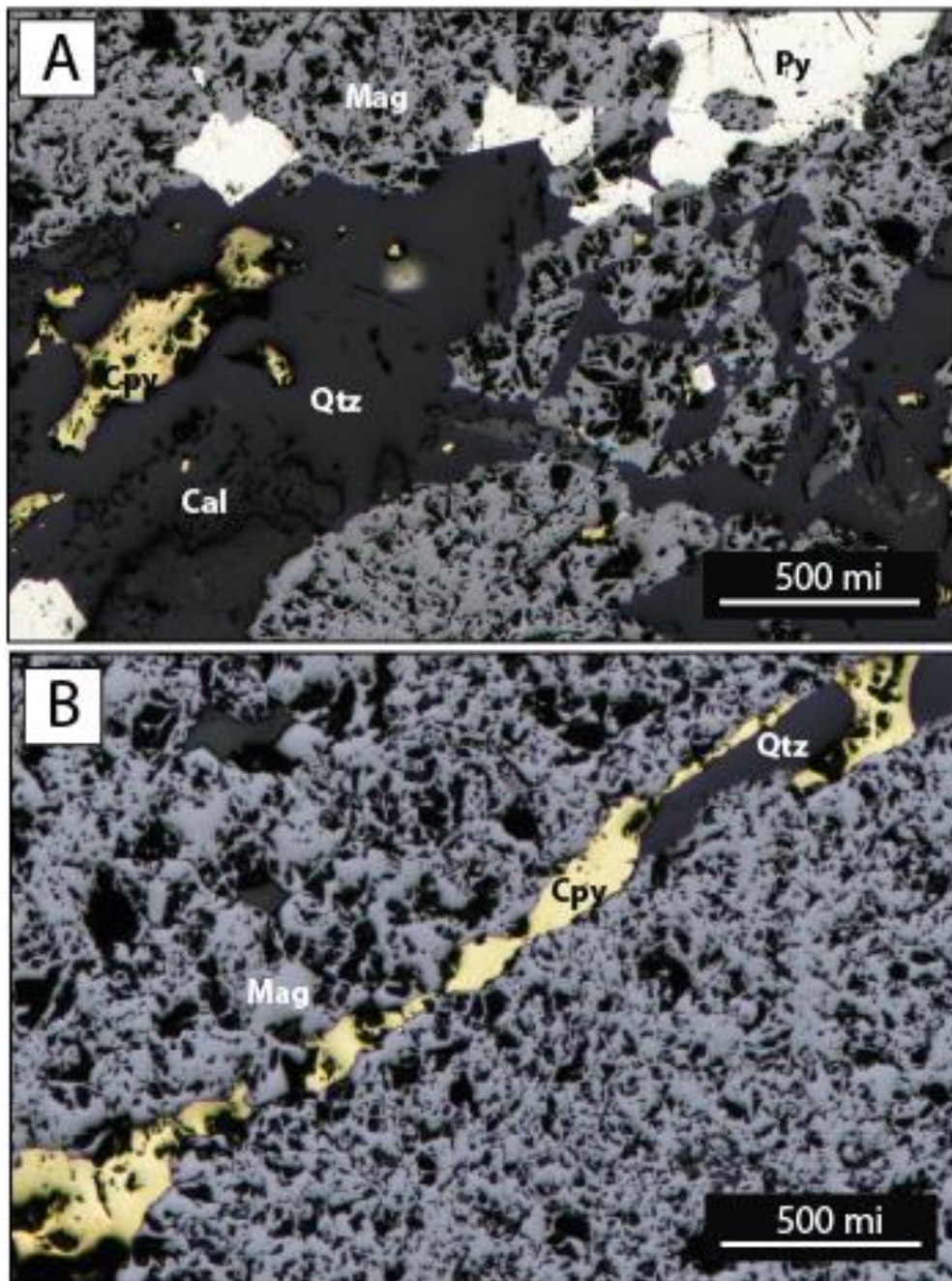
***Figure 4. 12*** Iron ore, **A**. Photomicrograph showing massive aggregate magnetite (Mag) and infilled vug compose of pyrite (Py), chalcopyrite (Cpy), quartz (Qtz) and calcite (Cal). **B**. Quartz- chalcopyrite veinlet cut through massive magnetite.
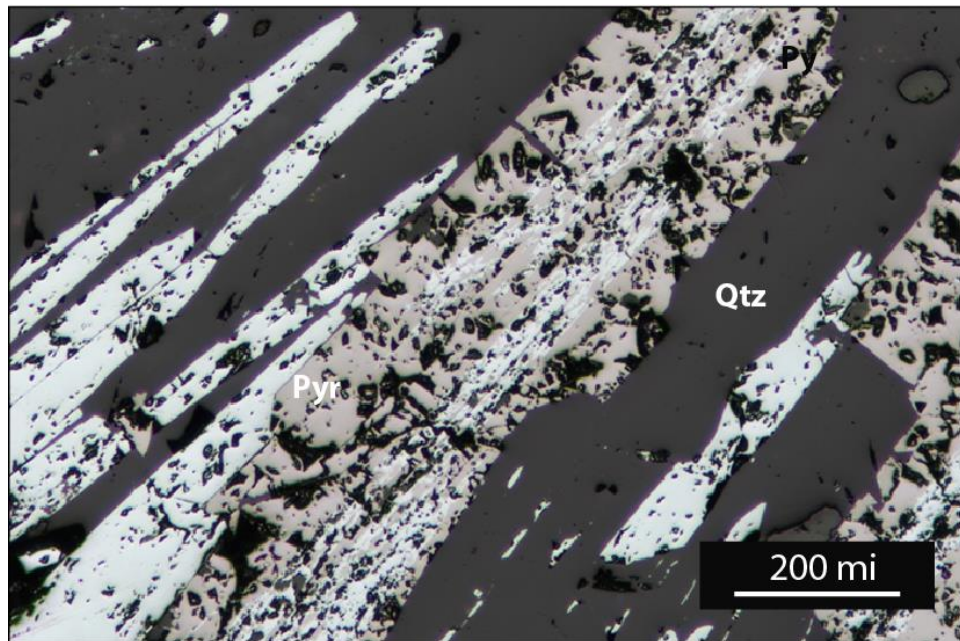
***Figure 4. 13***Photomicrograph of ore sample showing pyrrhotite (Pyr) and quartz (Qtz).

Quartz-amphibole-chlorite-sulfides mineralization (or stage 2) which occurs as veinlets (Fig. 4.14A), and are commonly cross cut the massive magnetite orebody (Figs. 4.12 and 4.13). This magnetite orebody is locally brecciated and filled up by veinlets of stage 2 assemblage (4.13A). Furthermore, pyrite and chalcopyrite whenever they occur in open space filling fracture they tend to associate with subhedral to euhedral quartz and calcite (Fig. 4.12A). This is suggesting that sulfide veinlets (Fig. 4.12B and 4.14A) were post-dated the magnetite formation or form toward late stage of magnetite mineralization. This quartz-amphibole-chlorite-sulfides veinlet is accompanied by strongly bleached in volcanic rocks (Fig. 4.14A). Amphibole minerals (e.g., tremolite and hornblende) are related to this quartz-amphibole-chlorite-sulfides veinlet (Figs. 4.14B to 4.15E). Biotites identified in some samples are likely to form during this mineralization stage (Fig. 4.15A and 4.15B).
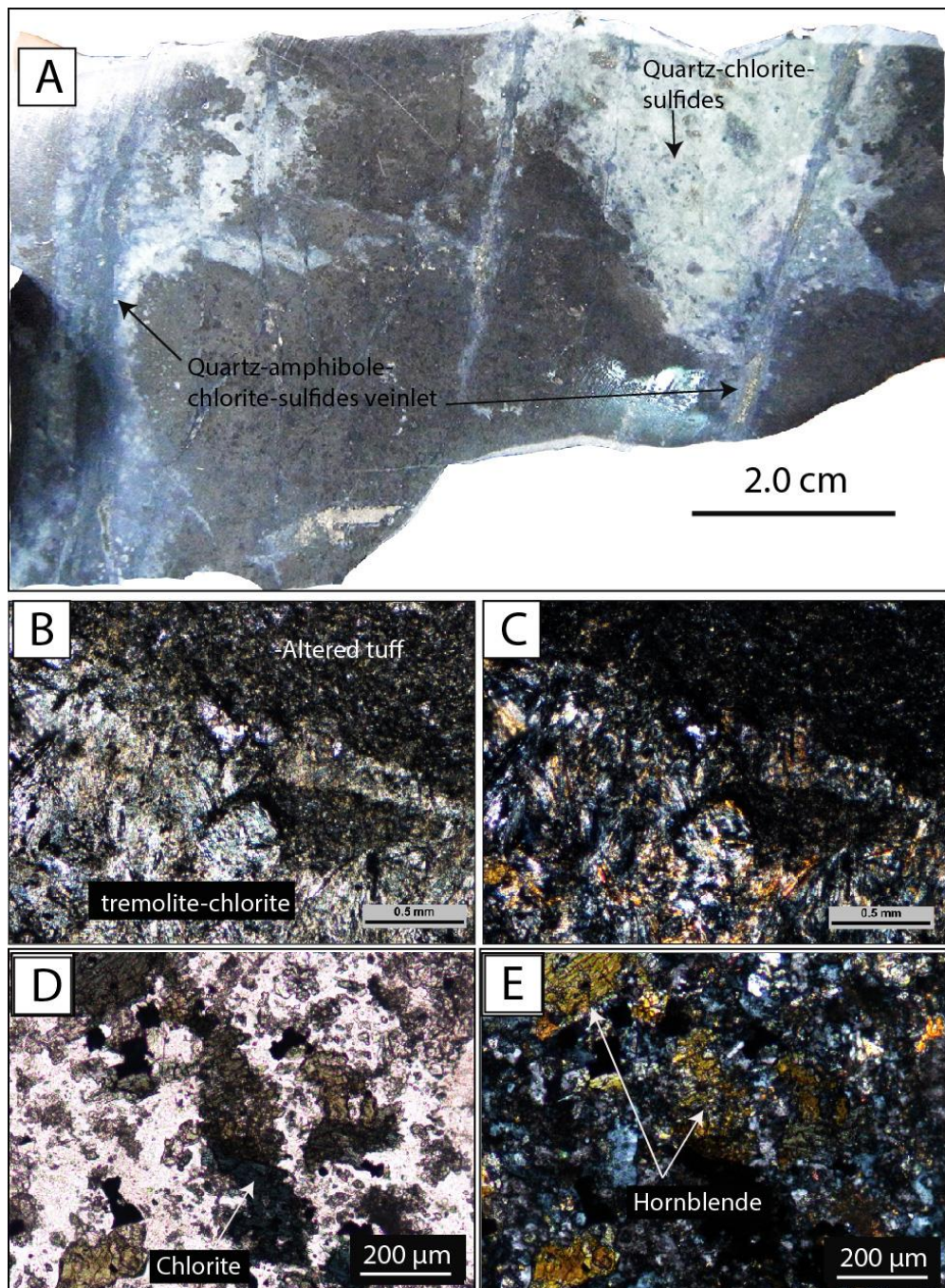
*Figure 4. 14*.Quartz-amphibole (tremolite)-chlorite-sulfides veinlet and associated alteration, **A**. Hand specimen showing pyrite in veinlets and quartz-amphibole-chlorite alteration, **B**. (ppl), **C**. (xpl) showing tremolite rich veinlet, **D**. (ppl) and **E**. (xpl) showing hornblende and chlorite.
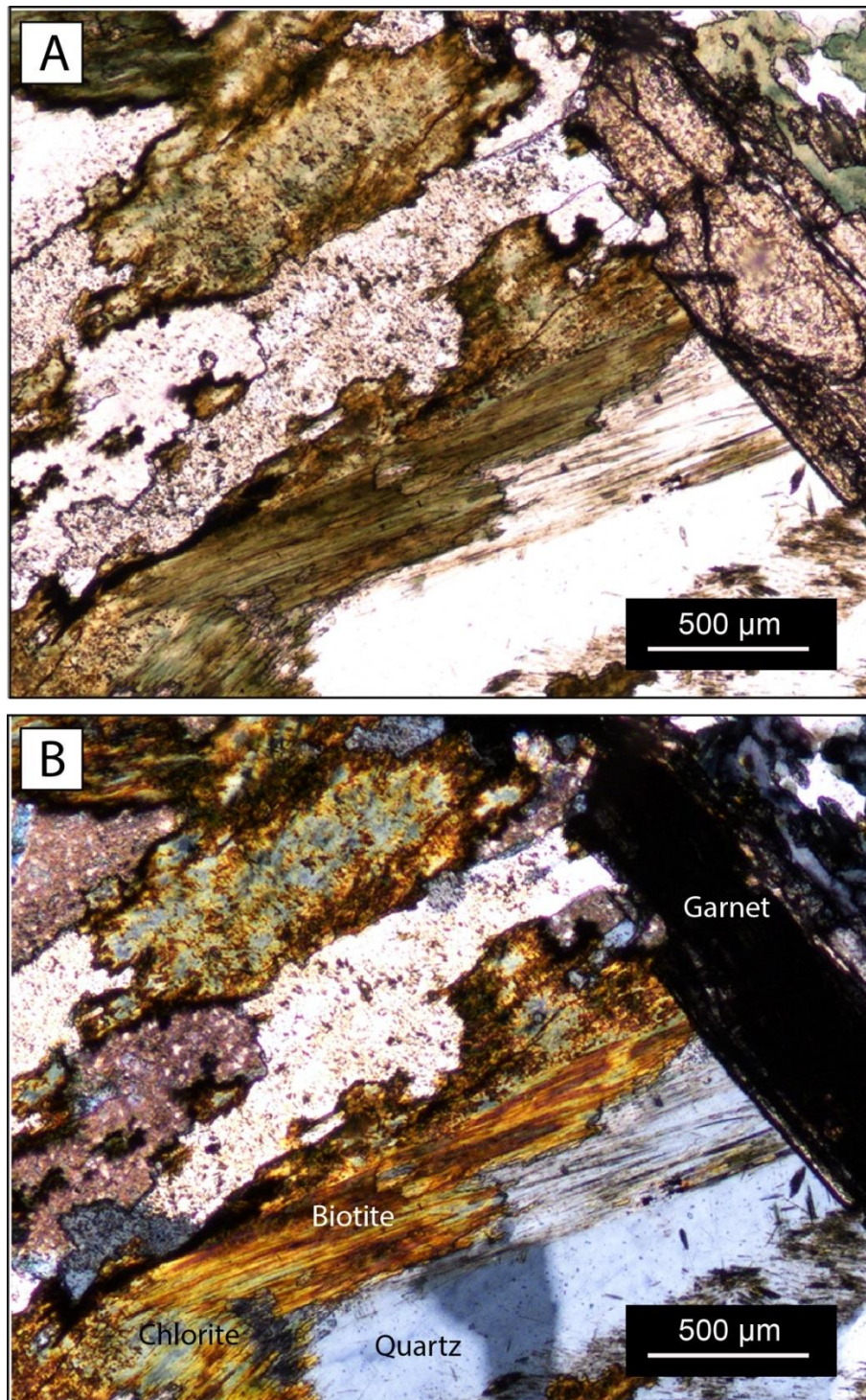
***Figure 4. 15*** Photomicrograph of garnet zone undergone lower temperature minerals showing secondary biotite and again altered to chlorite associated with garnet and quartz.

## 4.4. Retrograde Skarn

Quartz-amphibole-chlorite-sulfides veinlet (stage 2) associated alteration which is characterized by quartz-tremolite-hornblende ± biotite assemblage may include in retrograde skarn. However, as it is mineralized (or bearing ore minerals) veins/veinlets. Hence, it is preferred to describe in Section 4.3 (Mineralization Section). Retrograde skarn is particularly well developed around major fault especially on the hangingwall side (Fig. 3.2 and Fig. 4.16) at the southwestern part of the pit. Elsewhere, retrograde skarn is also identified including in pyroxene skarn veins/veinlets in basaltic andesite and/or basalt along the northern pit wall. However, the later one is less pervasive and unmappable. The retrograde skarn in the area mentioned above (Fig. 4.16) is clearly observed as it has a distinctive pinkish orange color in outcrop particularly on surface (Fig. 4.16). Here, volcaniclastic rocks contain pyroxene veinlets skarn were overprinted by epidote- chlorite ± calcite veinlets accompanied by strongly bleaching into light greenish gray to pale pink alteration (Figs. 4.16A and 4.16B). Chlorite and epidote are the most common retrograde skarn minerals at Khao Lek. In addition, calcite veinlets were also identified and often have similar orientation to epidote-chlorite ± calcite veinlets (Fig. 4.16A and 4.16B).
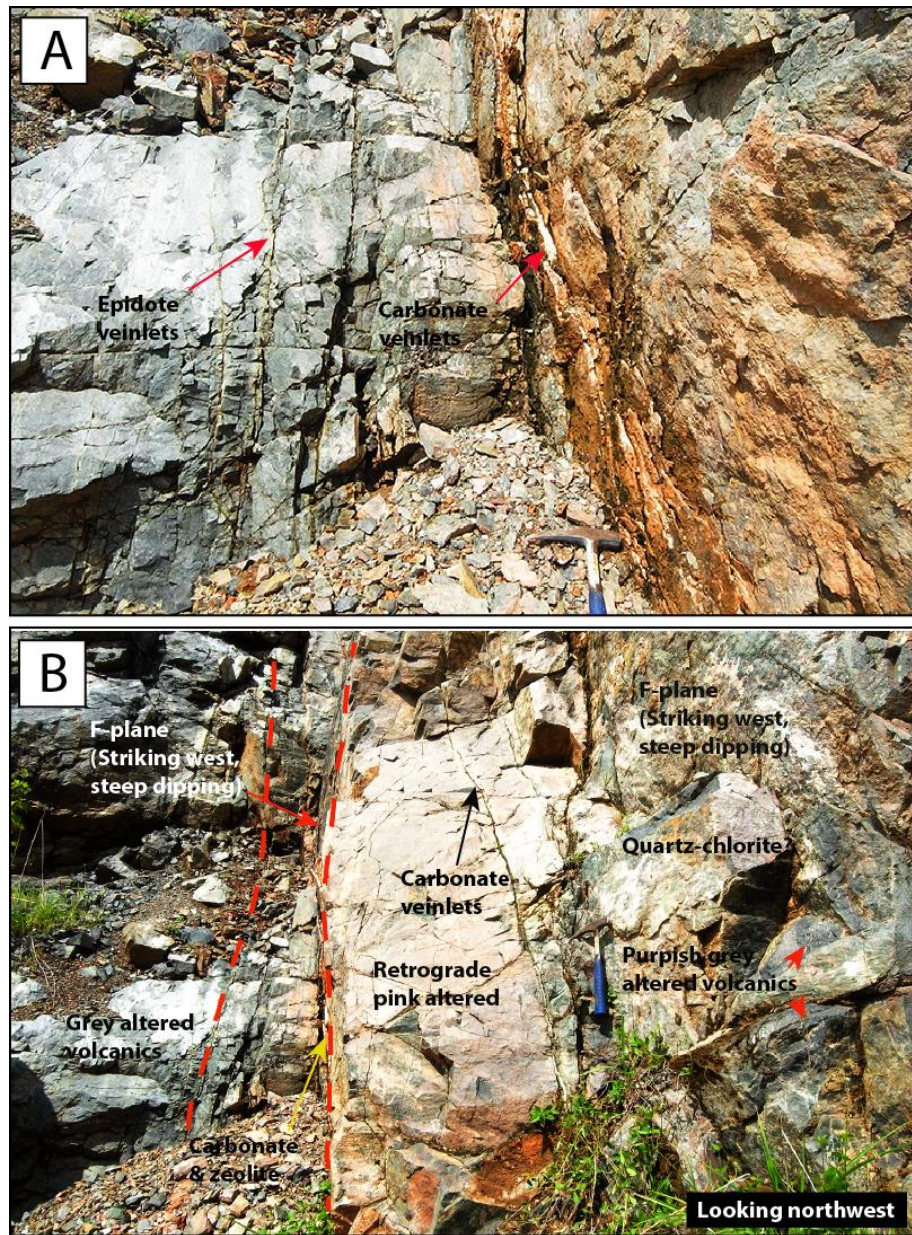
***Figure 4. 16*** Retrograde skarn, **A**. Photograph of volcanic rocks contain pyroxene skarn veinlets over printed by epidote-chlorite ± calcite veinlets and calcite veins/veinlets along major fault at southwestern part of the pit, B. Zooming of the area showing in Fig. 4.16A.

**Zeolite infilled breccia**

This low temperature infilled breccia, is probably the late which infilled or cementing brecciated basaltic dyke (Figs. 4.17A and 4.17B). Basaltic dyke might have been broken due to reactivation of the older fault that accommodated basalt then cementing by zeolite similar to identified at Chatree deposit (Salam, 2013).
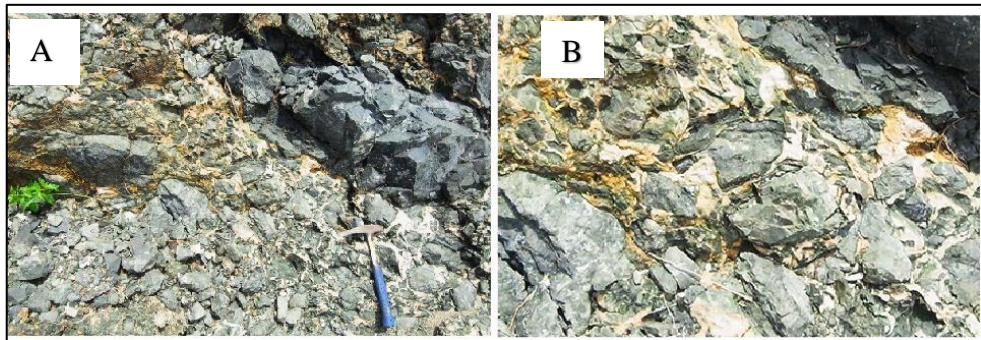


*Figure 4. 17* Photograph of basaltic dyke, Brecciated basalt at the foot of the northern pit wall. Noted that dark gray unbroken basalt portion (top right, left), Close-up part of Fig. 4.17A shows zeolite infilled breccia matrix (right).

# Chapter 5
# Mineral Chemistry

5.1. Introduction

This chapter is dealing with Electron Microprobe Analysis (EPMA) mainly undertaken on garnet and pyroxene in rock samples collected from Khao Lek mine (Fig. 3.2).

All sample preparations including thin sections, polished-thin sections, and polished sections were carried out at Department of Geology, Faculty of Science, Chulalongkorn University.

An advanced nondestructive analytical method, electron probe microanalyzer "EPMA" was performed with the JOEL model JXA 8100 base at the Geology Department. Calibration with pure oxides and mineral standards is taken place prior to analysis running under 15kV accelerating voltage with about $2.50 \ 10^{-8}$ A probe current with less than 1 micrometer of beam spot. Chemical compositions of the analyzed mineral samples are automatically undertaken ZAF correction and subsequently reported as oxides.

EPMA analysis technique may be used for various purposes; however, the following lists are concerned under this study.

- Accurate identification of opaque minerals and small or rare mineral grains can be applied from EPMA analyses.

- Petrographic description of rock samples may be improved as a result of accurate mineral identification leading to more proper rock classification.

- Geothermobarometry may be carried using appropriate coexisting mineral phases analyzed by  EPMA.

- Moreover, X-ray mapping technique can be applied to study zoned minerals and different phases occurred in the rock sample.

5.2. Results of EPMA analysis

5.2.1. Garnet

Garnets constitute a group of calc-silicate minerals, they occur mainly in the metamorphic rocks but they may be found in some igneous and sedimentary rocks. Garnet can be subdivided into the following end member:

- Pyrope (PYR): $Mg_3Al_2Si_3O_{12}$

- Almandine (ALM): $Fe_3^{2+}Al_2Si_3O_{12}$

- Spessartine (SPS): $Mn_3Al_2Si_3O_{12}$

- Grossular (GRO): $Ca_3Al_2Si_3O_{12}$

- Andradite (AND): $Ca_3 (Fe_3^{2+} + Ti)_2Si_3O_{12}$

- Uvarovite (UVA): $Ca_3Cr_2Si_3O_{12}$

- Hydrogrossular (HYD): $Ca_3Al_2Si_2O_8(SiO_4)_{1-m}(OH)_{4m}$

In this study, the formula of $(SPS,GRO)_xAND_y$ is uses to define composition of the analyzed garnets. Table 1a displays composition of analyzed garnet and its compositions are given below:

$$0.01 < (SPS,GRO) < 0.42 \quad and \quad 0.62 < AND < 1.00$$

The garnet from Khao Lek has compositions from spessartite-grossularite-andradite series to pure andradite (Table 1). This change is based on the exchange between $Al^{3+}$ and $Fe^{3+}$ in garnet structure and it play an important role related to their occurrence. Garnet collected from the area 2 and 6 from garnet-pyroxene skarn (Fig. 3.2) represent this series; Fe3+ and Al are occurred together (Table 1), however specimen which have more Al happened with a light yellowish, greenish color. In other hand, garnet taken from the area 4 near the ore body Fe3+ rich, is deep reddish brown to deep red and has high amount of Fe3+ and has zero Al (Table.1).

Formation of andradite (AND) at this stage is related to the injection of $Fe_2O_3$ from volcanic and intrusive protoliths and $SiO_2$ from the intrusive body into the impure

calcareous (Cc), limestone. This reaction occurs during the thermal and particularly the metasomatic skarn deposit formation.

$$3CaCO_3 \text{ (Cc)} + Fe_2O_3 + SiO_2 = CaFe_2Si_3O_{12} \text{ (And)} + 3CO_2$$
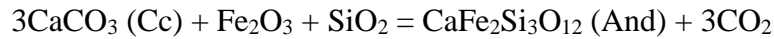
The results may suggest that the garnet from areas 2 and 6 in garnet-pyroxene skarn zone have similar composition which are classified spessartite-grossularite-andradite whereas garnet from area 4 and some grains from area 5 have andradite composition. This probably due to increasing of distance from intrusive sources but similar protolith type.

*Table 1. 1* EPMA results for garnet from areas 2, 4, 5, and 6.

| Sample ref. | 2 | 6_1 | 6_2 | 6_4 | 6_3 | 5 | 4_c1_f1 | 4_c1_f8 | 4_c1_f13 |
|---|---|---|---|---|---|---|---|---|---|
| $SiO_2$ | 36.904 | 36.645 | 36.422 | 35.887 | 35.488 | 34.743 | 34.408 | 34.397 | 34.333 |
| $Al_2O_3$ | 5.241 | 8.859 | 4.106 | 7.571 | 0.000 | 1.344 | 0.014 | 0.000 | 0.000 |
| $TiO_2$ | 0.015 | 0.017 | 0.015 | 0.012 | 0.007 | 0.000 | 0.000 | 0.013 | 0.014 |
| $Cr_2O_3$ | 0.008 | 0.014 | 0.000 | 0.012 | 0.012 | 0.006 | 0.012 | 0.000 | 0.031 |
| $Fe_2O_3$ | 0.000 | 0.000 | 0.000 | 0.000 | 0.000 | 0.000 | 0.000 | 0.000 | 0.000 |
| $FeO_{tot}$ | 22.787 | 18.311 | 24.631 | 19.820 | 29.354 | 27.702 | 30.613 | 30.351 | 30.524 |
| MnO | 0.797 | 1.010 | 0.724 | 1.026 | 0.424 | 0.372 | 0.726 | 0.687 | 0.540 |
| MgO | 0.030 | 0.036 | 0.024 | 0.021 | 0.056 | 0.008 | 0.008 | 0.049 | 0.013 |
| NiO | 0.005 | 0.013 | 0.000 | 0.033 | 0.000 | 0.018 | 0.000 | 0.006 | 0.001 |
| BaO | 0.023 | 0.010 | 0.001 | 0.014 | 0.019 | 0.022 | 0.012 | 0.050 | 0.000 |
| CaO | 34.205 | 34.295 | 33.864 | 34.278 | 33.689 | 33.802 | 33.224 | 33.399 | 33.280 |
| $Na_2O$ | 0.017 | 0.022 | 0.021 | 0.026 | 0.008 | 0.032 | 0.015 | 0.000 | 0.023 |
| $K_2O$ | 0.005 | 0.006 | 0.003 | 0.003 | 0.004 | 0.001 | 0.000 | 0.000 | 0.000 |
| **Total:** | 100.038 | 99.237 | 99.811 | 98.703 | 99.061 | 98.047 | 99.032 | 98.952 | 98.759 |
| Formula recalculated with 12 oxygenes, after Drop, 1987. | | | | | | | | | |
| Si | 2.965 | 2.927 | 2.948 | 2.896 | 2.938 | 2.891 | 2.858 | 2.859 | 2.859 |
| Al | 0.035 | 0.073 | 0.052 | 0.104 | 0.000 | 0.109 | 0.001 | 0.000 | 0.000 |
| Al | 0.461 | 0.762 | 0.339 | 0.617 | 0.000 | 0.023 | 0.000 | 0.000 | 0.000 |
| Ti | 0.001 | 0.001 | 0.001 | 0.001 | 0.000 | 0.000 | 0.000 | 0.001 | 0.001 |
| Cr | 0.001 | 0.001 | 0.000 | 0.001 | 0.001 | 0.000 | 0.001 | 0.000 | 0.002 |
| $Fe^{3+}$ | 1.531 | 1.223 | 1.667 | 1.338 | 2.033 | 1.928 | 2.127 | 2.110 | 2.126 |
| $Fe^{2+}$ | 0.000 | 0.000 | 0.000 | 0.000 | 0.000 | 0.000 | 0.000 | 0.000 | 0.000 |
| Mn | 0.054 | 0.068 | 0.050 | 0.070 | 0.030 | 0.026 | 0.051 | 0.048 | 0.038 |
| Mg | 0.004 | 0.004 | 0.003 | 0.003 | 0.007 | 0.001 | 0.001 | 0.006 | 0.002 |
| Ni | 0.000 | 0.001 | 0.000 | 0.002 | 0.000 | 0.001 | 0.000 | 0.000 | 0.000 |
| Ba | 0.001 | 0.000 | 0.000 | 0.000 | 0.001 | 0.001 | 0.000 | 0.002 | 0.000 |
| Ca | 2.944 | 2.935 | 2.937 | 2.964 | 2.989 | 3.014 | 2.957 | 2.974 | 2.969 |
| Na | 0.003 | 0.003 | 0.003 | 0.004 | 0.001 | 0.005 | 0.002 | 0.000 | 0.004 |
| K | 0.000 | 0.001 | 0.000 | 0.000 | 0.000 | 0.000 | 0.000 | 0.000 | 0.000 |
| **Total:** | 8.000 | 8.000 | 8.000 | 8.000 | 8.000 | 8.000 | 8.000 | 8.000 | 8.000 |

| Formula | Composition | Name | |
|---|---|---|---|
| $(Ca_{2.94 - 2.96} Mn_{0.05 - 0.07})(Fe^{3+}_{1.22 - 1.67}Al_{0.39 - 1.83})\ Si_3O_{12}$ | $(SPS,GRO)_{0.19 - 0.40}AND_{0.62 - 0.88}$ | Spessartite-Grossularite-Andradite | |
| $(Ca_{2.96 - 3.01}Mn_{0.03 - 0.05})(Fe^{3+}_{1.93 - 2.13}Al_{0.00 - 0.13})\ Si_3O_{12}$ | $(SPS,GRO)_{0.01 - 0.02}AND_{0.99 - 1.00}$ | Andradite | |

### 5.2.2. Results of pyroxene analysis

The EPMA analyzes for pyroxene are given in Tables 2.1, 2.2 and 2.3. The end-member composition of pyroxene is presented and listed as below:

| Composition | |
|---|---|
| Di. | a |
| Hd. | b |
| Jo. | c |
| Total | 1.00 |

The above abbreviations of Di, Hd, and Jo represent diopside, hedenbergite and johannsenite respectively.

Sample taken from the area 1 (Fig. 3.2) contains Mg-rich clinopyroxene, the component of diopside in this site is more than 80% mol per cent, these clinopyroxene belong to the solid solution hedenbergite-diopside series (Table 2.1). While clinopyroxene selected around the volcanic rock collected from area 3 and 4 (Fig. 3.2) has a high amount of $Fe^{2+}$ and Mg then classified as ferroaugite (Table 2.2) The results may be suggested that the pyroxene formed in volcanic protolith are rich in Mg which classified as hedenbergite-diopside series. This formation may reflect of high Mg volcanic sources. In contrast, pyroxene from area 3 and 4 which formed in limestone or close to limestone protolith. The pyroxene from these areas are high in $Fe^{2+}$ and Mg which is classified as ferroaugite. These pyroxenes may have influenced by Ca or probably Mg from limestone sources.

**Table 2. 1** EPMA results for pyroxene of sample collected from area 1.

| Sample ref. | 1_1 | 1_2 | 1_4 | 1_1-3 | 1_1-4 | 1_1-5 | 1_1-6 | 1_1-7 | 1_1-8 | 1_1-9 |
|---|---|---|---|---|---|---|---|---|---|---|
| $SiO_2$ | 53.280 | 53.152 | 53.082 | 53.271 | 52.612 | 53.321 | 53.327 | 53.675 | 53.661 | 53.698 |
| $Al_2O_3$ | 2.255 | 2.202 | 2.799 | 2.415 | 2.924 | 2.376 | 1.910 | 2.971 | 2.082 | 2.717 |
| $TiO_2$ | 0.245 | 0.213 | 0.037 | 0.124 | 0.066 | 0.114 | 0.152 | 0.000 | 0.018 | 0.100 |
| $Cr_2O_3$ | 0.022 | 0.000 | 0.000 | 0.028 | 0.000 | 0.024 | 0.040 | 0.000 | 0.020 | 0.000 |
| FeO Tot | 6.012 | 5.856 | 5.946 | 6.103 | 6.834 | 6.880 | 5.949 | 6.480 | 6.573 | 6.047 |
| MnO | 0.451 | 0.368 | 0.355 | 0.334 | 0.429 | 0.283 | 0.517 | 0.485 | 0.315 | 0.499 |
| MgO | 16.165 | 16.048 | 15.865 | 16.009 | 15.489 | 15.204 | 15.818 | 16.606 | 16.142 | 16.426 |
| NiO | 0.000 | 0.018 | 0.025 | 0.000 | 0.000 | 0.010 | 0.000 | 0.002 | 0.064 | 0.000 |
| BaO | 0.000 | 0.000 | 0.042 | 0.000 | 0.011 | 0.000 | 0.000 | 0.036 | 0.022 | 0.000 |
| CaO | 20.374 | 20.529 | 20.602 | 20.135 | 20.186 | 19.851 | 20.567 | 19.256 | 19.474 | 20.643 |
| $Na_2O$ | 0.355 | 0.334 | 0.246 | 0.262 | 0.205 | 0.430 | 0.291 | 0.274 | 0.221 | 0.238 |
| $K_2O$ | 0.018 | 0.097 | 0.024 | 0.013 | 0.022 | 0.176 | 0.122 | 0.068 | 0.094 | 0.043 |
| Total : | 99.177 | 98.817 | 99.023 | 98.694 | 98.778 | 98.669 | 98.693 | 99.853 | 98.686 | 100.411 |
| Formula recalculated with 6 oxygenes, after Droop, 1987. | | | | | | | | | | |
| Si | 1.970 | 1.972 | 1.967 | 1.981 | 1.961 | 1.989 | 1.985 | 1.969 | 1.998 | 1.960 |
| Al | 0.030 | 0.028 | 0.033 | 0.019 | 0.039 | 0.011 | 0.015 | 0.031 | 0.002 | 0.040 |
| Al | 0.068 | 0.068 | 0.089 | 0.086 | 0.089 | 0.094 | 0.069 | 0.098 | 0.089 | 0.077 |
| Ti | 0.007 | 0.006 | 0.001 | 0.003 | 0.002 | 0.003 | 0.004 | 0.000 | 0.001 | 0.003 |
| Cr | 0.001 | 0.000 | 0.000 | 0.001 | 0.000 | 0.001 | 0.001 | 0.000 | 0.001 | 0.000 |
| $Fe^{3+}$ | 0.000 | 0.000 | 0.000 | 0.000 | 0.000 | 0.000 | 0.000 | 0.000 | 0.000 | 0.000 |
| $Fe^{2+}$ | 0.186 | 0.182 | 0.184 | 0.190 | 0.213 | 0.215 | 0.185 | 0.199 | 0.205 | 0.185 |
| Mn | 0.014 | 0.012 | 0.011 | 0.011 | 0.014 | 0.009 | 0.016 | 0.015 | 0.010 | 0.015 |
| Mg | 0.891 | 0.887 | 0.876 | 0.887 | 0.860 | 0.846 | 0.878 | 0.908 | 0.896 | 0.894 |
| Ni | 0.000 | 0.001 | 0.001 | 0.000 | 0.000 | 0.000 | 0.000 | 0.000 | 0.002 | 0.000 |
| Ba | 0.000 | 0.000 | 0.001 | 0.000 | 0.000 | 0.000 | 0.000 | 0.001 | 0.000 | 0.000 |
| Ca | 0.807 | 0.816 | 0.818 | 0.802 | 0.806 | 0.794 | 0.820 | 0.757 | 0.777 | 0.807 |
| Na | 0.025 | 0.024 | 0.018 | 0.019 | 0.015 | 0.031 | 0.021 | 0.019 | 0.016 | 0.017 |
| K | 0.001 | 0.005 | 0.001 | 0.001 | 0.001 | 0.008 | 0.006 | 0.003 | 0.004 | 0.002 |
| Total : | 4.000 | 4.000 | 4.000 | 4.000 | 4.000 | 4.000 | 4.000 | 4.000 | 4.000 | 4.000 |
| Composition | | | | | | | | | | |
| Di. | 0.817 | 0.821 | 0.818 | 0.816 | 0.792 | 0.791 | 0.813 | 0.809 | 0.807 | 0.817 |
| Hd. | 0.170 | 0.168 | 0.172 | 0.174 | 0.196 | 0.201 | 0.172 | 0.177 | 0.184 | 0.169 |
| Jo. | 0.013 | 0.011 | 0.010 | 0.010 | 0.012 | 0.008 | 0.015 | 0.013 | 0.009 | 0.014 |
| Total | 1.000 | 1.000 | 1.000 | 1.000 | 1.000 | 1.000 | 1.000 | 1.000 | 1.000 | 1.000 |

Formula: $(Na_{0.01 - 0.03}Ca_{0.76 - 0.82}) (Mg_{0.85 - 0.90}Fe^{2+}_{0.18 - 0.21}Mn_{0.01 - 0.02}Al_{0.07 - 0.10})$

$(Si_{1.96 - 2}Al_{0.01 - 0.04}) O_6$

Name: Hedenbergite-diopside

**Table 2. 2**EPMA results for pyroxene of sample collected from areas 3 and 4

| Sample ref. | 3_c_1 | 3_c_2 | 3_c_3 | 3_c_1 -2 | 3_c_1 -5 | 3_b_1 -4 | 4_p_c2_9 | 4_p_c2_9 -1 | 4_p_c2_9 -2 |
|---|---|---|---|---|---|---|---|---|---|
| $SiO_2$ | 48.686 | 49.348 | 50.298 | 48.644 | 49.437 | 49.507 | 50.331 | 48.544 | 48.177 |
| $Al_2O_3$ | 1.631 | 1.690 | 0.525 | 1.359 | 0.346 | 1.602 | 2.534 | 1.728 | 2.261 |
| $TiO_2$ | 0.000 | 0.000 | 0.000 | 0.017 | 0.000 | 0.040 | 0.000 | 0.000 | 0.000 |
| $Cr_2O_3$ | 0.000 | 0.000 | 0.000 | 0.000 | 0.046 | 0.000 | 0.004 | 0.000 | 0.004 |
| FeO Tot | 27.427 | 26.604 | 26.121 | 26.685 | 26.997 | 25.487 | 25.131 | 26.757 | 26.893 |
| MnO | 0.988 | 1.374 | 0.973 | 1.164 | 1.004 | 0.979 | 0.699 | 0.998 | 0.539 |
| MgO | 8.744 | 9.144 | 9.367 | 9.744 | 9.107 | 8.254 | 9.161 | 10.245 | 9.048 |
| NiO | 0.000 | 0.000 | 0.029 | 0.034 | 0.030 | 0.056 | 0.002 | 0.042 | 0.000 |
| BaO | 0.010 | 0.000 | 0.000 | 0.000 | 0.060 | 0.000 | 0.000 | 0.000 | 0.000 |
| CaO | 11.866 | 11.777 | 11.865 | 11.912 | 12.266 | 13.712 | 11.376 | 10.265 | 11.618 |
| $Na_2O$ | 0.324 | 0.270 | 0.274 | 0.201 | 0.138 | 0.319 | 0.270 | 0.223 | 0.285 |
| $K_2O$ | 0.168 | 0.142 | 0.032 | 0.129 | 0.031 | 0.090 | 0.099 | 0.030 | 0.064 |
| Total | 99.844 | 100.349 | 99.484 | 99.889 | 99.462 | 100.046 | 99.607 | 98.832 | 98.889 |
| Formula recalculated with 6 oxygenes, after Droop, 1987. | | | | | | | | | |
| Si | 1.929 | 1.941 | 1.995 | 1.918 | 1.970 | 1.954 | 1.985 | 1.931 | 1.920 |
| Al | 0.071 | 0.059 | 0.005 | 0.063 | 0.016 | 0.046 | 0.015 | 0.069 | 0.080 |
| Al | 0.005 | 0.019 | 0.019 | 0.000 | 0.000 | 0.029 | 0.103 | 0.012 | 0.026 |
| Ti | 0.000 | 0.000 | 0.000 | 0.001 | 0.000 | 0.001 | 0.000 | 0.000 | 0.000 |
| Cr | 0.000 | 0.000 | 0.000 | 0.000 | 0.001 | 0.000 | 0.000 | 0.000 | 0.000 |
| $Fe^{3+}$ | 0.100 | 0.068 | 0.009 | 0.121 | 0.055 | 0.044 | 0.000 | 0.077 | 0.079 |
| $Fe^{2+}$ | 0.809 | 0.807 | 0.858 | 0.759 | 0.845 | 0.797 | 0.829 | 0.813 | 0.818 |
| Mn | 0.033 | 0.046 | 0.033 | 0.039 | 0.034 | 0.033 | 0.023 | 0.034 | 0.018 |
| Mg | 0.516 | 0.536 | 0.554 | 0.573 | 0.541 | 0.486 | 0.539 | 0.607 | 0.538 |
| Ni | 0.000 | 0.000 | 0.001 | 0.001 | 0.001 | 0.002 | 0.000 | 0.001 | 0.000 |
| Ba | 0.000 | 0.000 | 0.000 | 0.000 | 0.001 | 0.000 | 0.000 | 0.000 | 0.000 |
| Ca | 0.504 | 0.496 | 0.504 | 0.503 | 0.524 | 0.580 | 0.481 | 0.437 | 0.496 |
| Na | 0.025 | 0.021 | 0.021 | 0.015 | 0.011 | 0.024 | 0.021 | 0.017 | 0.022 |
| K | 0.008 | 0.007 | 0.002 | 0.006 | 0.002 | 0.005 | 0.005 | 0.002 | 0.003 |
| Total | 4.000 | 4.000 | 4.000 | 4.000 | 4.000 | 4.000 | 4.000 | 4.000 | 4.000 |

Sample from area 3.

Formula: $(Na_{0.01 - 0.02} Ca_{0.50 - 0.58} Mg_{0.49 - 0.57} Fe^{2+}_{0.76 - 0.86} Mn_{0.03 - 0.05} Fe^{3+}_{0.01 - 0.12})$
$(Si_{1.94 - 1.99} Al_{0.01 - 0.06}) O_6$

Composition: $Ens._{0.26 - 0.31}$ - $Fer._{0.44}$

Name: Ferroaugite

Sample from area 4.

Formula: $(Na_{0.02} Ca_{0.44 - 0.50} Mg_{0.54 - 0.61} Fe^{2+}_{0.81 - 0.83} Mn_{0.02})$
$(Si_{1.92 - 1.98} Al_{0.02 - 0.08}) O_6$

Composition: $Ens._{0.29 - 0.32}$ - $Fer._{0.44}$

Name: Ferroaugite

Where Ens., and Fer. represent. respectively enstatite and ferrosilite.
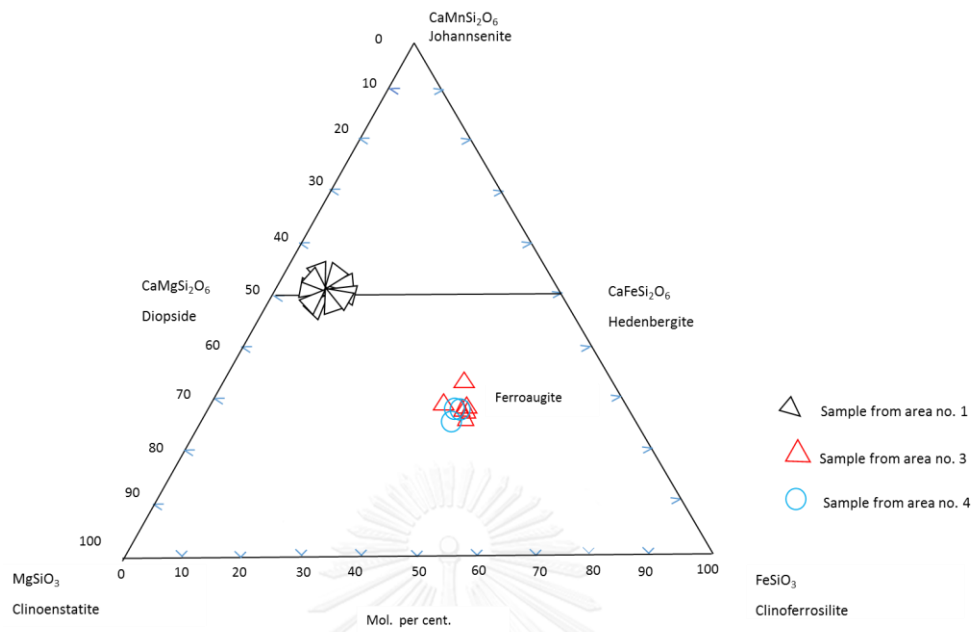
*Figure 5. 1* Triangle diagram of pyroxene collected on the areas 1, 3, and 4. (modified after Deer, W., A., 1966)

5.2.3 Results of iron ores analysis

The EPMA analyzes of magnetite is given in Table 3. The deficiency of the sum of oxides total, less than 96%, show that the fluid which participate to the formation of this iron ore contained some chemical elements and volatile which could not be determined through this EPMA method's.

*Table 5. 1* EPMA analysis of Khao Lek magnetite

| | | |
|---|---|---|
| SiO2 | 0.49 | 0.107 |
| Al2O3 | 0.03 | 0.03 |
| TiO2 | 0 | 0 |
| Cr2O3 | 0 | 0 |
| FeO | 94.92 | 94.92 |
| MnO | 0.05 | 0.08 |
| MgO | 0 | 0.003 |
| NiO | 0 | 0 |
| BaO | 0 | 0 |
| CaO | 0 | 0 |
| Na2O | 0 | 0 |
| K2O | 0 | 0 |
| Total | 95.49 | 95.14 |

# Chapter 6
# Discussion and conclusions

## 6.1 Discussion

### 6.1.1 Khao Lek skarn characterization

Field and petrographic investigations have provided information about the type and distribution as well as the relationships of igneous and metamorphic rocks in the Khao Lek area. The intrusion of probably diorite composition has thermally metamorphosed the rocks of the Permian limestone which is composed predominantly of limestone intercalated with chert nodules. At the same time, Permo-Triassic volcanics and volcaniclastic rocks which is composed of coherent volcanic rocks (basaltic andesite and basalt) and volcaniclastics include lapilli tuff, tuff and breccia of basaltic andesite to basaltic composition. Contact metamorphism and metasomatism occurred and series of metamorphic zone were identified and classified based on the mineral assemblage. A systematic zonal arrangement of rock types identified from the host rocks side to the intrusion rocks are; marble, pyroxene-wollastonite, skarn, pyroxene skarn, garnet pyroxene skarn and garnet skarn and contaminated dioritic skarn. The occurrences of both marble and skarn near dioritic intrusion and dyke suggest contact metamorphic origin for the high temperature marble and skarn minerals at Khao Lek.

From the zonal arrangement of marble and skarn rocks, it is deciphered the evolution of skarn formation at Khao Lek area into 3 stages; 1) metamorphic stage, 2) metasomatism stage, 3) retrograde stage.

1) Metamorphic stage was probably from shortly after the intrusion of dioritic rock. This stage occurred in responded to the emplacement of dioritic rock into the limestone of Tak Fah Formation with little or no introduction of chemichal component. The rock occurred at this stage was controlled chiefly by temperature and omposition and texture of the host rocks. For instance, the massive to thick bedded limestone protolith and volcanic and volcaniclastics were transformed into marble and hornfelsic volcanic rocks. The local exchange of chemical component of dissimilar lithology such

as quartz from chert and calcite from marble to form wollastonite and diopside is observed. This local exchange phenomena, could be formed during the early stage.

2) Metasomatic stage was characterized by the formation of pyroxene-wollastonite skarn, garnet-pyroxene skarn, pyroxene skarn, garnet skarn and contaminated dioritic dyke skarn. The development of these zonal skarns was likely to response to the mobility of elements as a small-scale exchange of $CO_2$, Ca and Mg rich fluid from the marble and Al, Si, Fe-rich fluid from the dioritic rock. The Al, Si and Fe contents should decrease gradually from intrusive rock side to the marble side and in contrast, concentration of Ca and $CO_2$ increase progressively away from the intrusive rock. For example, good mobility of Si combines with Ca to obtain wollastonite and moderate moblity of Al, Mg and Fe yield diopside and garnet respectively. These mineralogy zonations were likely to have replace marble, and are characteristically coarse-grained for example large garnet grains are abundant in garnet zone, garnet-pyroxene zone. Because the mineralogy of those skarn is simple and believe not reflect the composition or texture of the host marble, and the zonations are gradational in which garnet tends to replace other minerals. It is possible that these skarns were formed during the prograde metasomatic stage of the dioritic intrusion. Major iron mineralization represented by massive magnetite ore consisting of mainly magnetite, with trace of pyrite and chalcopyrite occurred along a major fault which could have been replaced the contaminated skarn at Khao Lek (or endoskarn). Minor magnetite mineralization also formed in garnet-pyroxene and pyroxene-wollastonite skarn at Khao Lek, might have been formed during this stage.

3) Retrograde alteration stage is characterized by a minor development of hydrous minerals, such as hornblende, tremolite, biotite, epidote, chlorite as well as quartz and calcite replacing high temperature mineral assemblages. Details investigation reveals that at two generations of fluids are responsible for retrograde alteration namely, 1) Quartz-amphibolite-chlorite-sulfide (pyrite, chalcopyrite) stage and 2) Epidote-chlorite/calcite stage and 3) Zeolite stage.

Minor iron and copper mineralization at Khao Lek was probably taken place after prograde stage as it also cross-cut mainly massive magnetite mineralization. Example of quart-amphibolite-chlorite-sulfide vein/veinlets are replacement of

hornblende in garnet (grossular garnet), tremolite in pyroxene (diopside) and quartz replaces wollastonite. During stage 2 (epidote-chlorite/ calcite) chlorite replaces biotite, hornblende and tremolite. This stage was probably formed during the declining temperature of dioritic intrusion/dyke and changing of fluid composition into a meteoric dominant component.

Since the prograde skarns at Khao Lek developed as a relative narrow shell surrounding the dioritic intrusion/dyke (although it has been observed only one side), and that there was only minor development of retrograde alteration particularly confined to the main fractures or fault that parallel to magnetite orebody and garnet skarn zone (or minor descent of meteoric dominated fluids). It is likely that these skarns were formed at relatively deep level (e.g., deeper than 1-2 km).

Generally, the main sulfide phase of activity usually occurs during the retrograde alteration. Since, ther is only minor retrograde alteration, hence the prospect for mineral exploration in the area is quite limited.

The skarn at Khao Lek can be classified as calcic-skarn based on its mineralogy. When consider in term of ore deposits that are hosted by skarns, this deposit can be classified as skarn deposit. It is classified as iron±copper skarn deposit according to common classification of Einaudi et al., 1981 and Meinert, 1993, which is based on the dominant metal i.e., Cu, Au, Pb-Zn,Fe, Mo, W and Sn.

**6.1.2 Comparision skarn deposits in LFB**

In LFB, skarn deposits are widely distributed from northern most in Laos (e.g., Phu Kham) through Loei-Udon Thani area (e.g., Puthep 1 and Puthep 2, Phu Thap Fah and Phu Lon), Phichit-Phetchabun area (e.g., Khao Phanom Pha and Khao Lek), Lopburi area (e.g., Khao Phra Ngam) and Prachinburi area (e.g., French Mine). These skarn deposits are divided into two types namely, oxidized skarn and reduced skarn (Khin Zaw et al., 2009). Some skarns in this region are clearly related to porphyry intrusions or porphyry-related skarn type which is mainly characterized by Cu-Au and Au deposit. However, other deposits that have mentioned above are less obvious or no direct links to porphyry intrusions. Skarn deposits in this region are also varying from Cu-Au skarn (e.g., Phu Kham and Phu Lon) to Au skarn (e.g., Phu Thap Fah, Khao

Phanom Pha and French Mine) and Fe-Cu skarn (e.g., Khao Lek and Khao Phra Ngam).

Many world class skarn deposits are hosted in carbonate rocks (both limestone and dolomite). However, some skarn deposits may occur in clastic and volcaniclastic rocks with minor limestone. Skarn deposits in the LFB shown with the following table tend to occur in clastic or volcaniclastic rocks. Within the LFB, there are variations for instance most skarn deposits in northern Laos and Loei area are confined clastic rocks that have minor limestone (e.g., Phu Kham, Puthep 1, Puthep 2, Phu Thap Fah and Phu Lon). In addition, Phu Kham also has volcaniclastics association. Skarn deposit at Khao Phanom Pha is the only deposit that occurs almost in the volcaniclastics and associated microdiorite intrusion. It has similar characters in comparison with other deposits in the LFB with an exception of no garnet skarn has been observed both intrusion and volcaniclastic protolith. Amphibole (tremolite) and biotite are well diatributed around orebodies. Regrading to source of intrusion responsible for skarn formation, skarn at Khao Lek seem to have unclear sources. In addition, skarn development is contrast in limestone in volcaniclastic in which skarn has a clear zoning and better developed in limestone than volcaniclastic rocks. Furthermore, skarn at Khao Phra Ngam has similar charaters as those in Loei-Udon Thani area.

Khao Phanom Pha is similar to Phu Thap Fah skarn deposit in which both deposits are classified as reduced skarn type. Other deposits are classified as oxidized skarn. In summary, skarn Cu-Au deposit in the LFB are hosted in Carboniferous, Devonian to Permian sequences of volcaniclastics, siliciclastic, calcareous shale and carbonate rocks intruded by Triassic intrusions. Most of strongly mineralized intrusion that responsible for skarn deposit in LFB are Early to Middle Triassic in age, whereas weakly mineralized systems (e.g., French mine, Singto and Ban Bothong) are mostly Late Triassic or younger in age (Khin Zaw et al., 2009).

Table 6. 1 Comparison of Khao Lek iron skarn with another skarn distributed in Loei Fold Belt (simplified from Khin Zaw et al. 2014 / Gondwana Research 26

| Location | Type of skarn | Host rocks | Intrusive rocks | Minerals assemblage | Sulphides / Oxides | Grades /reserves |
|---|---|---|---|---|---|---|
| Phu Kham (Cu–Au) Mine Laos | Porphyry related-skarn (oxidized) Advanced argillic overprint with possible link to high S epithermal system | -Volcaniclastics and interbedded limestone, red bed siltstone (Carboniferous–E. Permian) - Host volcanics: U–Pb zircon 306 ± 2 Ma | Diorite intrusion, U–Pb zircon 304 ± 1.5 Ma, 306.2 ± 1.4 Ma, 301 ± 3 Ma, 299 ± 3Ma; age of mineralization: Re–Os molybdenite 304.9 ± 1.7 Ma, 304.7 ± 1.7 Ma; K–Ar resetting age of 25.3 ± 1.6 Ma, 35.4 ± 1.7 Ma | Prograde skarn: garnet; Retrograde skarn: chlorite, epidote, carbonate, quartz, sericite, hematite; high-sulphidation with pyrophyllite at hanging wall zone | Chalcopyrite, pyrite, magnetite, bornite, hematite, tetrahedrite, galena, enargite, sphalerite, molybdenite, gold | |
| Phu Thap Fah (Au) – Loei Province – N.E. Thailand | Au skarn Reduced | Permian sedimentary sequence | Triassic granodiorite and micro diorite dikes | Prograde skarn: garnet, clinopyroxene, and quartz. Retrograde skarn: Amphibole, chlorite, epidote, quartz and carbonate | Chalcopyrite, pyrite, pyrrhotite, arsenopyrite. Gold, pyrite, bismuth, pyrrhotite, magnetite, chalcopyrite | 6.4 Mt at 2.19 g/t Au, 0.14% Cu & 3.9 g/t Ag |

| Location | Type of skarn | Host rocks | Intrusive rocks | Minerals assemblage | Sulphides / Oxides | Grades /reserves |
|---|---|---|---|---|---|---|
| Khao Phanom Pha (Au) Central Thailand | Skarn type (reduced) | Felsic andesite, volcaniclastic | | Prograde skarn: wollastonite, biotite; Retrograde skarn: quartz, tremolite, sericite; K–Ar age of sericite: 252 ± 5 Ma | - Pyrrhotite, pyrite, chalcopyrite, electrum<br>- Gold mineralization, up to 5m thick, in quartz–chlorite (±sericite–pyrite–arsenopyrite–pyrrhotite–chalcopyrite) veins (; Khin Zaw et al., 2007a).<br>- Visible gold in dark greenish to black chlorite bands<br>- Stockworks of quartz–actinolite–epidote (±sericite–chlorite–pyrite–pyrrhotite) cross-cut the wall rocks and occur up to 10 m from the central vein. | |

| Location | Type of skarn | Host rocks | Intrusive rocks | Minerals assemblage | Sulphides / Oxides | Grades /reserves |
|---|---|---|---|---|---|---|
| Khao Lek (Fe) Central Thailand | Porphyry related-skarn (oxidized) | Volcaniclastics and interbedded limestone (M. Permian, Saraburi group) | | Prograde skarn: Garnet, pyroxene, marble Retrograde skarn: Chlorite, epidote, tremolite/actinolite | Magnetite, hematite, chalcopyrite, pyrite | |
| Phu Lon (Cu,Fe,Au) prospect | Porphyry related-skarn (oxidized) | Limestone (Devonian) Volcaniclastics (U-Pb zircon: 359 ± 6Ma) | Diorite and quartz monzonite porphyry | Prograde skarn: Andradite, diopside Retrograde skarn: Chlorite, epidote, tremolite/actinolite, calcite | | |
| Khao Phra Ngam (Cu) prospect | Porphyry related-skarn (oxidized) | Limestone, siliciclastics (Permian | Granodiorite U–Pb zircon 208 ± 10 Ma | Prograde skarn: garnet, Retrograde skarn: quartz, epidote, chlorite, calcite | Chalcopyrite, magnetite, pyrite | |
| French Mine (Au, Cu, Mo) Central South Thailand | Au, Cu, Mo Porphyry related-skarn (oxidized) | Lower Middle Ratburi group; sandstone, massive siltstone, limestone, marble | Granodiorite U–Pb zircon 203 ± 8 Ma | Prograde skarn: garnet, pyroxene, wollastonite, albite, biotite; Retrograde skarn: quartz, epidote, chlorite, calcite, sericite. Illite, smectite | Chalcopyrite, pyrite, sphalerite, minor molybdenite | |

6.2. Conclusions

1. The deposit is hosted in Permian limestone of Tak Fa Formation and Late Permian-Early Triassic volcaniclastic rocks. The volcaniclastic rocks unit ranges in composition from basaltic andesite to basalt consisting of coherent rocks (e.g., basaltic andesite and basalt) and non-coherent (e.g., lapilli tuff, tuff and minor breccia).

2. In mine area, basaltic andesite and basalt are dominated the area. Permian limestone in the mine and its adjacent area were metamorphosed to calc-silicate rocks and marble partly due to the emplacement of diorite and granodiorite intrusions in the north and east of the mine area.

3. The medium- to coarse-grained marble exposed in mine area and associated with skarn alteration is likely to have responded to intrusion/dyke center close to the mine area rather than large diorite and granodiorite intrusion locate in the north and northeast.

4. Skarn occurs both in limestone and volcanic rocks. It is better developed in limestone than volcanic rocks. Skarn hosted in limestone shows zonation started with garnet skarn at proximal to intrusion to pyroxene skarn, garnet-pyroxene skarn, pyroxene-wollastonite skarn distal to intrusion.

5. Pyroxene skarn is the only skarn type that occurs in volcanics and it is characterized by pyroxene veinlets or pyroxene infilled vugs in volcanics mainly on the footwall. In addition, skarn also occurs in few meters wide dioritic dyke hosted in limestone (marble) in the center east of the pit.

6. Dyke skarn is the only well preserved endoskarn which is represented by garnet skarn at core, followed by garnet-pyroxene, pyroxene zone, narrow zone of wollastonite skarn and marble.

7. Mineralogical and chemically, there are variation within each skarn zone for example in garnet skarn in the western part of the zone it represented by dark brown, medium- to coarse-grained associated with mostly calcite whereas, at the eastern

part garnet is reddish brown to yellowish green and closely associated with pyroxene. This variation also observed in garnet-pyroxene zone in which mineral assemblage are varying from proximal to more distal to intrusion consistence with composition of garnet obtained from EPMA analyzes suggesting that garnet at proximal has andradite composition and at the distal become of spessartite-grossularite-andradite series. The above variation reflects source of fluid and type of protolith and its proximal and distal from source intrusion.

8. Diopside represent pyroxene skarn formed in volcanics protolith whereas, pyroxene hosted in or close to limestone protolith is represented by ferroaugite. These are likely reflected the influence of type of protolith more than distance to fluid sources.

9. Magnetite orebody is likely replaced the major endoskarn which was emplaced along ENE-WSW major fault as a dyke. This magnetite mineralization could well be formed prior or during retrograde skarn formation as indicated by cross cutting of quartz-amphibole-chlorite-sulfides and epidote-chlorite $\pm$ calcite and calcite vein/veinlets in magnetite orebody. These three veining systems are responsible for retrograde skarn alteration at the Khao Lek.

10. The skarn at Khao Lek can be classified as calcic skarn based on its mineralogy. When consider in terms of ore deposits that are hosted by skarns, this deposit can be classified as iron $\pm$ copper skarn deposit.

# REFERENCES

Audley-Charles, M., Ballantyne, P., and Hall, R., 1988, Mesozoic-Cenozoic rift-drift sequence of Asian fragments from Gondwanaland: Tectonophysics, v. 155, no. 1-4, p. 317-330.

Bunopas, S., 1981, Paleogeographic history of western Thailand and adjacent parts of Southeast Asia a plate tectonic interpretation: PhD Thesis, Victoria University of Wellington.

Bunopas, S., and Vella, P., Tectonic and geologic evolution of Thailand, *in* Proceedings Proceedings of a workshop on stratigraphic correlation of Thailand and Malaysia1983, Volume 1, p. 307-322.

Carter, A., and Clift, P. D., 2008, Was the Indosinian orogeny a Triassic mountain building or a thermotectonic reactivation event?: Comptes Rendus Geoscience, v. 340, no. 2, p. 83-93.

Carter, A., Roques, D., Bristow, C., and Kinny, P., 2001, Understanding Mesozoic accretion in Southeast Asia: significance of Triassic thermotectonism (Indosinian orogeny) in Vietnam: Geology, v. 29, no. 3, p. 211-214.

Charusiri, P., 1989, Lithophile Metallogenic Epochs of Thailand: A Geological and Geochronological Investigation. An unpublished Ph. D: D Thesis, Queen's University, Kingston, Ontaric, Canada.

Gatinsky, Y. G., Hutchison, C., Minh, N., and Tri, T., Tectonic evolution of southeast Asia, *in* Proceedings 27th International Geological Congress Report 51984, p. 225-240.

Hutchison, C. S., 1989, Geological evolution of South-east Asia, Clarendon Press Oxford.

Intasopa, S., 1993, Petrology and geochronology of the volcanic rocks of the central Thailand volcanic belt: PhD Thesis. Department of Geology, University of New Brunswick.

Kamvong, T., and Zaw, K., 2009, The origin and evolution of skarn-forming fluids from the Phu Lon deposit, northern Loei Fold Belt, Thailand: Evidence from fluid inclusion and sulfur isotope studies: Journal of Asian Earth Sciences, v. 34, no. 5, p. 624-633.

Kamvong, T., Zaw, K., and Harris, A., 2006, Geology and geochemistry of the Phu Lon copper-gold skarn deposit at the northern Loei Fold Belt, Northeast Thailand: ASEG Extended Abstracts, v. 2006, no. 1, p. 1-9.

Khositanont, S., 2008, Gold and iron–gold mineralization in the Sukhothai and Loei–Phetchabun Fold Belts: Unpublished PhD thesis, Chiang Mai University, Chiang Mai, Thailand University of Tasmania, Hobart, Australia, p. 185.

Metcalfe, I., 1988, Origin and assembly of south-east Asian continental terranes: Geological Society, London, Special Publications, v. 37, no. 1, p. 101-118.

Metcalfe, I., 2002, Permian tectonic framework and palaeogeography of SE Asia: Journal of Asian Earth Sciences, v. 20, no. 6, p. 551-566.

Nakornsri, 1981, Geology and Mineral ressources of Amphoe Ban Mi. Department of Mineral Resources. Geological Survey Report,: English summary), no. 3,, p. 1-36

Phajuy, B., Panjasawatwong, Y., and Osataporn, P., 2005, Preliminary geochemical study of volcanic rocks in the Pang Mayao area, Phrao, Chiang Mai, northern

Thailand: tectonic setting of formation: Journal of Asian Earth Sciences, v. 24, no. 6, p. 765-776.

Salam, A., 2013, A geological, geochemical and metallogenic study of the Chatree epithermal deposit, Phetchabun Province, central Thailand: University of Tasmania.

Salam, A., Zaw, K., Meffre, S., McPhie, J., and Lai, C.-K., 2014, Geochemistry and geochronology of the Chatree epithermal gold–silver deposit: Implications for the tectonic setting of the Loei Fold Belt, central Thailand: Gondwana Research, v. 26, no. 1, p. 198-217.

Shi, G. R., and Waterhouse, J. B., 1991, Sakmarian (Early Permian) brachiopod biogeography and major associations as related to terrane drift: Brachiopods Through Time, p. 355-365.

Sone, M., & Metcalfe, I.        , 2008a, Parallel Tethyan sutures and the Sukhothai Island arc system in Thailand. Proceeding of the international symposia on Geoscience Ressources and Environments of Asia Terranes (GREAT, 2008).

Tapponier, P., et al., 1982, Propagating extrusion tectonics in Asia: new insights from simple experiments with plasticine.: Geology, p. 611-616.

Tate, N. M., 2005, Discovery, geology and mineralization of the Phu Kham copper-gold deposit Lao PDR: Mineral Deposit Research: Meeting the global Challenge, p. 1077 – 1080.

Ueno, K., and Hisada, K.-i., 2001, The Nan-Uttaradit-Sa Kaeo Suture as a main Paleo-Tethyan Suture in Thailand: is it real?: Gondwana Research, v. 4, no. 4, p. 804-806.

Zaw, K., Meffre, S., Lai, C.-K., Burrett, C., Santosh, M., Graham, I., Manaka, T., Salam, A., Kamvong, T., and Cromie, P., 2014, Tectonics and metallogeny of mainland Southeast Asia—a review and contribution: Gondwana Research, v. 26, no. 1, p. 5-30.

Audley-Charles, M., Ballantyne, P., and Hall, R., 1988, Mesozoic-Cenozoic rift-drift sequence of Asian fragments from Gondwanaland: Tectonophysics, v. 155, no. 1-4, p. 317-330.

Bunopas, S., 1981, Paleogeographic history of western Thailand and adjacent parts of Southeast Asia a plate tectonic interpretation: PhD Thesis, Victoria University of Wellington.

Bunopas, S., and Vella, P., Tectonic and geologic evolution of Thailand, *in* Proceedings Proceedings of a workshop on stratigraphic correlation of Thailand and Malaysia1983, Volume 1, p. 307-322.

Carter, A., and Clift, P. D., 2008, Was the Indosinian orogeny a Triassic mountain building or a thermotectonic reactivation event?: Comptes Rendus Geoscience, v. 340, no. 2, p. 83-93.

Carter, A., Roques, D., Bristow, C., and Kinny, P., 2001, Understanding Mesozoic accretion in Southeast Asia: significance of Triassic thermotectonism (Indosinian orogeny) in Vietnam: Geology, v. 29, no. 3, p. 211-214.

Charusiri, P., 1989, Lithophile Metallogenic Epochs of Thailand: A Geological and Geochronological Investigation. An unpublished Ph. D: D Thesis, Queen's University, Kingston, Ontaric, Canada.

Gatinsky, Y. G., Hutchison, C., Minh, N., and Tri, T., Tectonic evolution of southeast Asia, *in* Proceedings 27th International Geological Congress Report 51984, p. 225-240.

Hutchison, C. S., 1989, Geological evolution of South-east Asia, Clarendon Press Oxford.

Intasopa, S., 1993, Petrology and geochronology of the volcanic rocks of the central Thailand volcanic belt: PhD Thesis. Department of Geology, University of New Brunswick.

Kamvong, T., and Zaw, K., 2009, The origin and evolution of skarn-forming fluids from the Phu Lon deposit, northern Loei Fold Belt, Thailand: Evidence from fluid inclusion and sulfur isotope studies: Journal of Asian Earth Sciences, v. 34, no. 5, p. 624-633.

Kamvong, T., Zaw, K., and Harris, A., 2006, Geology and geochemistry of the Phu Lon copper-gold skarn deposit at the northern Loei Fold Belt, Northeast Thailand: ASEG Extended Abstracts, v. 2006, no. 1, p. 1-9.

Khositanont, S., 2008, Gold and iron–gold mineralization in the Sukhothai and Loei–Phetchabun Fold Belts: Unpublished PhD thesis, Chiang Mai University, Chiang Mai, Thailand University of Tasmania, Hobart, Australia, p. 185.

Metcalfe, I., 1988, Origin and assembly of south-east Asian continental terranes: Geological Society, London, Special Publications, v. 37, no. 1, p. 101-118.

Metcalfe, I., 2002, Permian tectonic framework and palaeogeography of SE Asia: Journal of Asian Earth Sciences, v. 20, no. 6, p. 551-566.

Nakornsri, 1981, Geology and Mineral ressources of Amphoe Ban Mi. Department of Mineral Resources. Geological Survey Report,: English summary), no. 3,, p. 1-36

Phajuy, B., Panjasawatwong, Y., and Osataporn, P., 2005, Preliminary geochemical study of volcanic rocks in the Pang Mayao area, Phrao, Chiang Mai, northern Thailand: tectonic setting of formation: Journal of Asian Earth Sciences, v. 24, no. 6, p. 765-776.

Salam, A., 2013, A geological, geochemical and metallogenic study of the Chatree epithermal deposit, Phetchabun Province, central Thailand: University of Tasmania.

Salam, A., Zaw, K., Meffre, S., McPhie, J., and Lai, C.-K., 2014, Geochemistry and geochronology of the Chatree epithermal gold–silver deposit: Implications for the tectonic setting of the Loei Fold Belt, central Thailand: Gondwana Research, v. 26, no. 1, p. 198-217.

Shi, G. R., and Waterhouse, J. B., 1991, Sakmarian (Early Permian) brachiopod biogeography and major associations as related to terrane drift: Brachiopods Through Time, p. 355-365.

Sone, M., & Metcalfe, I.    , 2008a, Parallel Tethyan sutures and the Sukhothai Island arc system in Thailand. Proceeding of the international symposia on Geoscience Ressources and Environments of Asia Terranes (GREAT, 2008).

Tapponier, P., et al., 1982, Propagating extrusion tectonics in Asia: new insights from simple experiments with plasticine.: Geology, p. 611-616.

Tate, N. M., 2005, Discovery, geology and mineralization of the Phu Kham copper-gold deposit Lao PDR: Mineral Deposit Research: Meeting the global Challenge, p. 1077 – 1080.

Ueno, K., and Hisada, K.-i., 2001, The Nan-Uttaradit-Sa Kaeo Suture as a main Paleo-Tethyan Suture in Thailand: is it real?: Gondwana Research, v. 4, no. 4, p. 804-806.

Zaw, K., Meffre, S., Lai, C.-K., Burrett, C., Santosh, M., Graham, I., Manaka, T., Salam, A., Kamvong, T., and Cromie, P., 2014, Tectonics and metallogeny of mainland Southeast Asia—a review and contribution: Gondwana Research, v. 26, no. 1, p. 5-30.

Audley-Charles, M.G., 1988, Evolution of the southern margin of Tethys (North Australian region) from Early -Permian to Late Cretaceous.

Bunopas and Vella, 1983, Tectonic and geologic evolution of Thailand. Geological Society of Thailand/ Geological Society of Malaysia, 1, 307-322.

Bunopas, S., 1981, Paleogeographic history of western Thailand and adjacent parts of southeast Asia. A plate tectonic interpretation.

Carter, A. & Clift, P. D., 2008, was the Indosinian orogeny a Triassic mountain - building or a thermotectonic reactivation even? Compte rendus Geoscience, 340, 83-93.

Carter et al., 2001, Understanding Mesozoic accretion in Southeast Asia: significance of Triassic thermotectonism (Indosinian Orogeny) in Vietnam.

Charusiri, P., Clark, A., Farrar, E., Archibald, D., 1993, Granite belt in Thailand: evidence from the 40Ar/39Ar geochronological and geological synthesis. Journal of Asian Earth Sciences, v8, no 1-4, p127 -136

Deer, W.A., Howie, R.A., Zussman, J., 1966, An introduction to the Rock-forming Minerals. Longman Scientific & Technical Hong Kong.

Droop, G.T.R. 1987. A general equation for estimating Fe3+ concentrations in ferromagnesian silicates and oxides from microprobe analysis using stoichiometric criteria. Mineral magazine 51: 431 – 435.

Gatinsky et al., 1984, Tectonic evolution of Southeast Asia. 27th International Geological Congress.

Gatinsky, Y., G., and Hutchison C., S., 1984, Cathaysia, Gondwanaland and the palaeotethys in the evolution of continental Southeast Asia, GEOSEA, Geological society of Malaysia, 11 -12.

Ueno, K., Hisada, K., 2001, The Nan-Uttaradit-Sa Kaeo suture as a main Paleotethyan Suture in Thailand: Is it real? Gondwana Research 4, 804 -805.

Hutchison, C.S., 1989, Geological evolution of South-East Asia. Oxford Monographs on Geology and Geophysics, 13.

Intasopa, S., 1993, Petrology and Geochronogy of the volcanic rocks of the central Thailand volcanic belt.Unpublished PhD. Thesis, Univerity of New Brunswick, Canada.

Jungyusuk, N., et al., 1985, Cenozoic basalt of Thailand. Conference in Geology and Mineral Ressouces of Thailand, Nov 19-128, Bangkok.

Kamvong and Khin Zaw, 2009, Geochronological and metallogenic framework of Cu-Au skarn deposit along the Loei Fold Belt, Thailand and Lao PDR.

Kamvong, T., Zaw, K., 2009, The origin and evolution of skarn forming fluids from the Phu Lon deposit, northern LFB, Thailand: Evidence from fluids inclusion and sulfur isotope studies.

Khin Zaw, S. Meffre, C. Lai, C., Burrett, M. Santosh, I. Graham, T. Manaka, A. Salam, T. Kamvong, P. Cromie., 2014. Tectonics and metallogeny of mainland Southeast Asia- A review and contribution.

Khin Zaw et al.,2014, Tectonics and metallogeny of mainland Southeast Asia – a review and contribution. Gondwana research.

Khin Zaw et al, 2009, The origin and evoluation of skarn forming fluids from the Phu Lon deposit, northern Loei Fold Belt, Thailand.

Khin Zaw et al., 2008, Mineralogy and genesis of Phu Thap Fah gold skarn deposit Northeast Thailand: Implication for reduced gold skarn formation. IGC Norway 2008.

Khin Zaw, Meffre,S., 2007, Metallogenic relations and deposit scale studies, final report. Geochronology, Metallogenesis and Deposit styles of Loei Fold Belt in Thailand and Lao PDR.

Khin Zaw, et al., 2007, Geological setting alteration., mineralization and geochronology of Chatree epithermal gold silver deposit, Phetchabun Province, central Thailand.

Khositanont, S., 2008, Gold and iron-gold mineralization in the Sukhothai and Loei-Phetchabun fold Belts. Unpublished Ph. D. thesis, Chiang Mai University, pp, 186.

Meinert D. L., Dipple M. G., Nicolescu S., 2005, World Skarn Deposits – Economic Geology 100th Anniversary Volume - 2005

Metcalfe, I., 2002, Permian tectonic framework and paleogeography of Se Asia. Journal Asia Earth Science, 18, 691-712.

Müller, C. J., 1999, Geochemistry, fluid characteristic and evolution of the French mine gold skarn system, eastern Thailand. BSc (Hons) thesis, University of Tasmania, Hobart, Australia.

Nakornsri, 1981, Geology and Mineral ressources of Amphoe Ban Mi. Department of Mineral Resources. Geological Survey Report, no 3, 1-36 (English summary).

Phajuy, B. et al., 2005, Preliminary geochemical study of volcanic rocks in the Pang Mayao area. Phrao Chiang Mai, northern of Thailand: tectonic setting of formation. Journal of Asia Earth Sciences, 24, 765-776.

Salam A., Khin Zaw, Meffre, S., McPhie, J., C., 2014, Geochemistry and geochronology of the Chatree epithermal gold-siver deposit: Implication for the tectonic setting of the Loei fold belt, Central Thailand. Gondwana Research, V.26, p 198-217

Salam, A., et al., 2007, Geological setting, alteration, mineralization and geochronology of Chatree epithermal gold-silver deposit, Phetchabun Province, Central Thailand.

Sharusiri, P., 1989, Lithophile metallogenetic epochs of Thailand: a geological and geochronological investigation. PhD. Thesis, Queen's University, Kingston, Canada.

Sone, M., & Metcalfe, I., 2008a, Parallel Tethyan sutures in mainland Southeast Asia: New insight for Paleotethys closure and implication for the indosinian orogeny. Comptes rendus Geosciences. 340, 166-179.

Sone, M., & Metcalfe, I., 2008a, Parallel Tethyan sutures and the Sukhothai Island arc system in Thailand. Proceeding of the international symposia on Geoscience Ressources and Environments of Asia Terranes (GREAT, 2008).

Tate, N. M., 2005, Discovery, geology and mineralization of the Phu Kham copper-gold deposit Lao PDR, Mineral Deposit Research: Meeting the global Challenge, p 1077 – 1080

Tapponier, P., et al., 1982, Propagating extrusion tectonics in Asia: new insights from simple experiments with plasticine. Geology, 10, 611-616.
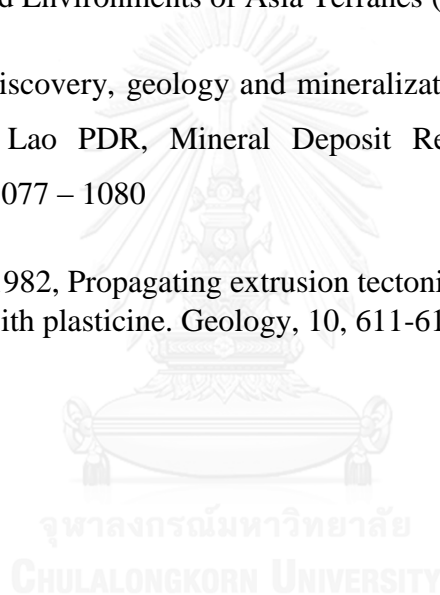
APPENDIX

Appendix A : EPMA results for garnet

| sample ref | 6_c1_p11 | 6_c1_p12 | 6_c1_p13 | 6_c1_p14 | 6_c1_p21 | 6_c1_p22 | 6_c1_p23 | 6_c1_p24 | 6_c1_p31 |
|---|---|---|---|---|---|---|---|---|---|
| SiO2 | 35.027 | 35.009 | 35.187 | 36.118 | 36.451 | 36.146 | 36.339 | 37.105 | 36.718 |
| Al2O3 | 0.017 | 0 | 0.029 | 7.867 | 7.458 | 6.354 | 6.732 | 10.731 | 7.645 |
| TiO2 | 0.009 | 0 | 0.022 | 0 | 0 | 0.055 | 0 | 0.05 | 0 |
| Cr2O3 | 0 | 0 | 0.022 | 0.017 | 0 | 0.007 | 0 | 0.025 | 0 |
| FeO | 29.341 | 28.861 | 28.781 | 19.691 | 19.884 | 21.682 | 20.941 | 15.868 | 19.29 |
| MnO | 0.342 | 0.34 | 0.388 | 0.84 | 0.856 | 0.798 | 0.748 | 1.286 | 0.997 |
| MgO | 0.044 | 0.032 | 0.049 | 0.045 | 0.004 | 0.034 | 0.014 | 0.009 | 0.015 |
| NiO | 0 | 0.001 | 0 | 0 | 0 | 0 | 0 | 0.017 | 0 |
| BaO | 0 | 0 | 0 | 0.02 | 0 | 0 | 0 | 0 | 0.009 |
| CaO | 33.519 | 33.577 | 33.449 | 34.542 | 34.443 | 34.004 | 34.048 | 34.214 | 34.13 |
| Na2O | 0.003 | 0.02 | 0.028 | 0.03 | 0.041 | 0.018 | 0.016 | 0.024 | 0.042 |
| K2O | 0 | 0 | 0.001 | 0.017 | 0 | 0.008 | 0.023 | 0 | 0.001 |
| Total | 98.302 | 97.84 | 97.956 | 99.187 | 99.137 | 99.106 | 98.861 | 99.329 | 98.847 |

| sample ref | 6_c1_p32 | 6_c1_p33 | 6_c2_p11 | 6_c2_p12 | 6_c2_p13 | 6_c2_p14 | 6_c2_p11 | 6_c2_p12 | 6_c2_p13 |
|---|---|---|---|---|---|---|---|---|---|
| SiO2 | 35.541 | 36.713 | 35.428 | 35.762 | 35.723 | 34.817 | 35.342 | 35.719 | 35.893 |
| Al2O3 | 7.223 | 7.98 | 0.03 | 0.015 | 0.005 | 0 | 0.543 | 0.071 | 0.015 |
| TiO2 | 0 | 0 | 0.035 | 0 | 0 | 0.035 | 0.028 | 0 | 0 |
| Cr2O3 | 0 | 0 | 0 | 0 | 0.032 | 0.004 | 0 | 0.003 | 0 |
| FeO | 19.714 | 19.373 | 29.925 | 28.838 | 28.716 | 28.499 | 28.759 | 29.209 | 29.09 |
| MnO | 0.828 | 0.905 | 0.421 | 0.365 | 0.407 | 0.507 | 0.464 | 0.487 | 0.436 |
| MgO | 0.035 | 0.055 | 0.042 | 0.054 | 0.039 | 0.032 | 0.01 | 0.044 | 0.035 |
| NiO | 0.035 | 0.021 | 0 | 0.004 | 0 | 0.02 | 0 | 0 | 0.008 |
| BaO | 0 | 0.009 | 0.002 | 0 | 0 | 0 | 0 | 0 | 0.051 |
| CaO | 33.423 | 34.128 | 33.428 | 33.73 | 33.526 | 33.76 | 33.285 | 33.482 | 33.467 |
| Na2O | 0.156 | 0.011 | 0.035 | 0.038 | 0.028 | 0 | 0.003 | 0.004 | 0.026 |
| K2O | 0.022 | 0 | 0.008 | 0.017 | 0.017 | 0.022 | 0.016 | 0.011 | 0.005 |
| Total | 96.977 | 99.195 | 99.354 | 98.823 | 98.493 | 97.696 | 98.45 | 99.03 | 99.026 |

| sample ref | 6_c2_p14 | 6_c2_p21 | 6_c2_p22 | 6_c2_p31 | 6_c2_p32 | 6_c2_p33 | 6_c2_p34 | 6_c3_p11 | 6_c3_p12 |
|---|---|---|---|---|---|---|---|---|---|
| SiO2 | 35.512 | 37.005 | 36.833 | 35.095 | 35.531 | 35.385 | 35.621 | 35.366 | 35.816 |
| Al2O3 | 0.005 | 6.125 | 6.162 | 0.001 | 0.016 | 0.004 | 0.02 | 0 | 0 |
| TiO2 | 0.061 | 0.01 | 0 | 0.039 | 0.001 | 0.025 | 0 | 0.024 | 0 |
| Cr2O3 | 0.004 | 0.001 | 0 | 0 | 0.007 | 0.017 | 0.012 | 0 | 0.037 |
| FeO | 28.861 | 21.914 | 22.055 | 28.791 | 29.487 | 29.301 | 29.581 | 28.964 | 29.287 |
| MnO | 0.506 | 0.909 | 0.841 | 0.402 | 0.442 | 0.433 | 0.436 | 0.402 | 0.444 |
| MgO | 0.048 | 0 | 0.029 | 0.043 | 0.048 | 0.037 | 0.042 | 0.014 | 0.027 |
| NiO | 0 | 0 | 0 | 0 | 0.006 | 0.014 | 0 | 0 | 0 |
| BaO | 0 | 0 | 0 | 0 | 0.022 | 0 | 0 | 0 | 0 |
| CaO | 33.26 | 34.121 | 34.044 | 33.422 | 33.555 | 33.806 | 33.338 | 33.426 | 33.656 |
| Na2O | 0.028 | 0.012 | 0.015 | 0.041 | 0 | 0.015 | 0.003 | 0.028 | 0.014 |
| K2O | 0 | 0 | 0.002 | 0 | 0.011 | 0 | 0.003 | 0.02 | 0.011 |
| Total | 98.285 | 100.097 | 99.981 | 97.834 | 99.126 | 99.037 | 99.056 | 98.244 | 99.292 |

| sample ref | 6_c3_p13 | 6_c3_p21 | 6_c3_p22 | 6_c3_p23 | 6_c3_p31 | 6_c3_p32 | 6_c3_p33 | 6_c4_p11 | 6_c4_p12 |
|---|---|---|---|---|---|---|---|---|---|
| SiO2 | 35.488 | 34.945 | 35.268 | 34.558 | 34.594 | 34.658 | 35.16 | 35.585 | 35.527 |
| Al2O3 | 0 | 0 | 0 | 0 | 0.015 | 0.024 | 0 | 6.011 | 6.069 |
| TiO2 | 0.015 | 0 | 0.023 | 0.015 | 0.049 | 0 | 0.005 | 0 | 0 |
| Cr2O3 | 0 | 0 | 0 | 0 | 0.01 | 0 | 0 | 0.028 | 0 |
| FeO | 29.14 | 29.176 | 29.042 | 29.86 | 29.476 | 29.54 | 29.635 | 21.692 | 20.993 |
| MnO | 0.388 | 0.456 | 0.476 | 0.464 | 0.552 | 0.45 | 0.439 | 0.819 | 0.904 |
| MgO | 0.06 | 0.056 | 0.026 | 0.011 | 0.022 | 0.036 | 0.081 | 0.017 | 0.046 |
| NiO | 0 | 0.006 | 0 | 0.002 | 0.007 | 0.023 | 0 | 0.011 | 0 |
| BaO | 0 | 0.008 | 0 | 0 | 0 | 0 | 0.058 | 0 | 0 |
| CaO | 33.891 | 33.496 | 33.543 | 33.427 | 33.539 | 33.293 | 33.519 | 34.056 | 32.571 |
| Na2O | 0.007 | 0.02 | 0.019 | 0.004 | 0 | 0.011 | 0.004 | 0.02 | 0.007 |
| K2O | 0 | 0.001 | 0.014 | 0 | 0 | 0 | 0 | 0.011 | 0.005 |
| Total | 98.989 | 98.164 | 98.411 | 98.341 | 98.264 | 98.035 | 98.901 | 98.25 | 96.122 |

| sample ref | 6_c4_p13 | 6_c4_p21 | 6_c4_p22 | 6_c4_p23 | 6_c4_p31 | 6_c4_p32 | 6_c4_p33 | 5_c_p11 | 5_c_p12 | 5_c_p13 | 5_c_p14 |
|---|---|---|---|---|---|---|---|---|---|---|---|
| SiO2 | 35.68 | 34.843 | 34.371 | 34.401 | 35.895 | 36.145 | 35.62 | 35.072 | 35.597333 | 34.413 | 34.333 |
| Al2O3 | 6.002 | 0.022 | 0.013 | 0.079 | 7.752 | 7.492 | 7.468 | 1.015 | 0.874 | 1.673 | 0.338 |
| TiO2 | 0 | 0.04 | 0 | 0 | 0.037 | 0 | 0 | 0 | 0 | 0 | 0 |
| Cr2O3 | 0 | 0.009 | 0 | 0 | 0 | 0.037 | 0 | 0 | 0.009 | 0.011 | 0 |
| FeO | 21.913 | 28.637 | 29.632 | 29.524 | 19.8 | 19.579 | 20.08 | 28.307 | 28.325 | 27.097 | 28.57 |
| MnO | 0.855 | 0.459 | 0.416 | 0.45 | 1 | 1.074 | 1.005 | 0.368 | 0.289 | 0.375 | 0.258 |
| MgO | 0.025 | 0.05 | 0.052 | 0.042 | 0.023 | 0.018 | 0.022 | 0.011 | 0.027 | 0.004 | 0.002 |
| NiO | 0.013 | 0.016 | 0.026 | 0.018 | 0.076 | 0.019 | 0.003 | 0.028 | 0.014 | 0.007 | 0.029 |
| BaO | 0 | 0 | 0.001 | 0 | 0.018 | 0 | 0.025 | 0.012 | 0 | 0.032 | 0 |
| CaO | 33.957 | 33.448 | 33.394 | 33.534 | 34.311 | 34.239 | 34.285 | 33.618 | 33.363 | 33.985 | 33.308 |
| Na2O | 0.019 | 0.011 | 0.008 | 0.006 | 0.011 | 0.009 | 0.058 | 0.033 | 0.154 | 0.031 | 0.089 |
| K2O | 0 | 0.002 | 0.012 | 0 | 0 | 0 | 0.009 | 0 | 0.022 | 0.001 | 0.007 |
| Total | 98.464 | 97.537 | 97.925 | 98.054 | 98.923 | 98.612 | 98.575 | 98.464 | 97.467 | 97.629 | 96.934 |

| sample ref. | 2_c1_p21 | 2_c1_p22 | 2_c1_p23 | 2_c1_p41 | 2_c1_p42 | 2_c1_p43 | 2_c1_p51 | 2_c1_p52 | 2_c1_p53 | 2_c1_p61 |
|---|---|---|---|---|---|---|---|---|---|---|
| SiO2 | 36.893 | 36.604 | 35.161 | 37.407 | 36.8 | 36.45 | 36.983 | 36.901 | 37.035 | 36.832 |
| Al2O3 | 4.963 | 4.881 | 1.16 | 4.711 | 4.656 | 4.387 | 6.24 | 5.758 | 6.283 | 4.405 |
| TiO2 | 0 | 0.011 | 0 | 0 | 0 | 0.042 | 0 | 0.063 | 0 | 0.065 |
| Cr2O3 | 0 | 0 | 0.01 | 0.024 | 0.018 | 0 | 0 | 0 | 0 | 0 |
| Fe2O3 | | | | | | | | | | |
| FeO | 23.43 | 23.321 | 27.967 | 23.341 | 23.713 | 23.396 | 21.483 | 22.134 | 21.802 | 23.141 |
| MnO | 0.333 | 0.407 | 0.737 | 0.974 | 0.846 | 0.691 | 1.013 | 0.834 | 1.084 | 0.772 |
| MgO | 0.082 | 0.074 | 0.024 | 0.03 | 0 | 0.034 | 0.017 | 0.019 | 0.029 | 0.023 |
| NiO | 0 | 0.032 | 0 | 0 | 0 | 0 | 0 | 0.014 | 0 | 0 |
| BaO | 0 | 0.015 | 0.008 | 0 | 0 | 0 | 0.099 | 0.066 | 0.028 | 0 |
| CaO | 34.604 | 34.855 | 33.026 | 33.82 | 34.036 | 33.717 | 34.001 | 34.101 | 34.014 | 33.99 |
| Na2O | 0.037 | 0.034 | 0.026 | 0 | 0.018 | 0.01 | 0 | 0 | 0.025 | 0.014 |
| K2O | 0.007 | 0.011 | 0 | 0.015 | 0 | 0.009 | 0 | 0 | 0 | 0.01 |
| Total | 100.349 | 100.245 | 98.119 | 100.322 | 100.087 | 98.736 | 99.836 | 99.89 | 100.3 | 99.252 |

| sample ref. | 2_c1_p62 | 2_c1_p63 | 2_c1_p71 | 2_c1_p72 | 2_c1_p73 | 2_c1_p81 | 2_c1_p82 | 2_c1_p83 | 2_c2_p11 | 2_c2_p12 |
|---|---|---|---|---|---|---|---|---|---|---|
| SiO2 | 35.987 | 35.543 | 36.047 | 36.683 | 35.992 | 36.209 | 35.799 | 35.851 | 36.395 | 36.068 |
| Al2O3 | 4.36 | 4.673 | 5.707 | 5.273 | 6.235 | 5.169 | 5.346 | 5.695 | 10.051 | 8.986 |
| TiO2 | 0 | 0 | 0 | 0 | 0 | 0.009 | 0.068 | 0.01 | 0.011 | 0 |
| Cr2O3 | 0 | 0 | 0.026 | 0.034 | 0 | 0.021 | 0.006 | 0 | 0 | 0 |
| Fe2O3 | | | | | | | | | | |
| FeO | 23.308 | 22.87 | 20.974 | 22.715 | 20.984 | 22.72 | 22.596 | 21.994 | 16.676 | 17.881 |
| MnO | 0.681 | 0.829 | 1.029 | 0.906 | 1.135 | 0.883 | 0.625 | 0.873 | 1.219 | 1.215 |
| MgO | 0.042 | 0.015 | 0.035 | 0 | 0.054 | 0 | 0.044 | 0.012 | 0.005 | 0.012 |
| NiO | 0 | 0.005 | 0.016 | 0 | 0.006 | 0.043 | 0 | 0 | 0.018 | 0 |
| BaO | 0.013 | 0.025 | 0.017 | 0 | 0 | 0.031 | 0.008 | 0 | 0 | 0 |
| CaO | 33.893 | 33.854 | 34.035 | 34.427 | 33.943 | 34.09 | 34.72 | 34.508 | 34.104 | 34.105 |
| Na2O | 0.08 | 0.06 | 0.007 | 0.022 | 0.025 | 0.002 | 0.023 | 0.045 | 0.025 | 0.031 |
| K2O | 0.019 | 0 | 0.012 | 0 | 0.012 | 0 | 0.01 | 0 | 0 | 0 |
| Total | 98.383 | 97.874 | 97.905 | 100.06 | 98.386 | 99.177 | 99.245 | 98.988 | 98.504 | 98.298 |

| sample ref. | 2_c2_p13 | 2_c2_p21 | 2_c2_p22 | 2_c2_p23 | 2_c2_p31 | 2_c2_p32 | 2_c2_p33 | 2_c2_p41 | 2_c2_p42 | 2_c2_p43 |
|---|---|---|---|---|---|---|---|---|---|---|
| SiO2 | 36.06 | 35.896 | 36.533 | 35.918 | 36.452 | 35.611 | 36.834 | 35.714 | 35.776 | 34.645 |
| Al2O3 | 9.502 | 10.342 | 9.91 | 10.088 | 6.764 | 7.416 | 9.159 | 4.661 | 2.932 | 2.008 |
| TiO2 | 0 | 0.101 | 0 | 0.039 | 0 | 0 | 0 | 0 | 0 | 0.014 |
| Cr2O3 | 0.025 | 0.017 | 0.022 | 0.041 | 0.009 | 0 | 0.003 | 0 | 0.034 | 0.016 |
| Fe2O3 | | | | | | | | | | |
| FeO | 17.267 | 16.254 | 16.862 | 16.371 | 20.801 | 19.599 | 17.642 | 22.964 | 25.808 | 26.786 |
| MnO | 1.099 | 1.012 | 1.015 | 0.798 | 0.883 | 0.861 | 0.977 | 0.856 | 0.632 | 0.555 |
| MgO | 0.023 | 0.005 | 0.027 | 0.025 | 0.033 | 0.029 | 0.023 | 0.007 | 0.013 | 0.006 |
| NiO | 0.018 | 0 | 0 | 0.001 | 0 | 0.01 | 0 | 0.042 | 0.049 | 0.027 |
| BaO | 0.041 | 0.023 | 0.041 | 0 | 0 | 0.025 | 0.005 | 0 | 0 | 0 |
| CaO | 33.825 | 34.002 | 34.368 | 34.309 | 33.826 | 34.231 | 34.054 | 33.953 | 33.973 | 33.197 |
| Na2O | 0.059 | 0.009 | 0.015 | 0.043 | 0 | 0.027 | 0.024 | 0.056 | 0.014 | 0.057 |
| K2O | 0.009 | 0.026 | 0.01 | 0.027 | 0 | 0.001 | 0 | 0.014 | 0.014 | 0.028 |
| Total | 97.928 | 97.687 | 98.803 | 97.66 | 98.768 | 97.81 | 98.721 | 98.267 | 99.245 | 97.339 |

| sample ref. | 2_c2_p51 | 2_c2_p52 | 2_c2_p53 | 2_c2_p61 | 2_c2_p62 | 2_c2_p63 | 2_c2_p71 | 2_c2_p72 | 2_c2_p73 | 2_c2_p81 |
|---|---|---|---|---|---|---|---|---|---|---|
| SiO2 | 34.334 | 34.642 | 34.98 | 34.667 | 34.552 | 34.81 | 34.144 | 34.302 | 33.469 | 34.146 |
| Al2O3 | 0.428 | 0.337 | 0.75 | 0 | 0.022 | 0.026 | 0.186 | 0.167 | 0.212 | 0.678 |
| TiO2 | 0 | 0 | 0 | 0 | 0.109 | 0 | 0 | 0 | 0 | 0.059 |
| Cr2O3 | 0 | 0.02 | 0.012 | 0.007 | 0.033 | 0 | 0 | 0.015 | 0 | 0.027 |
| Fe2O3 | | | | | | | | | | |
| FeO | 28.185 | 28.568 | 28.139 | 29.527 | 29.309 | 29.32 | 29.436 | 28.958 | 28.886 | 28.22 |
| MnO | 0.609 | 0.583 | 0.655 | 0.476 | 0.465 | 0.448 | 0.519 | 0.581 | 0.448 | 0.562 |
| MgO | 0.049 | 0.068 | 0.069 | 0.102 | 0.097 | 0.127 | 0.002 | 0.027 | 0.026 | 0.09 |
| NiO | 0.046 | 0.011 | 0 | 0.043 | 0.016 | 0 | 0 | 0.006 | 0 | 0.014 |
| BaO | 0 | 0 | 0 | 0.089 | 0 | 0.011 | 0.031 | 0 | 0 | 0.025 |
| CaO | 33.482 | 33.303 | 33.473 | 33.475 | 33.355 | 33.394 | 33.498 | 33.242 | 33.287 | 33.525 |
| Na2O | 0.03 | 0.015 | 0.018 | 0 | 0.033 | 0.035 | 0 | 0.033 | 0.031 | 0.011 |
| K2O | 0 | 0 | 0.016 | 0.02 | 0.008 | 0.015 | 0.002 | 0 | 0.007 | 0.019 |
| Total | 97.163 | 97.547 | 98.112 | 98.406 | 97.999 | 98.186 | 97.818 | 97.331 | 96.366 | 97.376 |

| sample ref. | 2_c2_p82 | 2_c2_p83 | 2_c2_p101 | 2_c2_p102 | 2_c2_p103 | 2_c3_p11 | 2_c3_p12 | 2_c3_p13 | 2_c3_p14 | 2_c3_p17 |
|---|---|---|---|---|---|---|---|---|---|---|
| SiO2 | 34.569 | 35.114 | 35.288 | 35.317 | 35.835 | 35.281 | 36.186 | 35.503 | 36.257 | 34.652 |
| Al2O3 | 0.554 | 0.111 | 8.408 | 4.72 | 4.564 | 4.295 | 3.766 | 3.556 | 6.348 | 0.154 |
| TiO2 | 0.009 | 0 | 0 | 0 | 0 | 0 | 0 | 0 | 0 | 0 |
| Cr2O3 | 0 | 0 | 0 | 0.01 | 0 | 0.019 | 0 | 0 | 0.025 | 0 |
| Fe2O3 | | | | | | | | | | |
| FeO | 27.277 | 29.152 | 17.461 | 22.253 | 22.73 | 22.552 | 23.763 | 23.703 | 21.338 | 29.393 |
| MnO | 0.539 | 0.428 | 0.692 | 0.891 | 0.797 | 0.788 | 0.742 | 0.695 | 0.968 | 0.524 |
| MgO | 0.073 | 0.079 | 0.058 | 0 | 0.022 | 0.012 | 0.043 | 0.035 | 0.024 | 0 |
| NiO | 0.046 | 0.019 | 0.061 | 0.003 | 0.032 | 0.015 | 0 | 0 | 0 | 0 |
| BaO | 0.073 | 0 | 0 | 0 | 0 | 0 | 0.041 | 0 | 0 | 0 |
| CaO | 32.952 | 33.113 | 34.631 | 33.682 | 33.782 | 34.125 | 34.123 | 34.076 | 34.266 | 33.439 |
| Na2O | 1.192 | 0.016 | 0.019 | 0.002 | 0.021 | 0.003 | 0.012 | 0.014 | 0.019 | 0.103 |
| K2O | 0.013 | 0.024 | 0.017 | 0.028 | 0 | 0 | 0.02 | 0.023 | 0.009 | 0.012 |
| Total | 97.297 | 98.056 | 96.635 | 96.906 | 97.783 | 97.09 | 98.696 | 97.605 | 99.254 | 98.277 |

| sample ref. | 2_c3_p18 | 2_c3_p21 | 2_c3_p22 | 2_c3_p23 | 2_c3_p31 | 2_c3_p32 | 2_c3_p33 |
|---|---|---|---|---|---|---|---|
| SiO2 | 34.706 | 36.871 | 37.678 | 36.698 | 36.729 | 36.691 | 36.869 |
| Al2O3 | 0.122 | 10.85 | 9.487 | 9.995 | 7.097 | 6.331 | 5.656 |
| TiO2 | 0 | 0 | 0 | 0 | 0 | 0 | 0.023 |
| Cr2O3 | 0 | 0.015 | 0 | 0.024 | 0.023 | 0 | 0.032 |
| Fe2O3 | | | | | | | |
| FeO | 28.898 | 16.179 | 17.296 | 17.04 | 19.247 | 21.018 | 21.954 |
| MnO | 0.629 | 1.064 | 1.121 | 1.043 | 0.995 | 0.962 | 0.89 |
| MgO | 0.021 | 0.008 | 0.026 | 0.013 | 0.042 | 0.013 | 0.084 |
| NiO | 0.013 | 0.018 | 0 | 0.037 | 0 | 0 | 0.034 |
| BaO | 0.012 | 0.013 | 0 | 0 | 0.044 | 0 | 0.074 |
| CaO | 33.355 | 34.241 | 34.172 | 34.136 | 34.469 | 33.972 | 34.184 |
| Na2O | 0.029 | 0.018 | 0.028 | 0.03 | 0 | 0.02 | 0 |
| K2O | 0.005 | 0.005 | 0.028 | 0.002 | 0 | 0 | 0 |
| Total | 97.79 | 99.282 | 99.836 | 99.018 | 98.646 | 99.007 | 99.8 |

## Appendix B: EPMA results for pyroxene

| Sample ref. | 1_1 | 1_2 | 1_4 | 1_5 | 1_6 | 1_7 | 1_1-2 | 1_1-3 | 1_1-4 | 1_1-5 | 1_1-6 | 1_1-7 | 1_1-8 | 1_1-9 |
|---|---|---|---|---|---|---|---|---|---|---|---|---|---|---|
| SiO2 | 53.28 | 53.152 | 53.082 | 55.113 | 55.22 | 52.862 | 52.233 | 53.271 | 52.612 | 53.321 | 53.327 | 53.675 | 53.661 | 53.698 |
| Al2O3 | 2.255 | 2.202 | 2.799 | 27.906 | 27.827 | 30.291 | 2.836 | 2.415 | 2.924 | 2.376 | 1.91 | 2.971 | 2.082 | 2.717 |
| TiO2 | 0.245 | 0.213 | 0.037 | 0.042 | 0.116 | 0.08 | 0.207 | 0.124 | 0.066 | 0.114 | 0.152 | 0 | 0.018 | 0.1 |
| Cr2O3 | 0.022 | 0 | 0 | 0 | 0 | 0 | 0 | 0.028 | 0 | 0.024 | 0.04 | 0 | 0.02 | 0 |
| Fe2O3 | | | | | | | | | | | | | | |
| FeO | 6.012 | 5.856 | 5.946 | 0.817 | 1.05 | 0.421 | 6.364 | 6.103 | 6.834 | 6.88 | 5.949 | 6.48 | 6.573 | 6.047 |
| MnO | 0.451 | 0.368 | 0.355 | 0.041 | 0.013 | 0 | 0.458 | 0.334 | 0.429 | 0.283 | 0.517 | 0.485 | 0.315 | 0.499 |
| MgO | 16.165 | 16.048 | 15.865 | 0.091 | 0.111 | 0.051 | 15.457 | 16.009 | 15.489 | 15.204 | 15.818 | 16.606 | 16.142 | 16.426 |
| NiO | 0 | 0.018 | 0.025 | 0 | 0.029 | 0 | 0.037 | 0 | 0 | 0.01 | 0 | 0.002 | 0.064 | 0 |
| BaO | 0 | 0 | 0.042 | 0 | 0 | 0.087 | 0 | 0 | 0.011 | 0 | 0 | 0.036 | 0.022 | 0 |
| CaO | 20.374 | 20.529 | 20.602 | 10.882 | 10.638 | 11.365 | 20.405 | 20.135 | 20.186 | 19.851 | 20.567 | 19.256 | 19.474 | 20.643 |
| K2O | 0.018 | 0.097 | 0.024 | 0.156 | 0.126 | 0.09 | 0.102 | 0.013 | 0.022 | 0.176 | 0.122 | 0.068 | 0.094 | 0.043 |
| Na2O | 0.355 | 0.334 | 0.246 | 5.866 | 5.064 | 4.058 | 0.297 | 0.262 | 0.205 | 0.43 | 0.291 | 0.274 | 0.221 | 0.238 |
| Total | 99.177 | 98.817 | 99.023 | 100.914 | 100.194 | 99.305 | 98.396 | 98.694 | 98.778 | 98.669 | 98.693 | 99.853 | 98.686 | 100.411 |

| Sample ref. | 4_c2_9 | 4_c2_9-1 | 4_c2_9-2 | 3_c_1 | 3_c_2 | 3_b_1 | 3_c_3 | 3_c_1-1 | 3_c_1-2 | 3_c_1-3 | 3_c_1-4 | 3_c_1-5 |
|---|---|---|---|---|---|---|---|---|---|---|---|---|
| $SiO_2$ | 50.331 | 48.544 | 48.177 | 48.686 | 49.348 | 48.861 | 50.298 | 48.962 | 48.644 | 49.345 | 49.415 | 49.437 |
| $Al_2O_3$ | 2.534 | 1.728 | 2.261 | 1.631 | 1.69 | 0.87 | 0.525 | 0.632 | 1.359 | 0.541 | 0.539 | 0.346 |
| $TiO_2$ | 0 | 0 | 0 | 0 | 0 | 0 | 0 | 0 | 0.017 | 0 | 0 | 0 |
| $Cr_2O_3$ | 0.004 | 0 | 0.004 | 0 | 0 | 0 | 0 | 0.038 | 0 | 0 | 0.03 | 0.046 |
| FeO Tot | 25.131 | 26.757 | 26.893 | 27.427 | 26.604 | 26.587 | 26.121 | 26.976 | 26.685 | 26.966 | 26.679 | 26.997 |
| MnO | 0.699 | 0.998 | 0.539 | 0.988 | 1.374 | 1.171 | 0.973 | 0.972 | 1.164 | 0.716 | 0.865 | 1.004 |
| MgO | 9.161 | 10.245 | 9.048 | 8.744 | 9.144 | 9.255 | 9.367 | 8.767 | 9.744 | 9.276 | 8.804 | 9.107 |
| NiO | 0.002 | 0.042 | 0 | 0 | 0 | 0 | 0.029 | 0.029 | 0.034 | 0.01 | 0.015 | 0.03 |
| BaO | 0 | 0 | 0 | 0.01 | 0 | 0 | 0 | 0 | 0 | 0 | 0.017 | 0.06 |
| CaO | 11.376 | 10.265 | 11.618 | 11.866 | 11.777 | 11.449 | 11.865 | 11.946 | 11.912 | 12.168 | 12.033 | 12.266 |
| $Na_2O$ | 0.27 | 0.223 | 0.285 | 0.324 | 0.27 | 0.241 | 0.274 | 0.192 | 0.201 | 0.198 | 0.223 | 0.138 |
| $K_2O$ | 0.099 | 0.03 | 0.064 | 0.168 | 0.142 | 0.093 | 0.032 | 0.108 | 0.129 | 0.066 | 0.071 | 0.031 |
| Total | 99.607 | 98.832 | 98.889 | 99.844 | 100.349 | 98.527 | 99.484 | 98.622 | 99.889 | 99.286 | 98.691 | 99.462 |

| Sample ref. | 3_c_1-6 | 3_c_1-7 | 3_c_2-5 | 3_b_1-2 | 3_b_1-4 | 3_b_1-5 | 3_c_3-1 | 3_c_3-2 | 3_c_3-3 | 3_c_3-4 | 3_c_3-5 |
|---|---|---|---|---|---|---|---|---|---|---|---|
| SiO2 | 49.708 | 49.097 | 49.692 | 49.298 | 49.507 | 49.994 | 49.636 | 49.405 | 50.324 | 50.274 | 50.544 |
| Al2O3 | 0.464 | 0.705 | 0.559 | 0.609 | 1.602 | 0.931 | 0.562 | 0.4 | 0.495 | 0.447 | 0.569 |
| TiO2 | 0 | 0 | 0 | 0 | 0.04 | 0.043 | 0 | 0 | 0.013 | 0 | 0.035 |
| Cr2O3 | 0.015 | 0.015 | 0 | 0.05 | 0 | 0 | 0 | 0.011 | 0 | 0 | 0 |
| FeO Tot | 26.686 | 26.965 | 26.655 | 26.904 | 25.487 | 26.238 | 27.278 | 26.537 | 25.71 | 26.004 | 25.583 |
| MnO | 0.987 | 0.727 | 0.925 | 0.935 | 0.979 | 1.039 | 0.861 | 0.841 | 0.924 | 0.915 | 0.814 |
| MgO | 8.55 | 8.851 | 8.416 | 9.113 | 8.254 | 8.516 | 8.993 | 8.983 | 9.102 | 9.053 | 8.798 |
| NiO | 0 | 0.028 | 0 | 0 | 0.056 | 0.015 | 0.021 | 0 | 0.018 | 0 | 0.033 |
| BaO | 0 | 0 | 0.023 | 0.005 | 0 | 0 | 0 | 0 | 0 | 0 | 0 |
| CaO | 11.998 | 12.234 | 11.711 | 11.992 | 13.712 | 11.81 | 12.163 | 12.246 | 12.188 | 12.218 | 11.944 |
| Na2O | 0.16 | 0.242 | 0.261 | 0.245 | 0.319 | 0.242 | 0.2 | 0.149 | 0.22 | 0.161 | 0.202 |
| K2O | 0.049 | 0.072 | 0.078 | 0.05 | 0.09 | 0.129 | 0.046 | 0.039 | 0.052 | 0.062 | 0.041 |
| Total | 98.617 | 98.936 | 98.32 | 99.201 | 100.046 | 98.957 | 99.76 | 98.611 | 99.033 | 99.147 | 98.563 |

# VITA

The author was born on July 1963 at Antananarivo Madagascar. A long strike which affected his University study obligated him to work as technician at the ex-Laboratoire National des Mines for two years. After trained for nine months in "Mineralogy of raw materials and Environment" at the Bundes Geogewichaften of Rohstoff (BGR) in Hannover Germany, He went back to the "Ecole Supérieure Polytechniques d'Ivontovorona Antananarivo"- University of Antananarivo to achieve his graduation as Mining Engineer. This cursus, followed of three months in Sustainable Development of Mining training courses at the MINTEC Institute Kosaka Japan allowed him to occupy successively the post of Chief of Division of Mines and Geology at the Direction des Mines d'Antananarivo Province for seven years, Responsible of  Mines and Geology at Fianarantsoa Province, and Responsible of Small Scale Mining Environment at the Cellule Environementale des Mines of the Ministry of Mines,  to came back as Responsible of Mines and Geology at Antananarivo Province. Before coming in Thailand, He has been integrated as controller of mining and geological activities for the whole country.